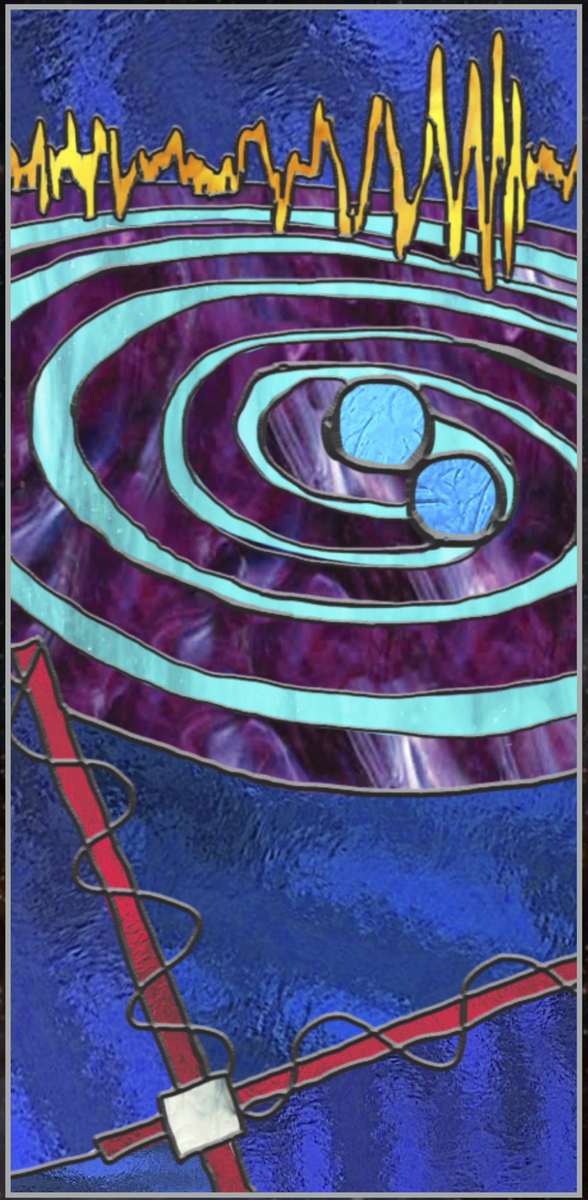
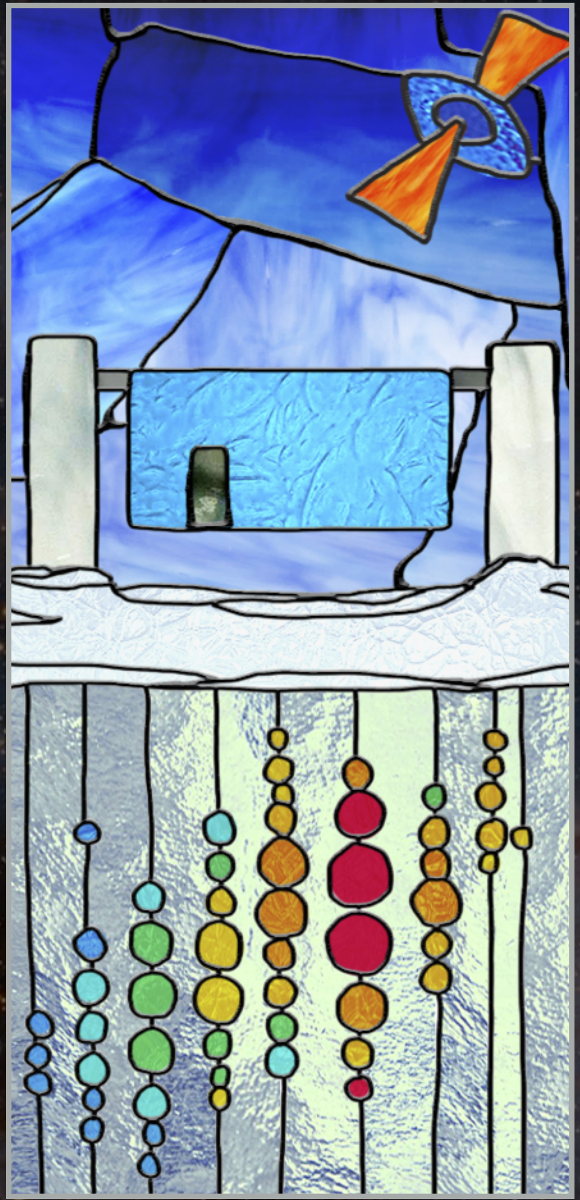
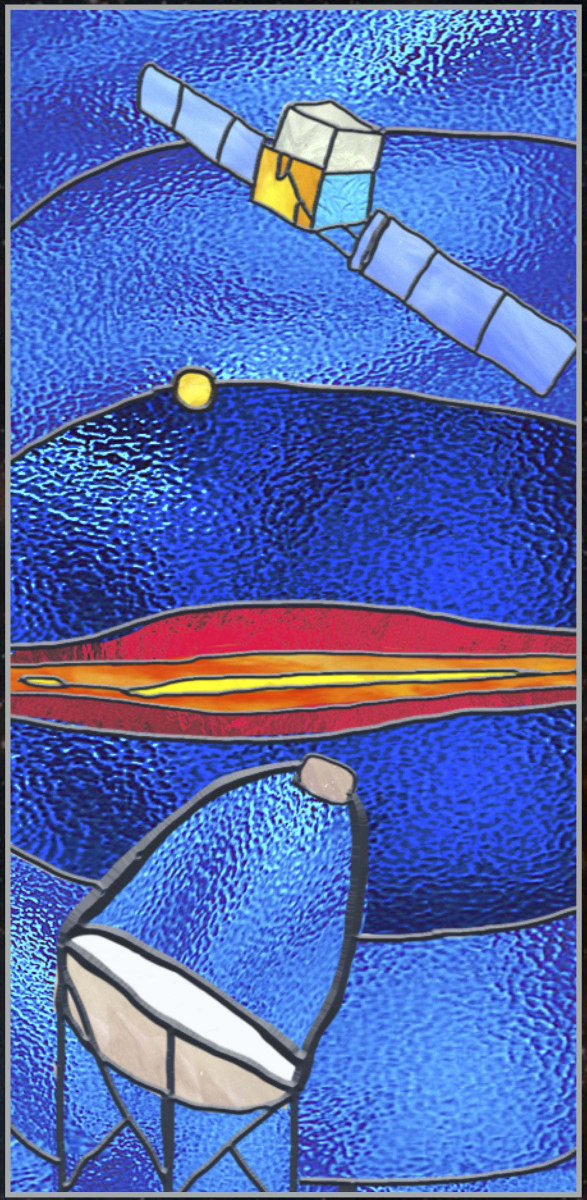

Cosmic Ray Anisotropies: Observation & Interpretation

Markus Ahlers
Niels Bohr Institute

Georges Lemaître Chair 2023

VILLUM FONDEN

KØBENHAVNS UNIVERSITET

Cosmic Rays

- Cosmic rays (CRs) are **energetic nuclei** and (at a lower level) leptons.
- Spectrum follows a **power-law** over many orders of magnitude, indicating a **non-thermal origin**.
- CRs below the **knee (few PeV)** dominated by Galactic sources
- CRs above the **ankle (few EeV)** dominated by extragalactic sources

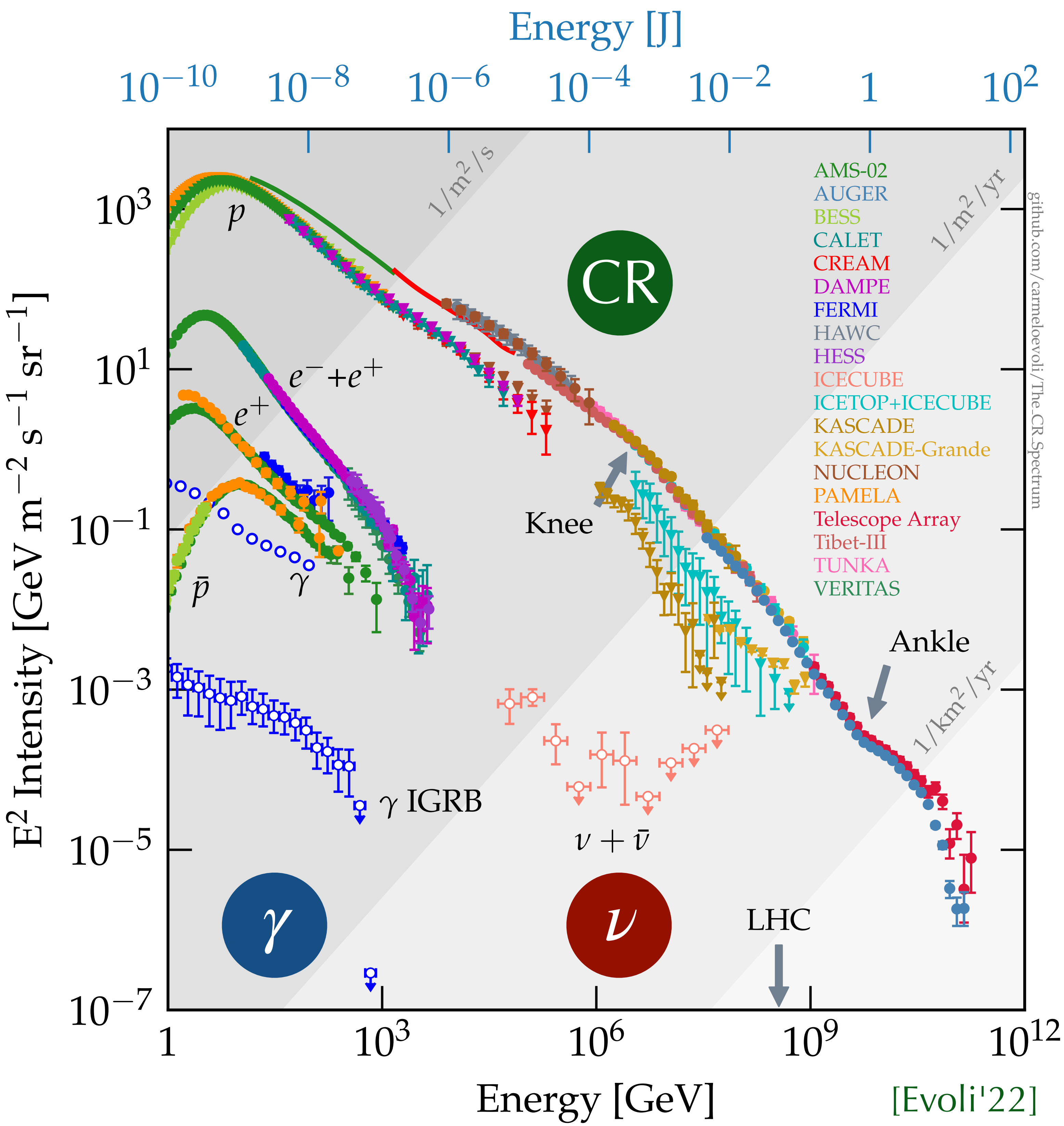

[Evoli'22]

Galactic Cosmic Rays

- *Standard paradigm*: Galactic CRs accelerated in supernova remnants

  [Baade & Zwicky'34]
  [Ginzburg & Sirovatskii'64]

- diffusive shock acceleration:

$$n_{\rm CR} \propto E^{-\Gamma}$$

- rigidity-dependent escape from Galaxy:

$$n_{\rm CR} \propto E^{-\Gamma-\delta}$$

- Arrival directions of cosmic rays are scrambled by magnetic fields.

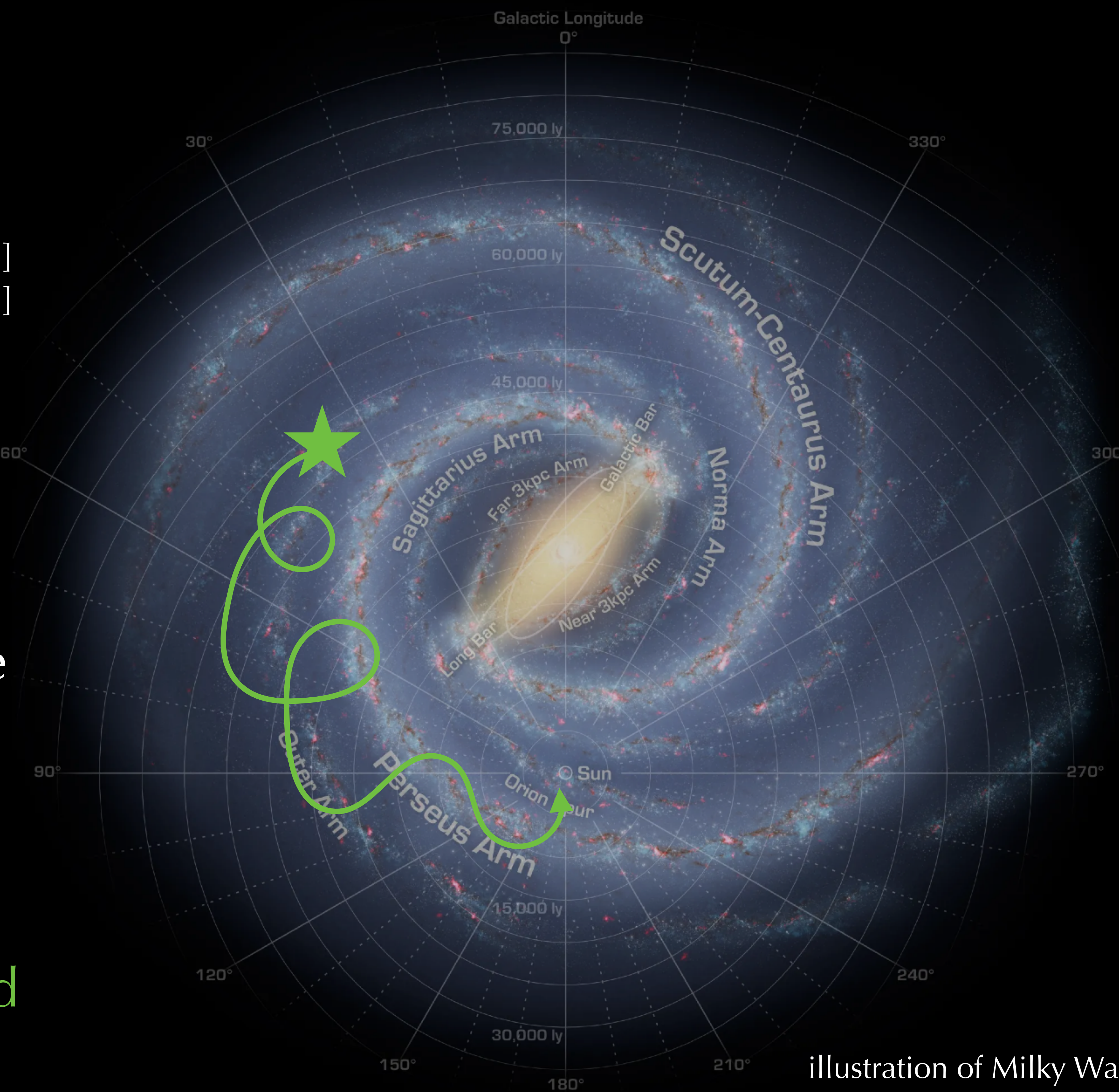

illustration of Milky Way
[Credit: NASA]

Galactic Cosmic Rays Anisotropy

Cosmic ray anisotropies up to the level of **one-per-mille** at various energies

(Super-Kamiokande, Milagro, ARGO-YBJ, EAS-TOP, Tibet ASγ, IceCube, HAWC)

$$\delta I = \frac{F_{\rm CR}}{\langle F_{\rm CR}\rangle_{4\pi}} - 1$$

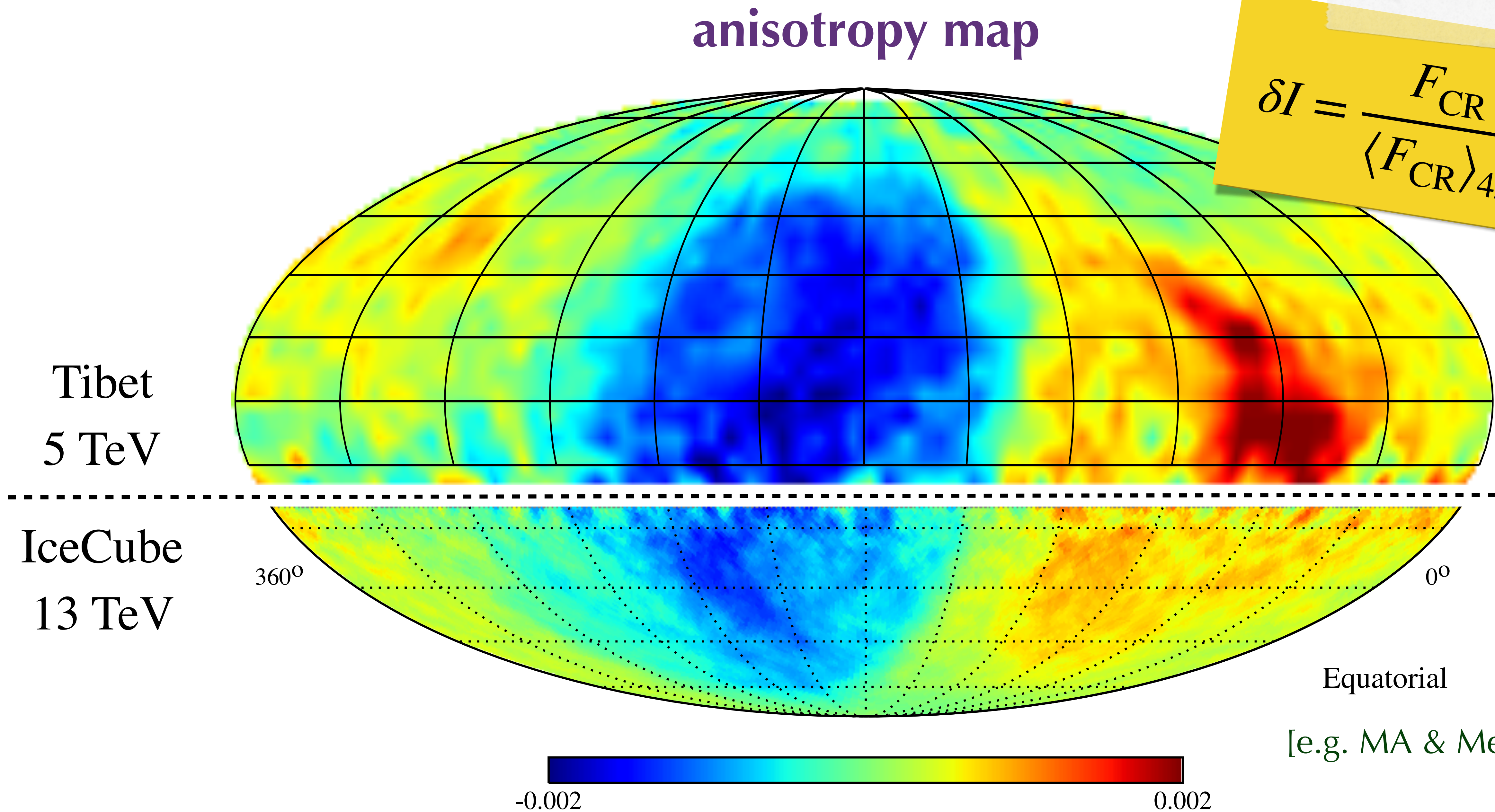

[e.g. MA & Mertsch'16]

Galactic Cosmic Rays Anisotropy

Cosmic ray anisotropies up to the level of **one-per-mille** at various energies

(Super-Kamiokande, Milagro, ARGO-YBJ, EAS-TOP, Tibet ASγ, IceCube, HAWC)

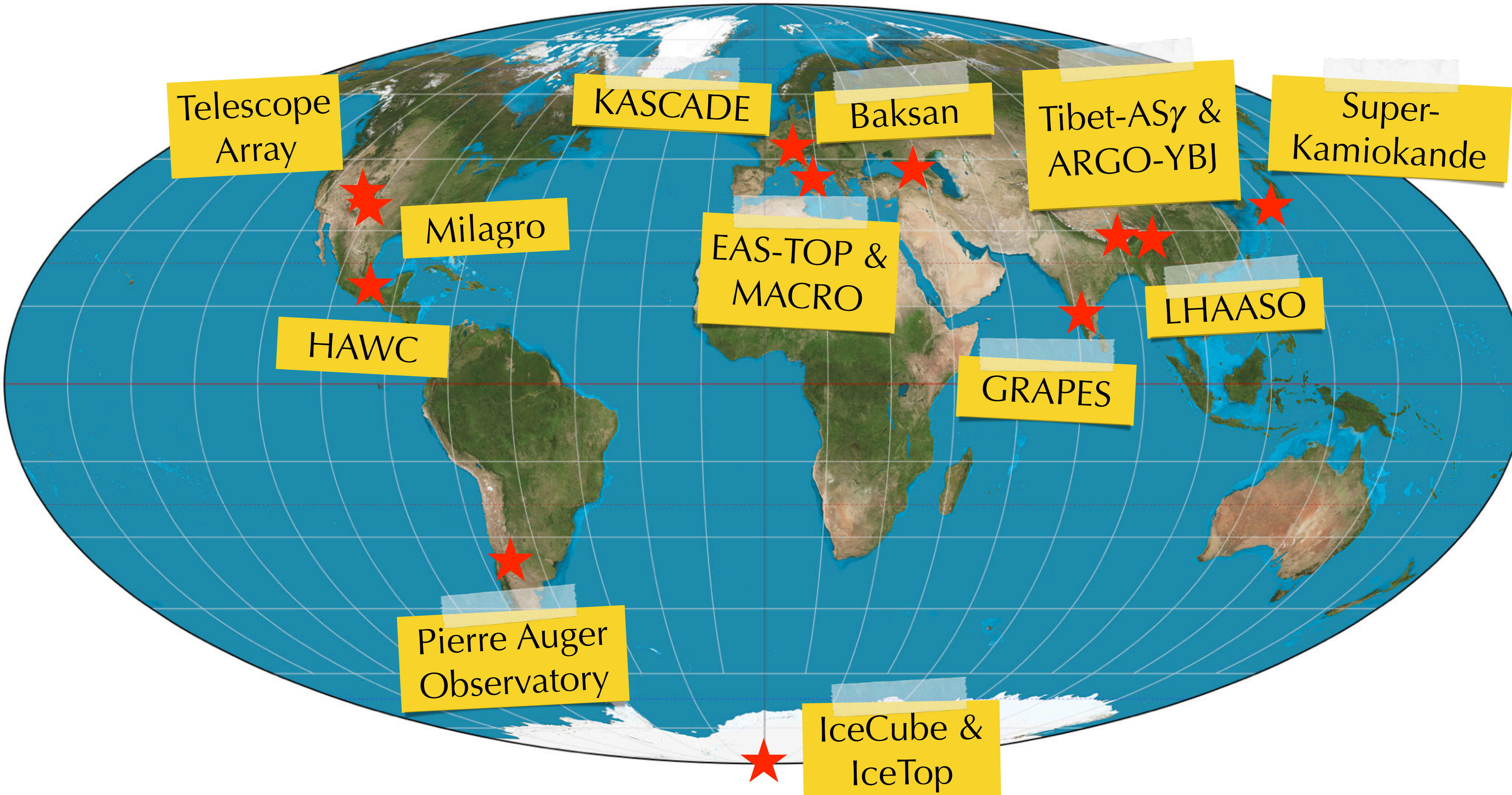

Ground-Based Observations

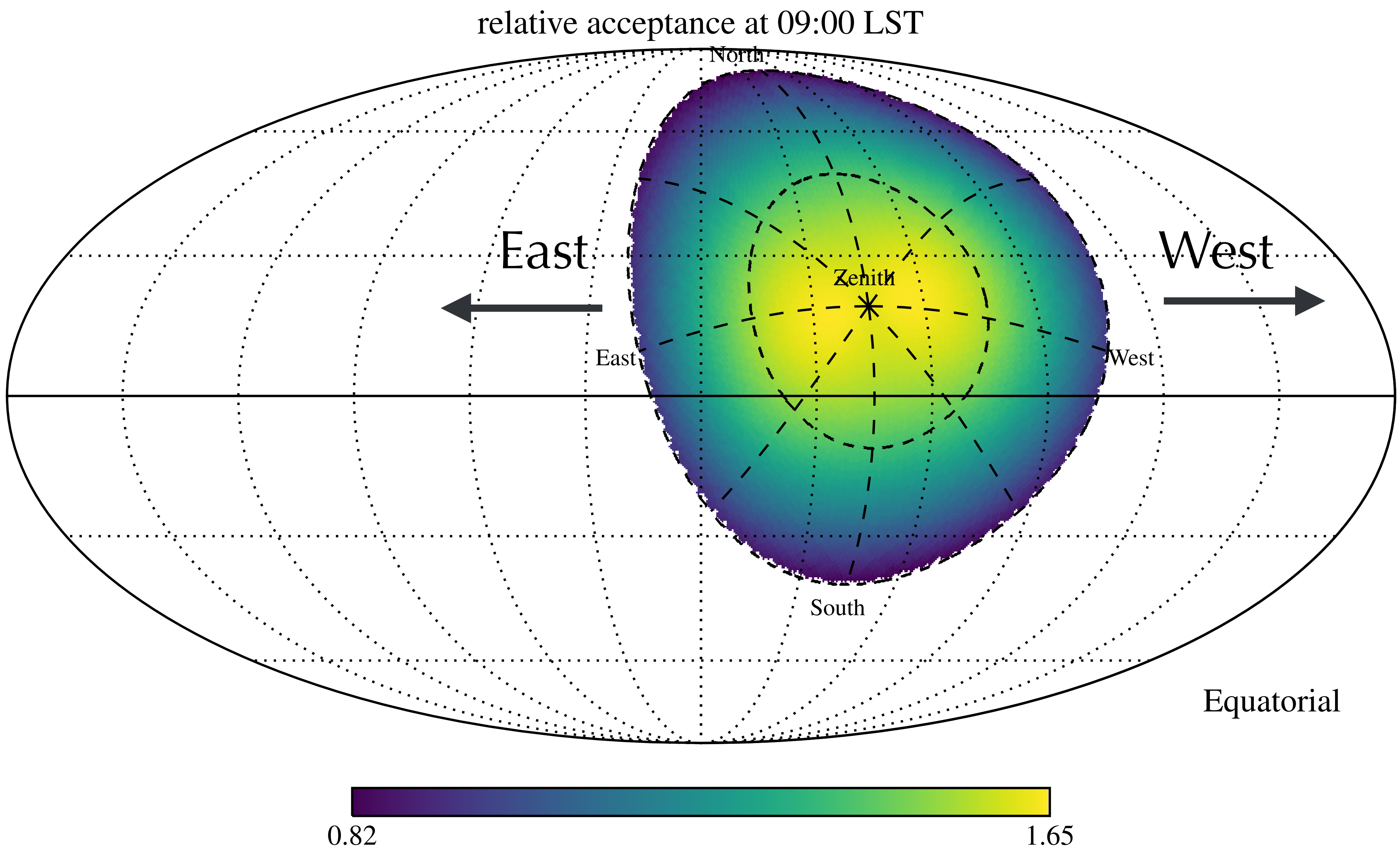

Field of View (FoV) of ground-based detector (e.g. HAWC at geographic latitude 19°) sweeps across the Sky over 24h.

Galactic Cosmic Rays Anisotropy

No significant variation of TeV-PeV anisotropy over the time scale of $\mathcal{O}(10)$ years.

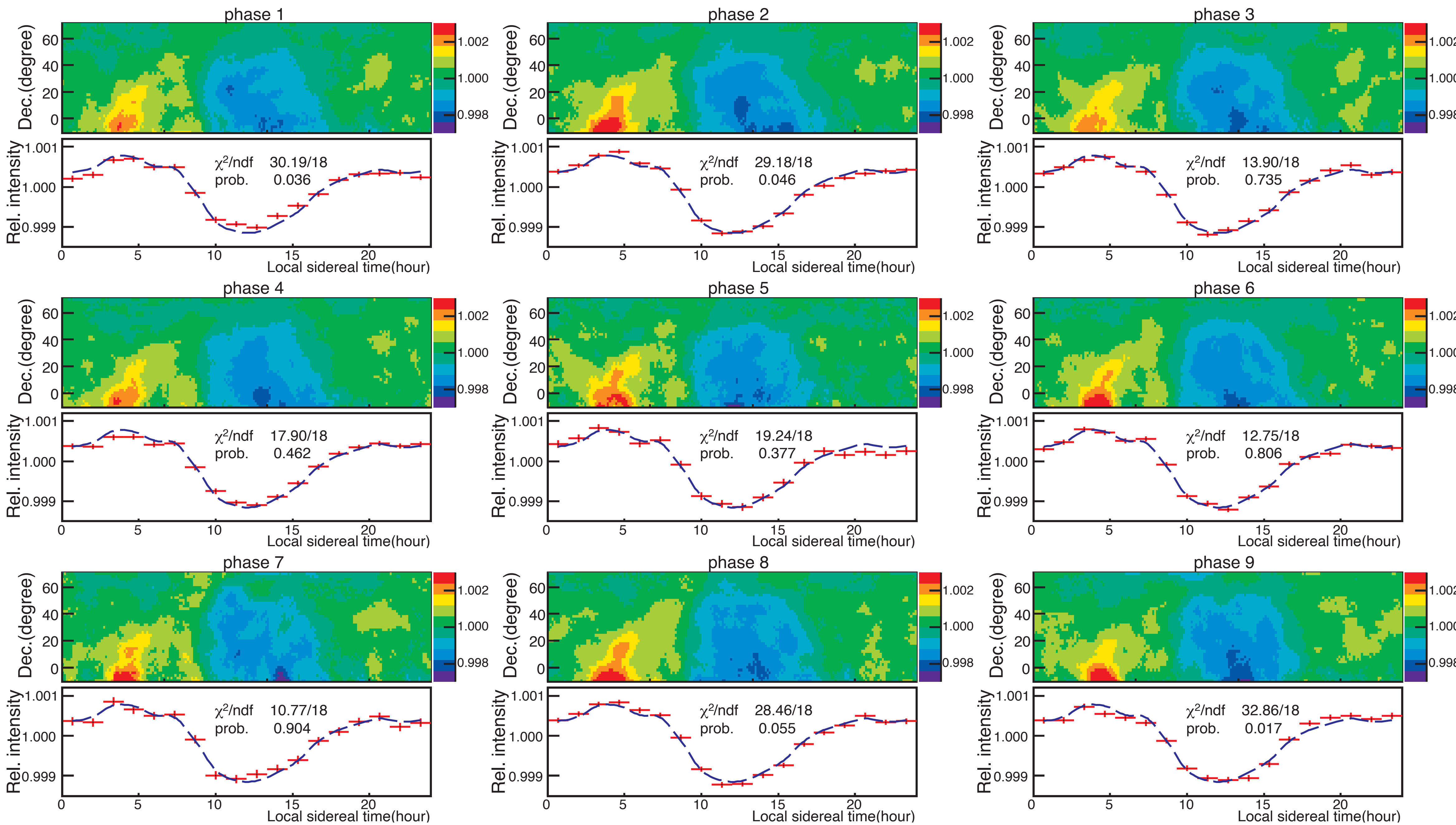

[Tibet-ASγ '10]

Large-Scale Anisotropy

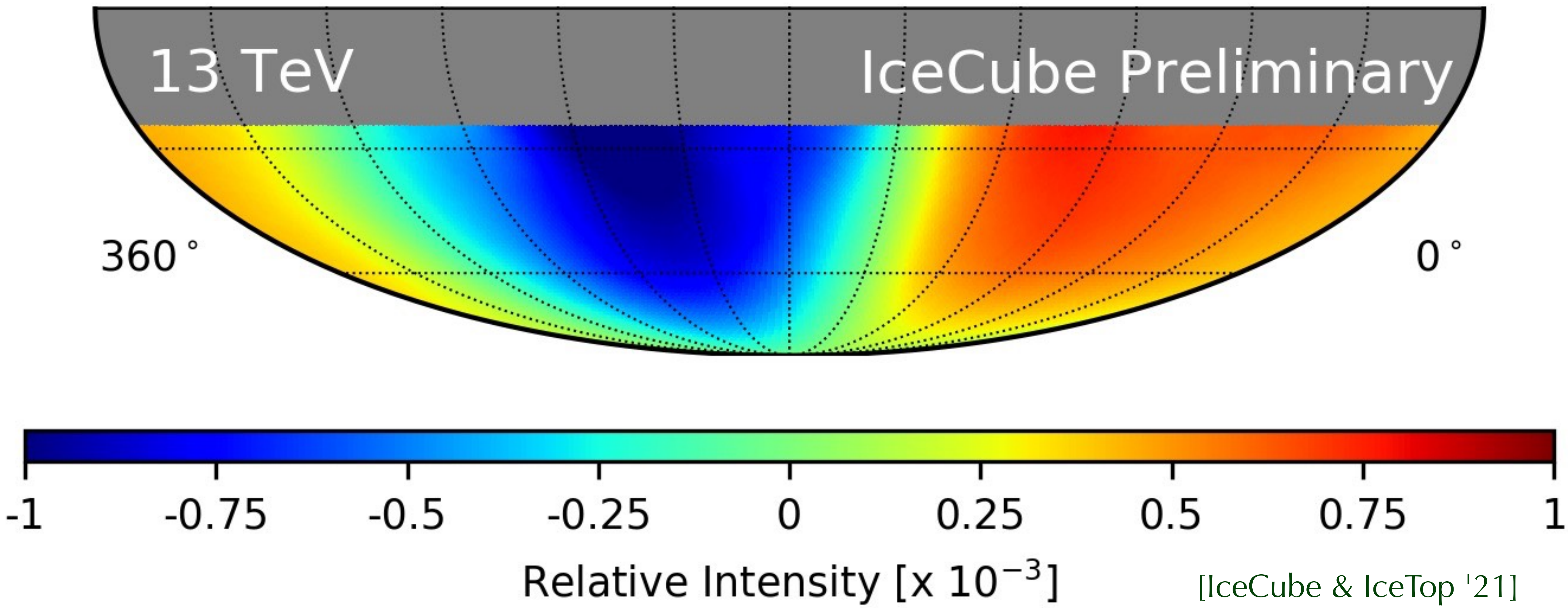

[IceCube & IceTop '21]

Amplitude of large-scale dipole anisotropy has strong energy dependence with a phase flip around 100 TeV.

Large-Scale Anisotropy

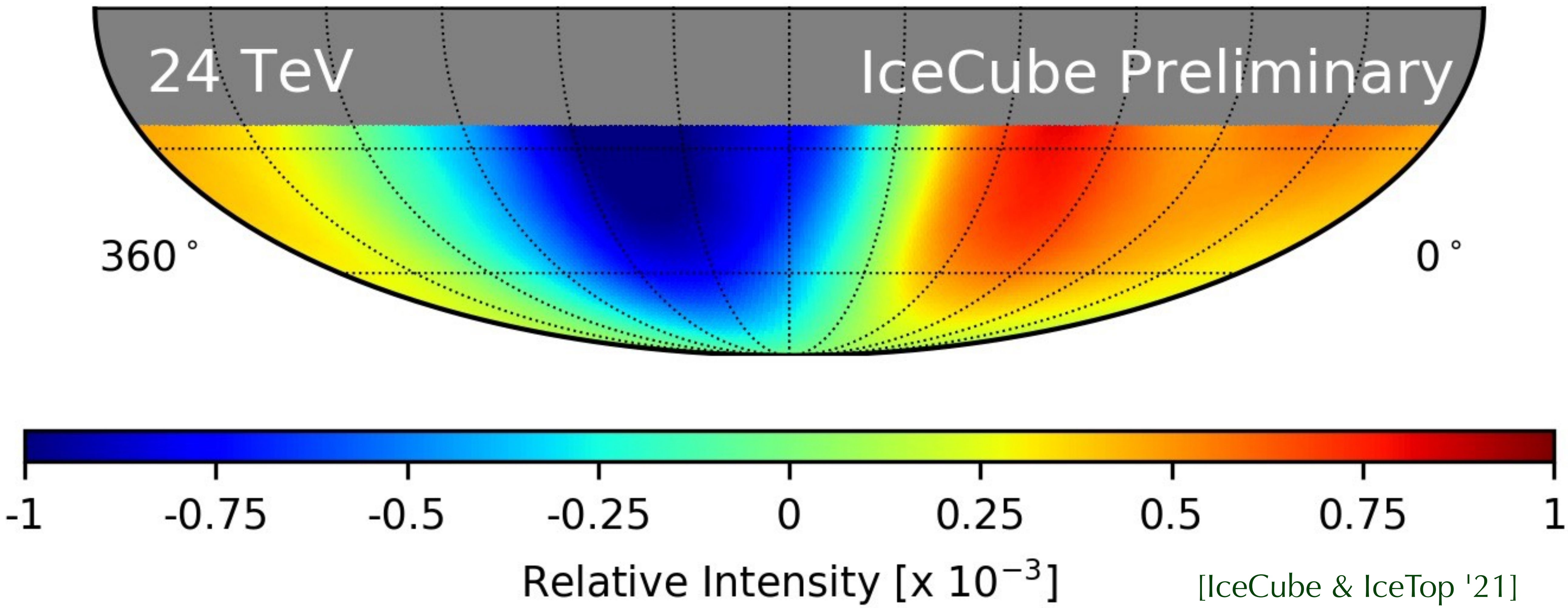

[IceCube & IceTop '21]

Amplitude of large-scale dipole anisotropy has strong energy dependence with a phase flip around 100 TeV.

Large-Scale Anisotropy

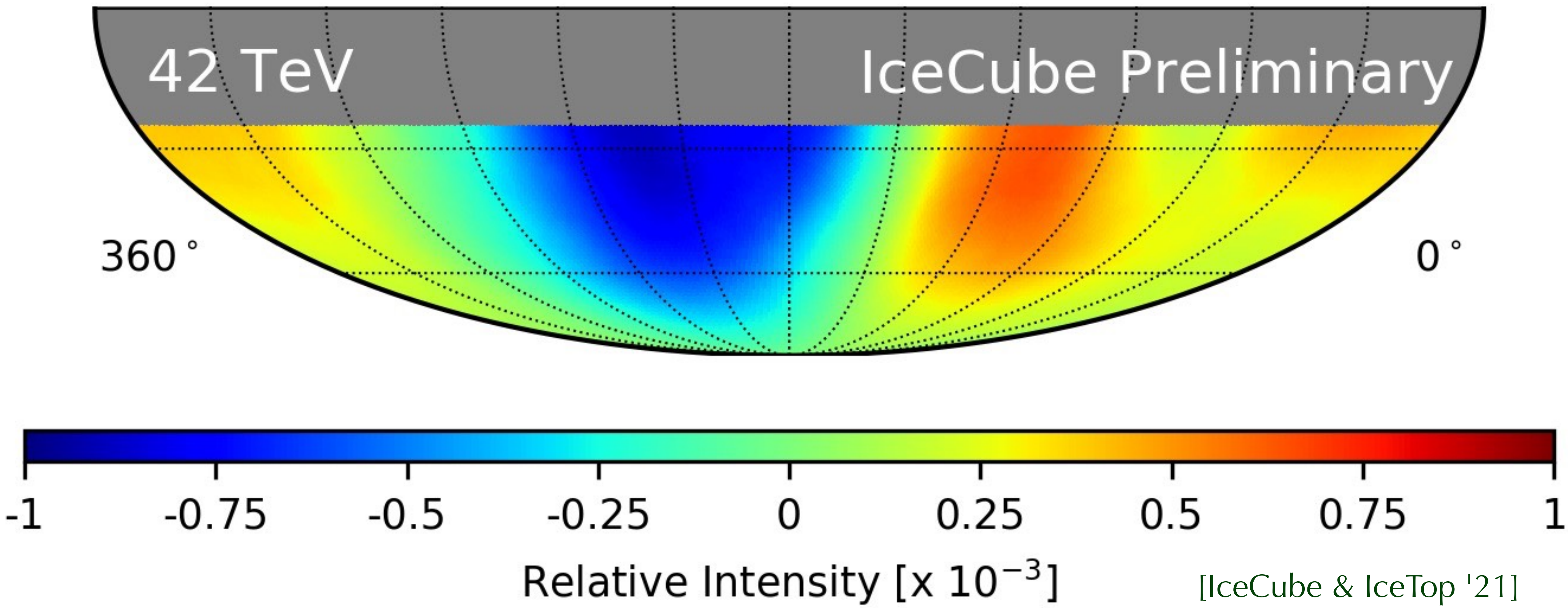

[IceCube & IceTop '21]

Amplitude of large-scale dipole anisotropy has strong energy dependence with a phase flip around 100 TeV.

Large-Scale Anisotropy

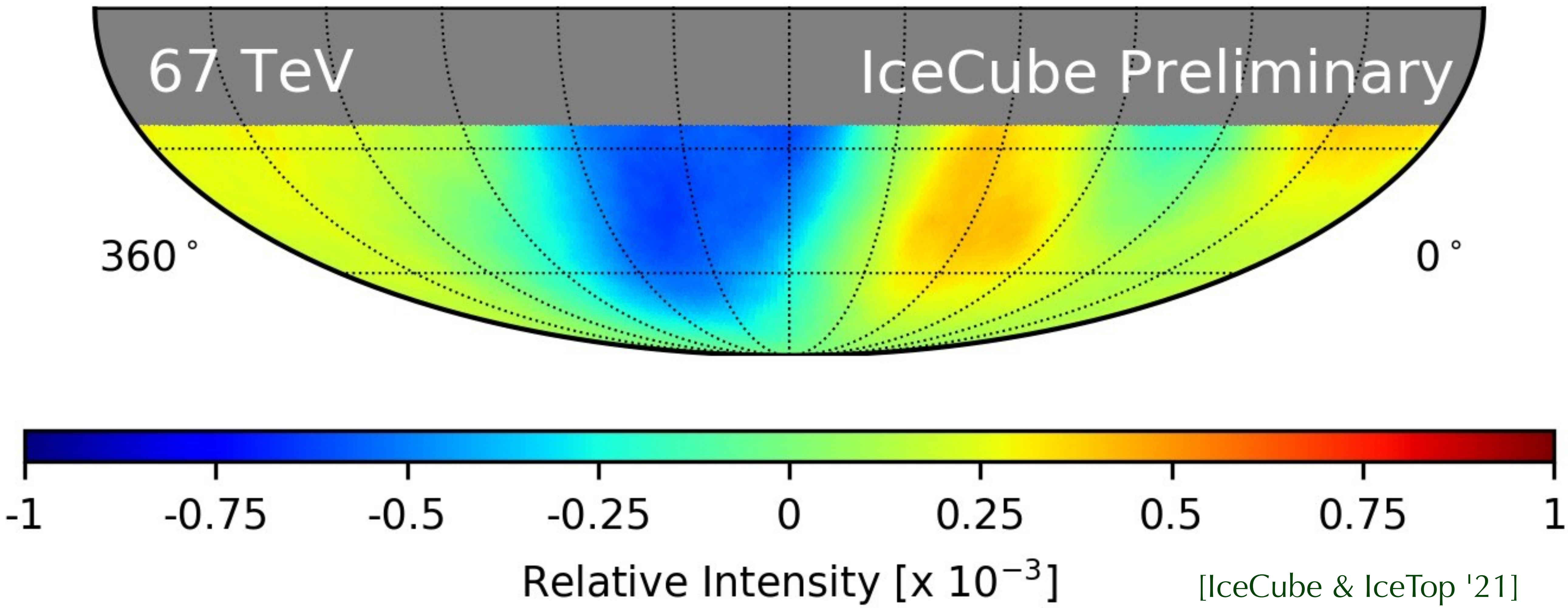

[IceCube & IceTop '21]

Amplitude of large-scale dipole anisotropy has strong energy dependence with a phase flip around 100 TeV.

Large-Scale Anisotropy

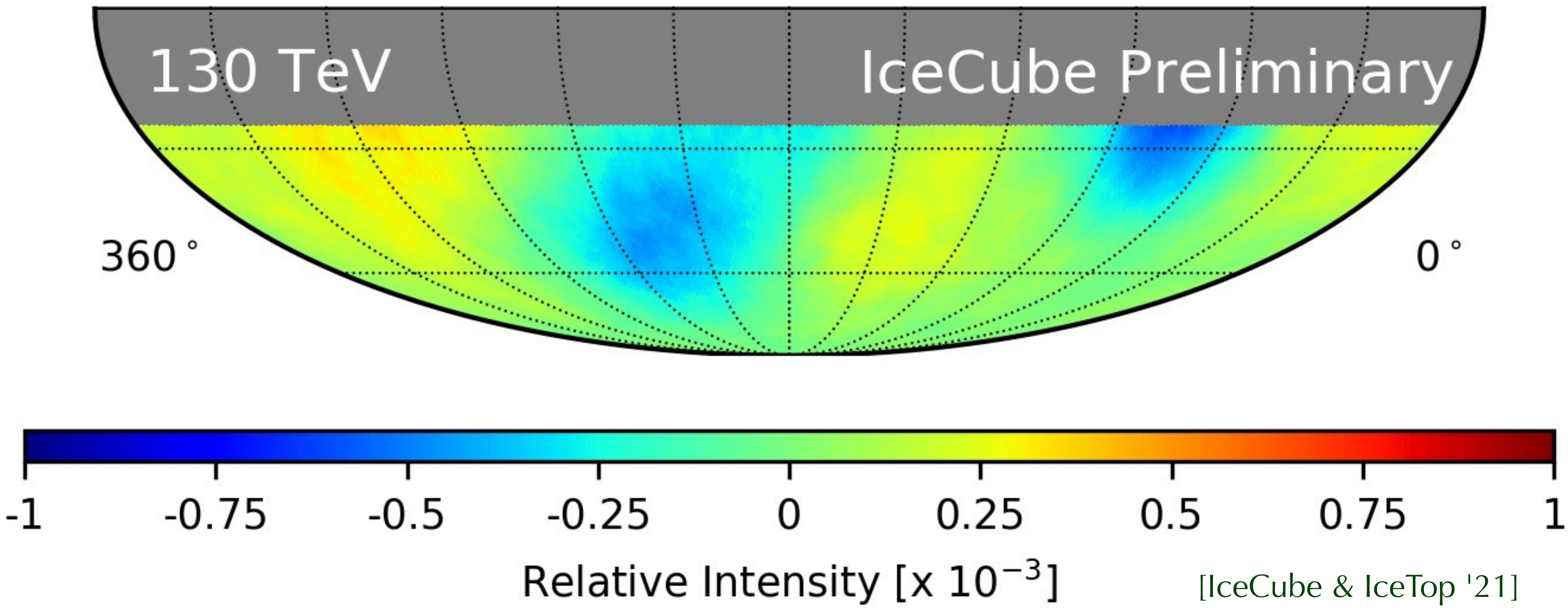

[IceCube & IceTop '21]

Amplitude of large-scale dipole anisotropy has strong energy dependence with a phase flip around 100 TeV.

Large-Scale Anisotropy

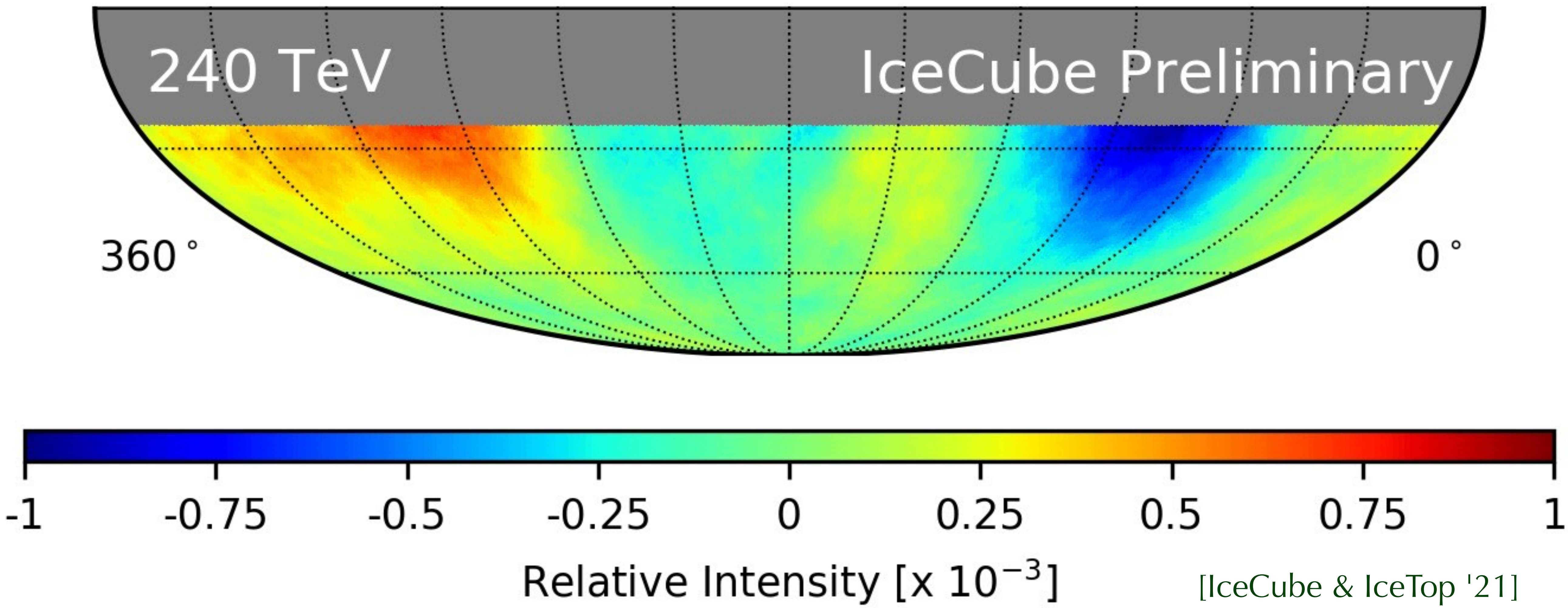

[IceCube & IceTop '21]

Amplitude of large-scale dipole anisotropy has strong energy dependence with a phase flip around 100 TeV.

Large-Scale Anisotropy

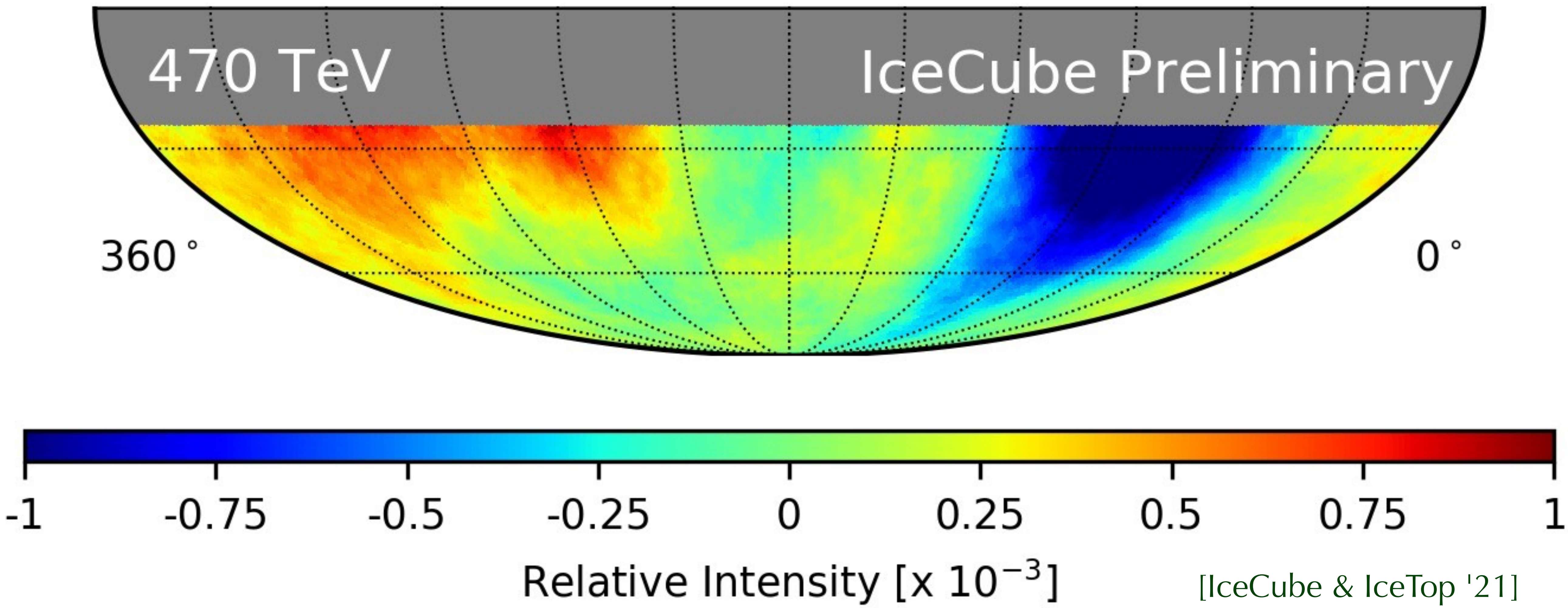

[IceCube & IceTop '21]

Amplitude of large-scale dipole anisotropy has strong energy dependence with a phase flip around 100 TeV.

Large-Scale Anisotropy

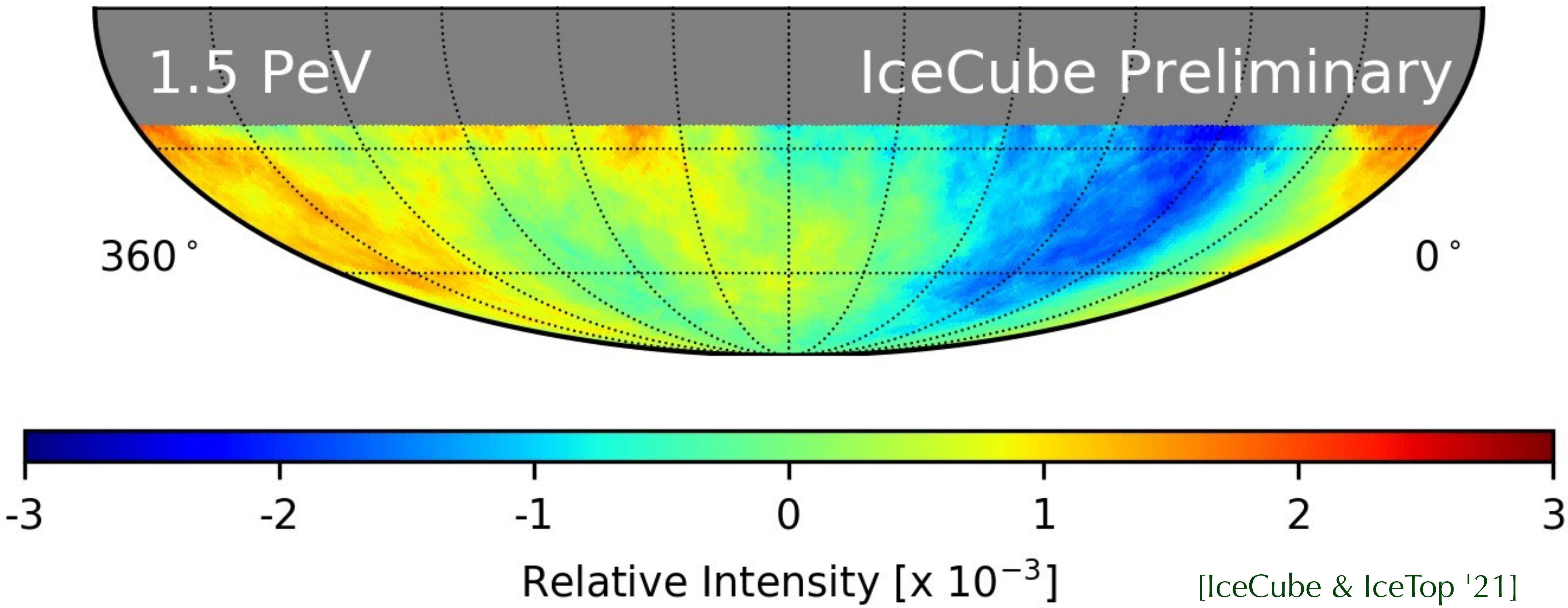

[IceCube & IceTop '21]

Amplitude of large-scale dipole anisotropy has strong energy dependence with a phase flip around 100 TeV.

Large-Scale Anisotropy

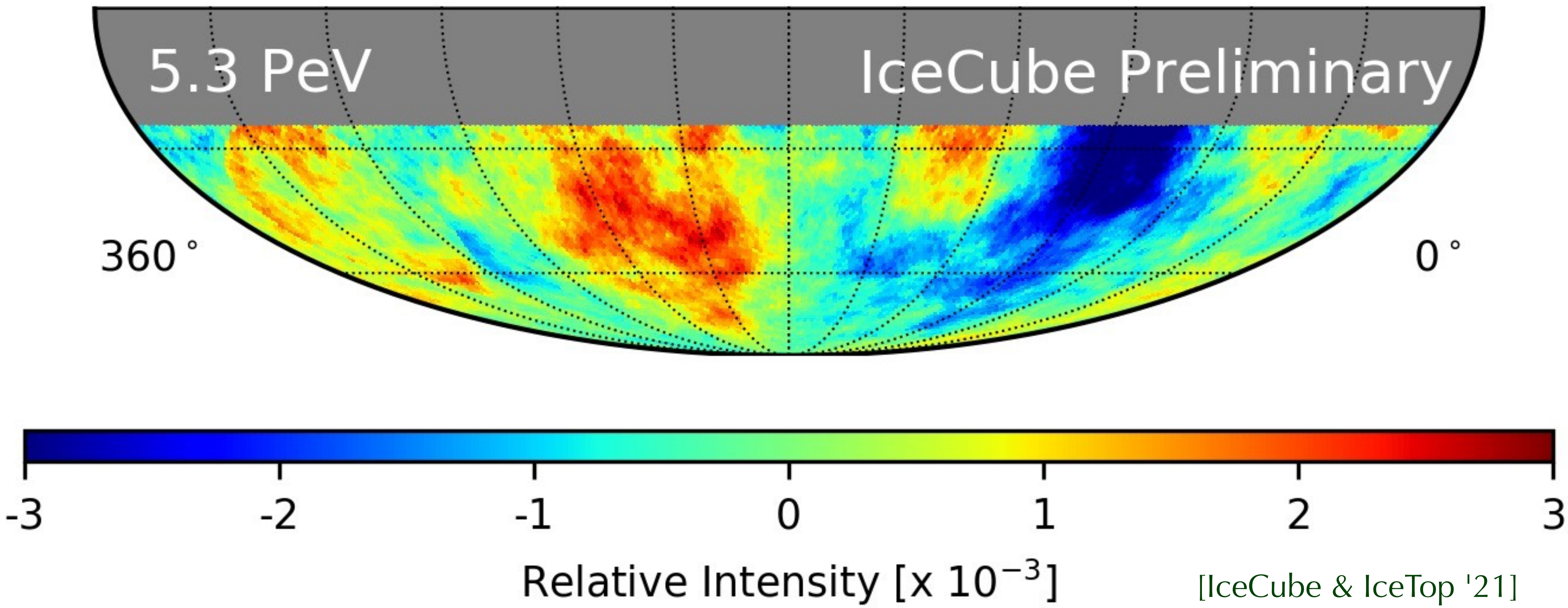

[IceCube & IceTop '21]

Amplitude of large-scale dipole anisotropy has strong energy dependence with a phase flip around 100 TeV.

Dipole Anisotropy of UHE CRs

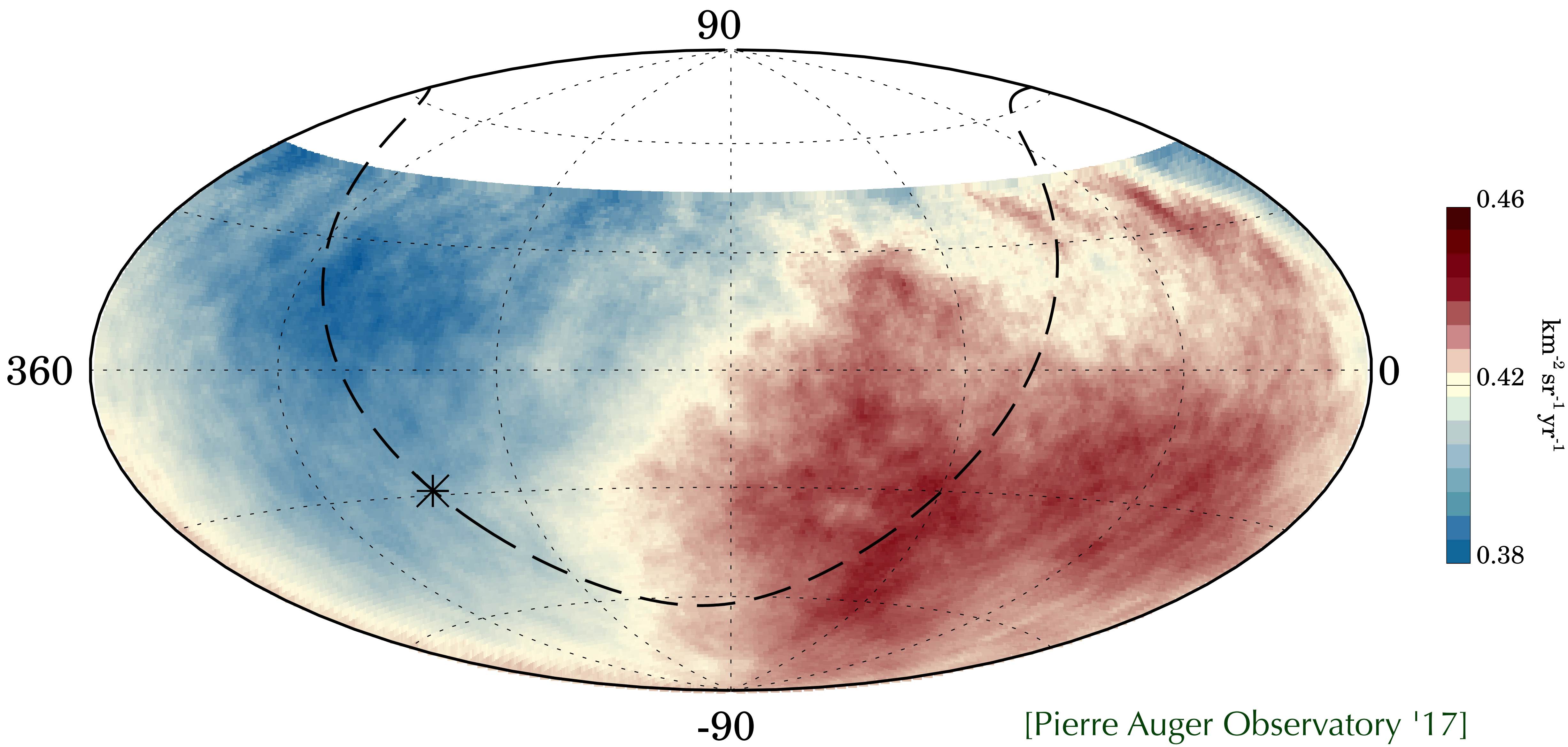

[Pierre Auger Observatory '17]

Energy [EeV]	Dipole component d_z	Dipole component $d_\perp$	Dipole amplitude d	Dipole declination δ_d [°]	Dipole right ascension α_d [°]
4 to 8	-0.024 ± 0.009	$0.006^{+0.007}_{-0.003}$	$0.025^{+0.010}_{-0.007}$	-75^{+17}_{-8}	80 ± 60
8	-0.026 ± 0.015	$0.060^{+0.011}_{-0.010}$	$0.065^{+0.013}_{-0.009}$	-24^{+12}_{-13}	100 ± 10

Issues with Reconstructions

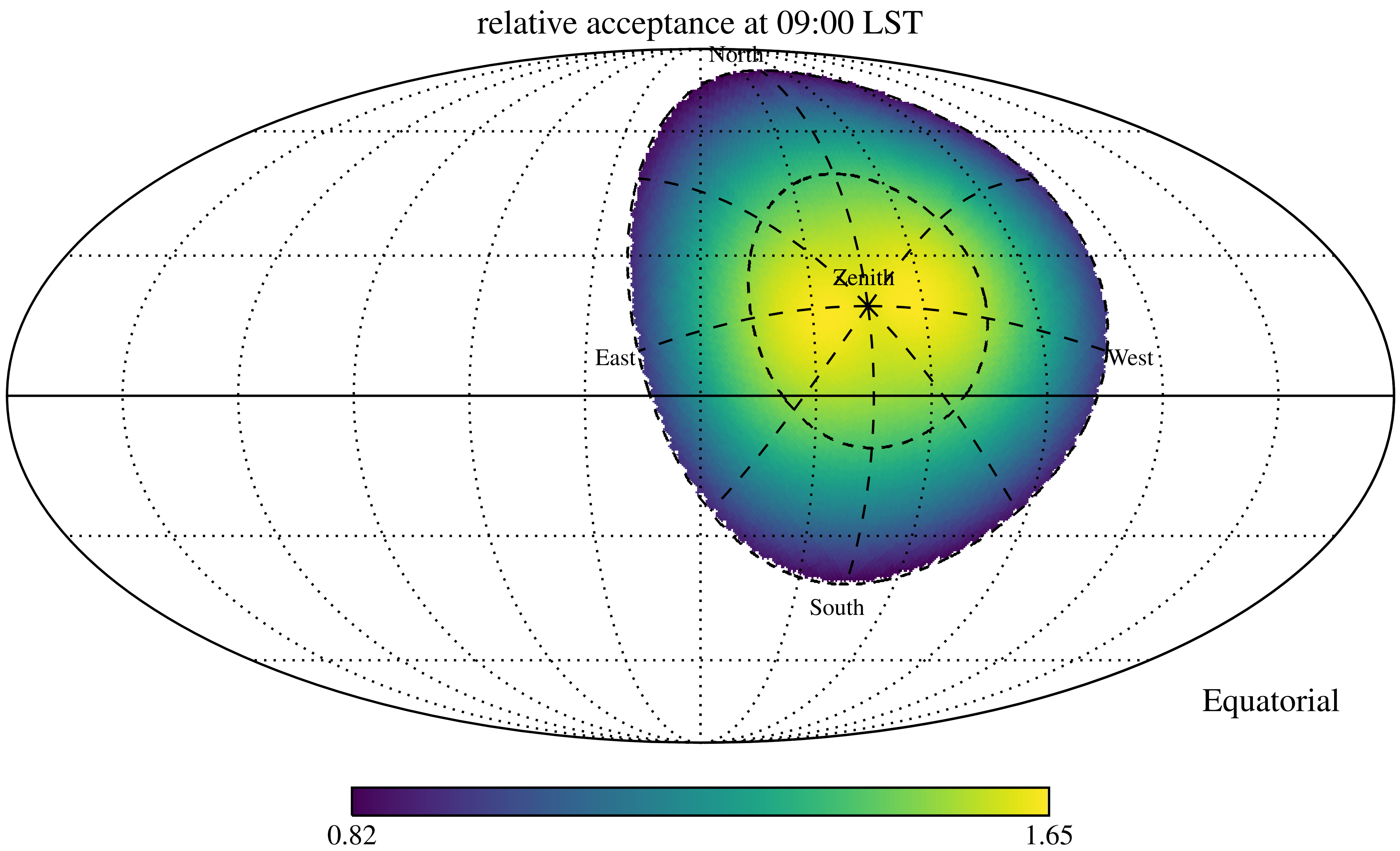

Ground-based detectors needs to be calibrated by the CR data it collects while it sweeps across the sky over 24h.

Issues with Reconstructions

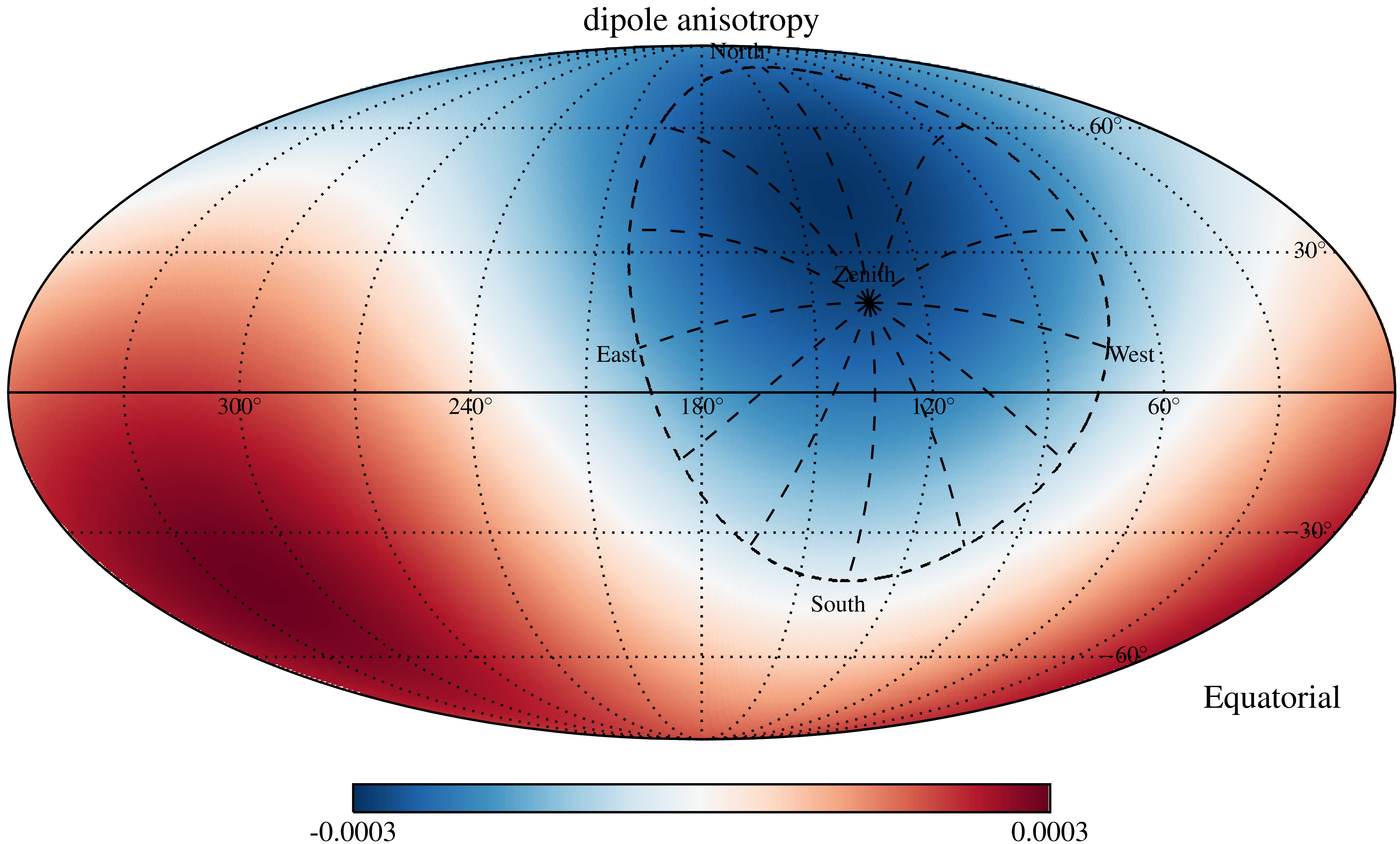

True CR dipole is defined by amplitude A and direction (α, δ).

Observable dipole is projected onto equatorial plane: $A' = A\cos\delta$

[Iuppa & Di Sciascio'13; MA *et al.*'15]

Issues with Reconstructions

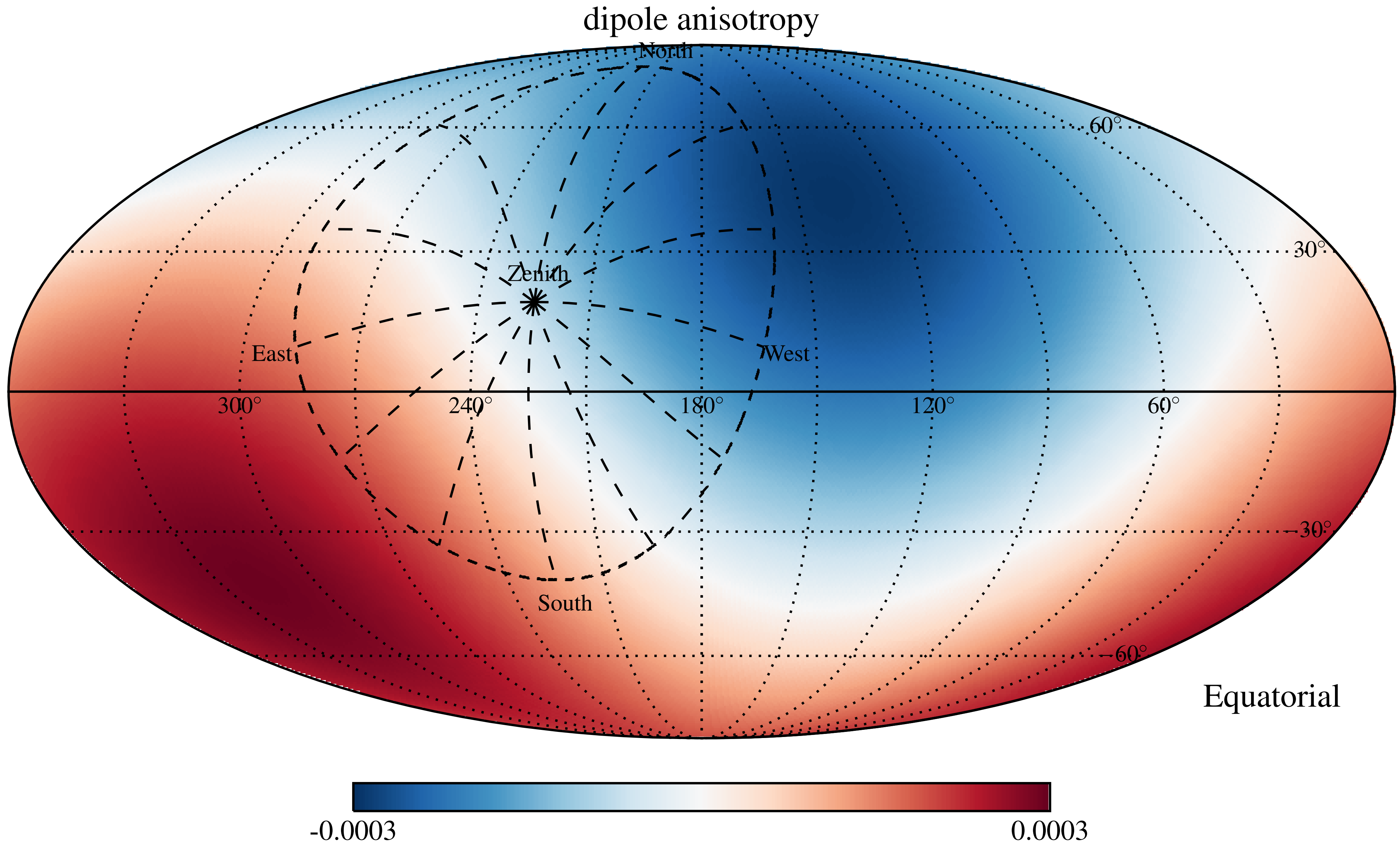

True CR dipole is defined by amplitude A and direction (α, δ).

Observable dipole is projected onto equatorial plane: $A' = A\cos\delta$

[Iuppa & Di Sciascio'13; MA *et al.*'15]

Issues with Reconstructions

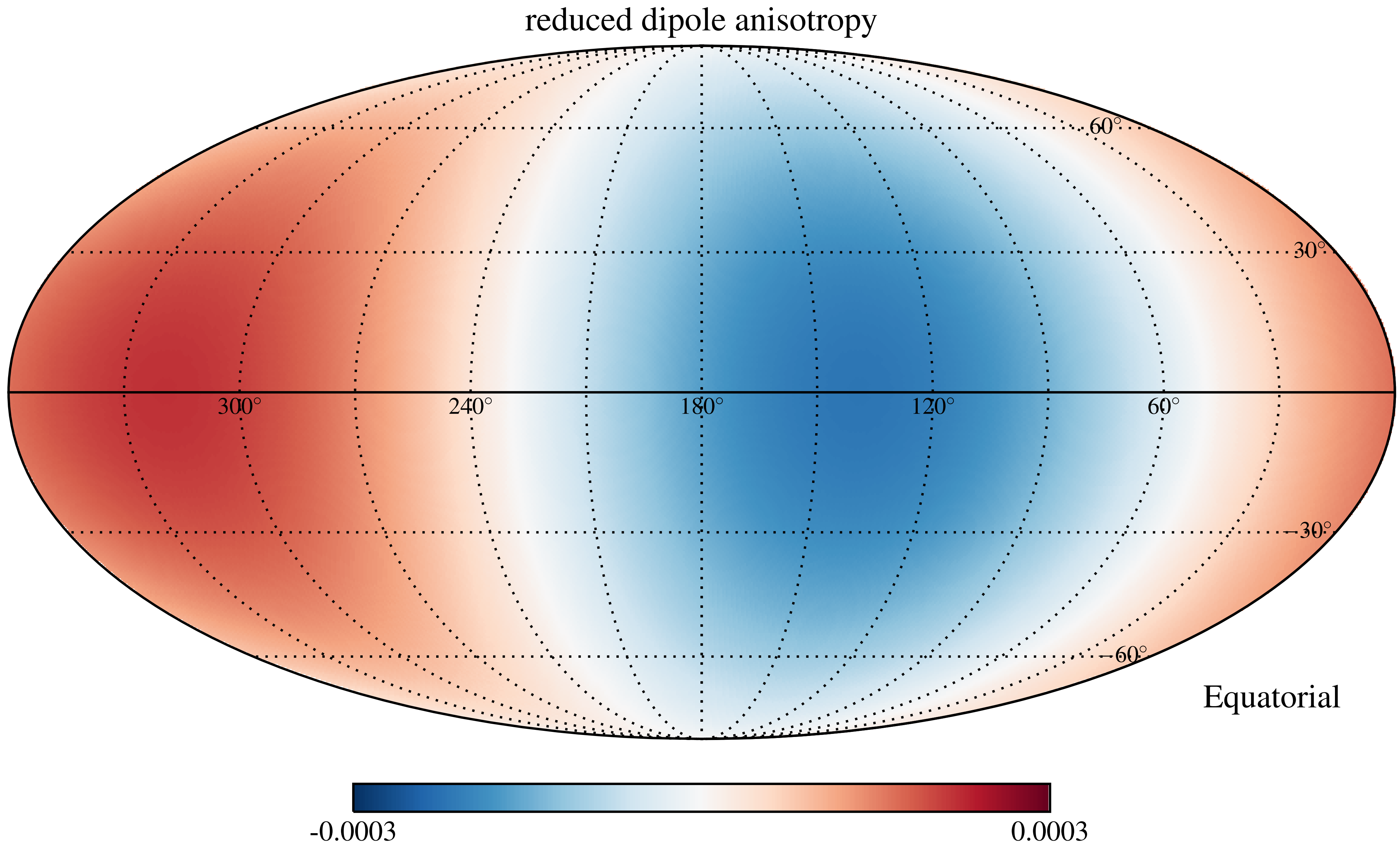

True CR dipole is defined by amplitude A and direction (α, δ).

Observable dipole is projected onto equatorial plane: $A' = A\cos\delta$

[Iuppa & Di Sciascio'13; MA *et al.*'15]

Dipole Anisotropy

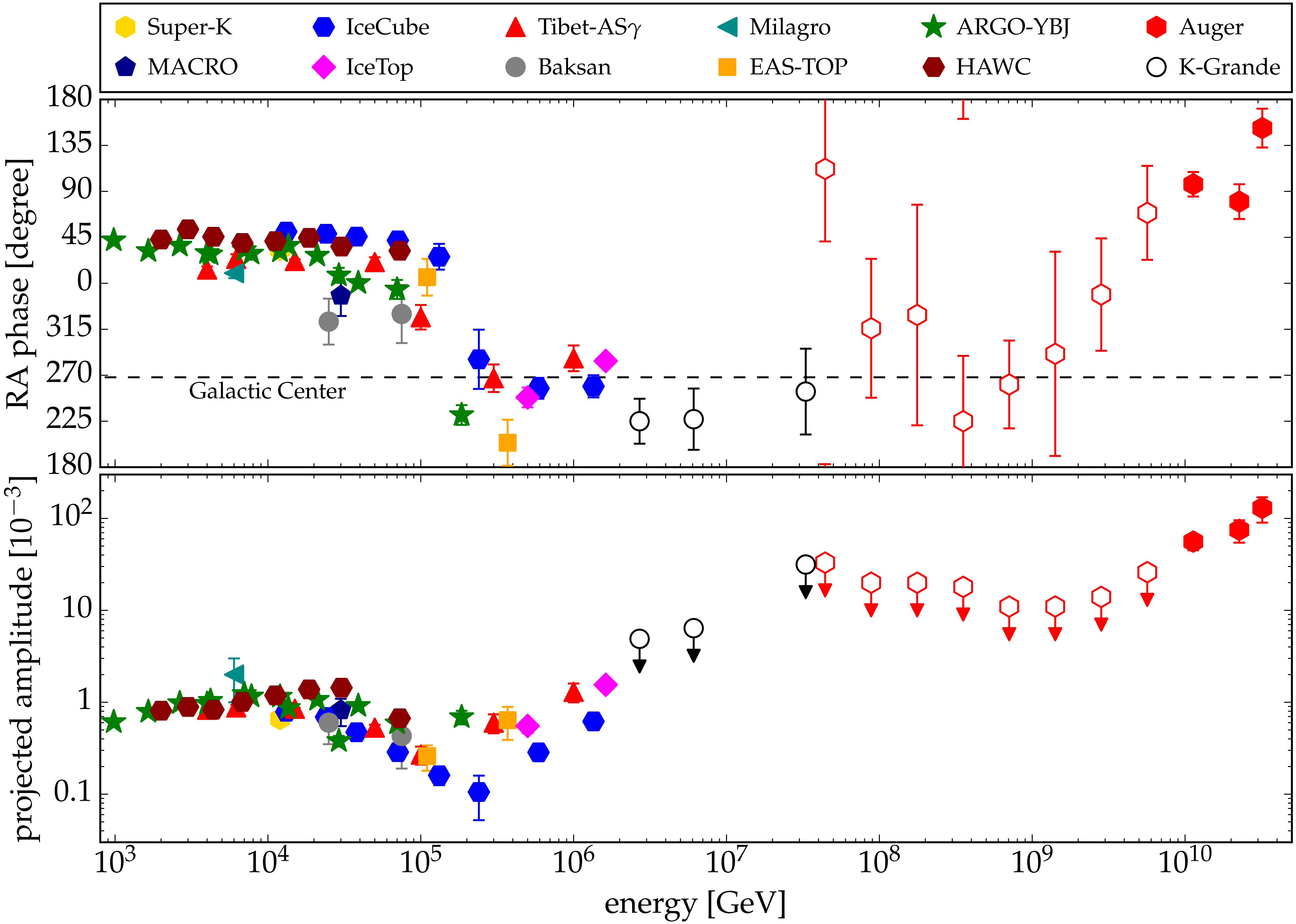

Reconstruction

- data has **strong time dependence**
  - detector deployment/maintenance
  - atmospheric conditions (day/night, seasons)
  - power outages, etc.
- **local anisotropy** of detector:
  - non-uniform geometry
- two analysis strategies:
  - **Monte-Carlo & monitoring** (limited by systematic uncertainties)
  - **data-driven likelihood methods** (limited by statistical uncertainties)

Example: Auger data > 8 EeV

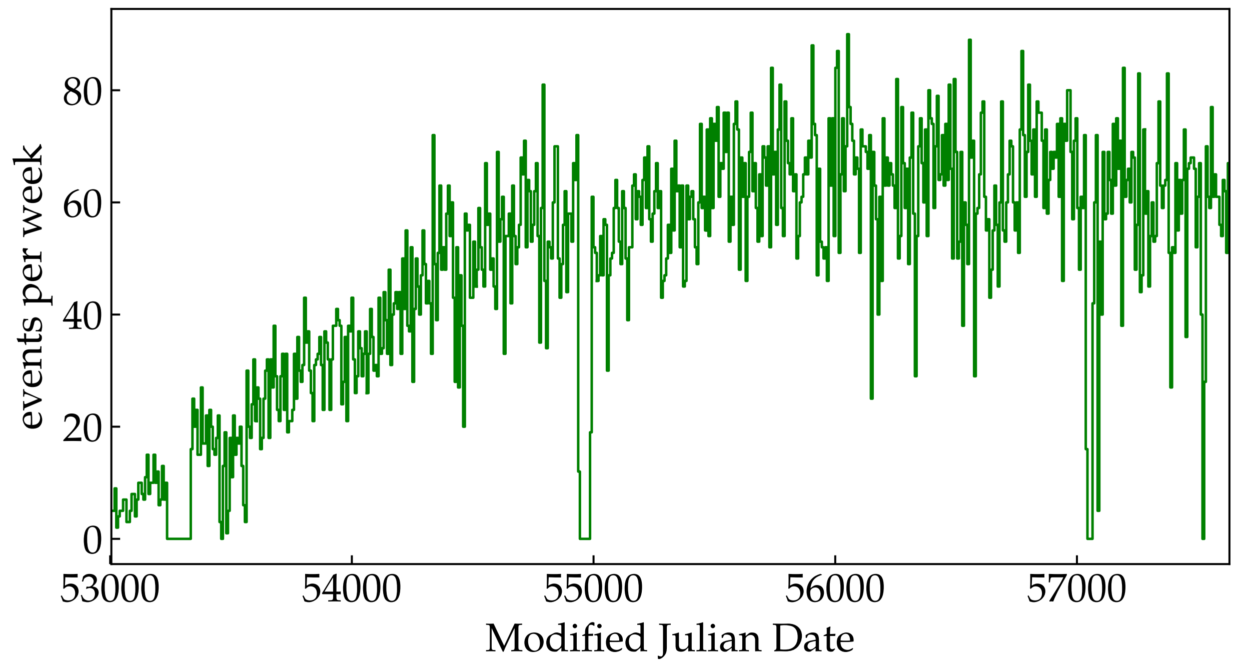

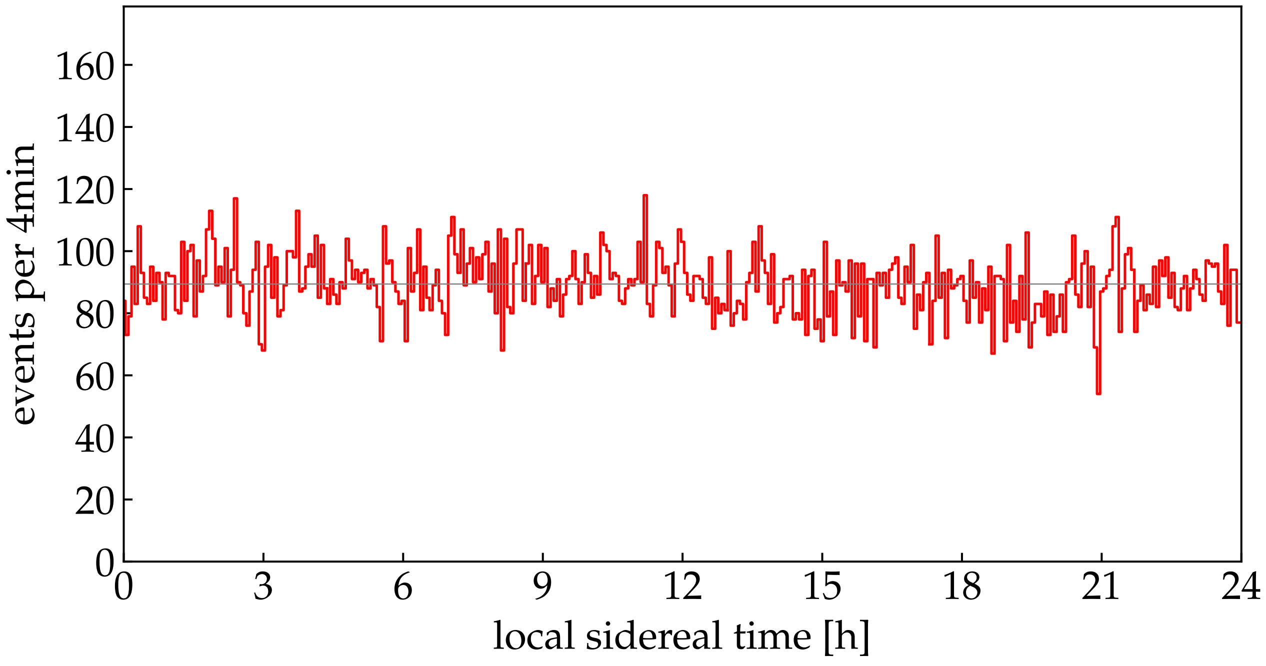

[Pierre Auger Observatory'17; MA'18]

East-West Method

- Strong time variation of CR background level can be compensated by differential methods. [e.g. Bonino *et al.*'11]
- **East-West asymmetry**:

$$A_{\rm EW}(t) \equiv \frac{N_{\rm E}(t) - N_{\rm W}(t)}{N_{\rm E}(t) + N_{\rm W}(t)} \simeq \underbrace{\Delta\alpha \frac{\partial}{\partial\alpha}\delta I(\alpha,0)}_{\text{assuming dipole!}} + \underbrace{\text{const}}_{\text{local asym.}}$$

- For instance, Auger data > 8EeV:

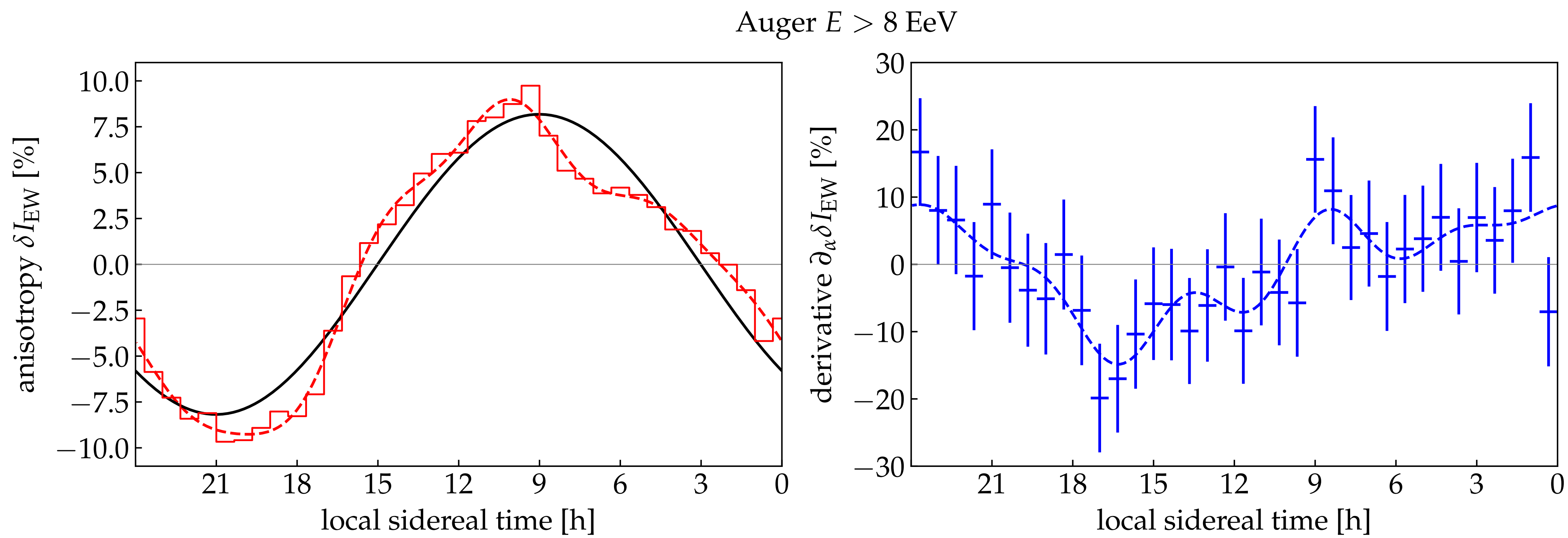

- best-fit dipole from EW method: (8.2 ± 1.4) % and $\alpha_d = 135^\circ \pm 10^\circ$

Likelihood Reconstruction

- East-West method introduces cross-talk between higher multipoles, regardless of the field of view.
- Alternatively, data can be analyzed to simultaneously reconstruct:
  - **relative acceptance** $\mathscr{A}(\varphi, \theta)$ (in local coordinates)
  - **relative intensity** $\mathscr{I}(\alpha, \delta)$ (in equatorial coordinates)
  - **background rate** $\mathscr{N}(t)$ (in sidereal time)
- expected number of CRs observed in sidereal time bin τ and local "pixel" i:

$$\mu_{\tau i} = \mu(\mathscr{I}_{\tau i}, \mathscr{N}_{\tau}, \mathscr{A}_{i})$$

- reconstruction **likelihood**:

[*MA et al.*'15]

$$\mathscr{L}(\mathbf{n}\,|\,\mathscr{I}, \mathscr{N}, \mathscr{A}) = \prod_{\tau i} \frac{(\mu_{\tau i})^{n_{\tau i}} e^{-\mu_{\tau i}}}{n_{\tau i}!}$$

- Maximum LH can be reconstructed by iterative methods.
- used in joint IceCube & HAWC analysis

[IceCube & HAWC '18]

Likelihood Reconstruction

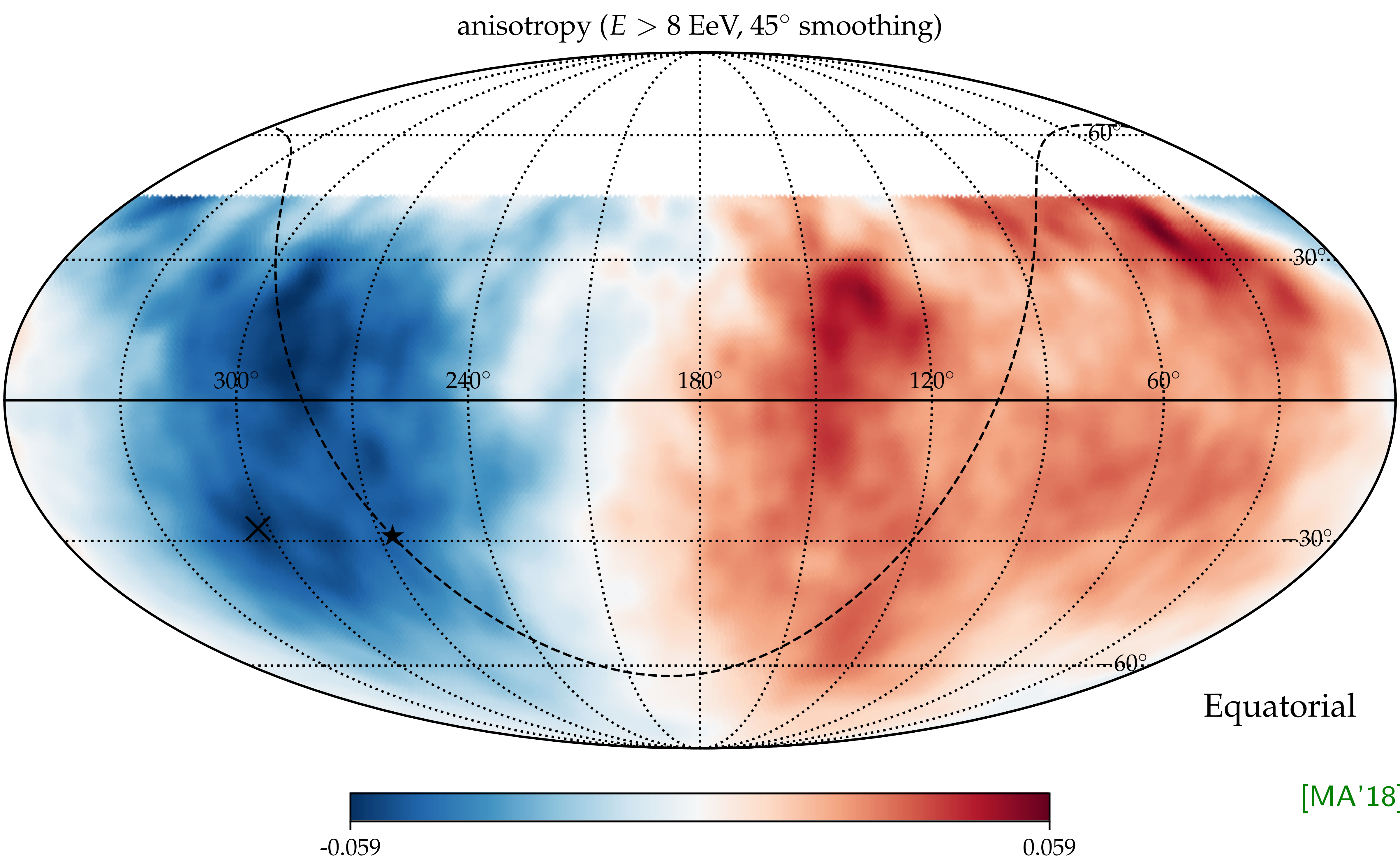

[MA'18]

Method can also be applied to high-energy data beyond the knee, *e.g.* Auger.

Likelihood Reconstruction

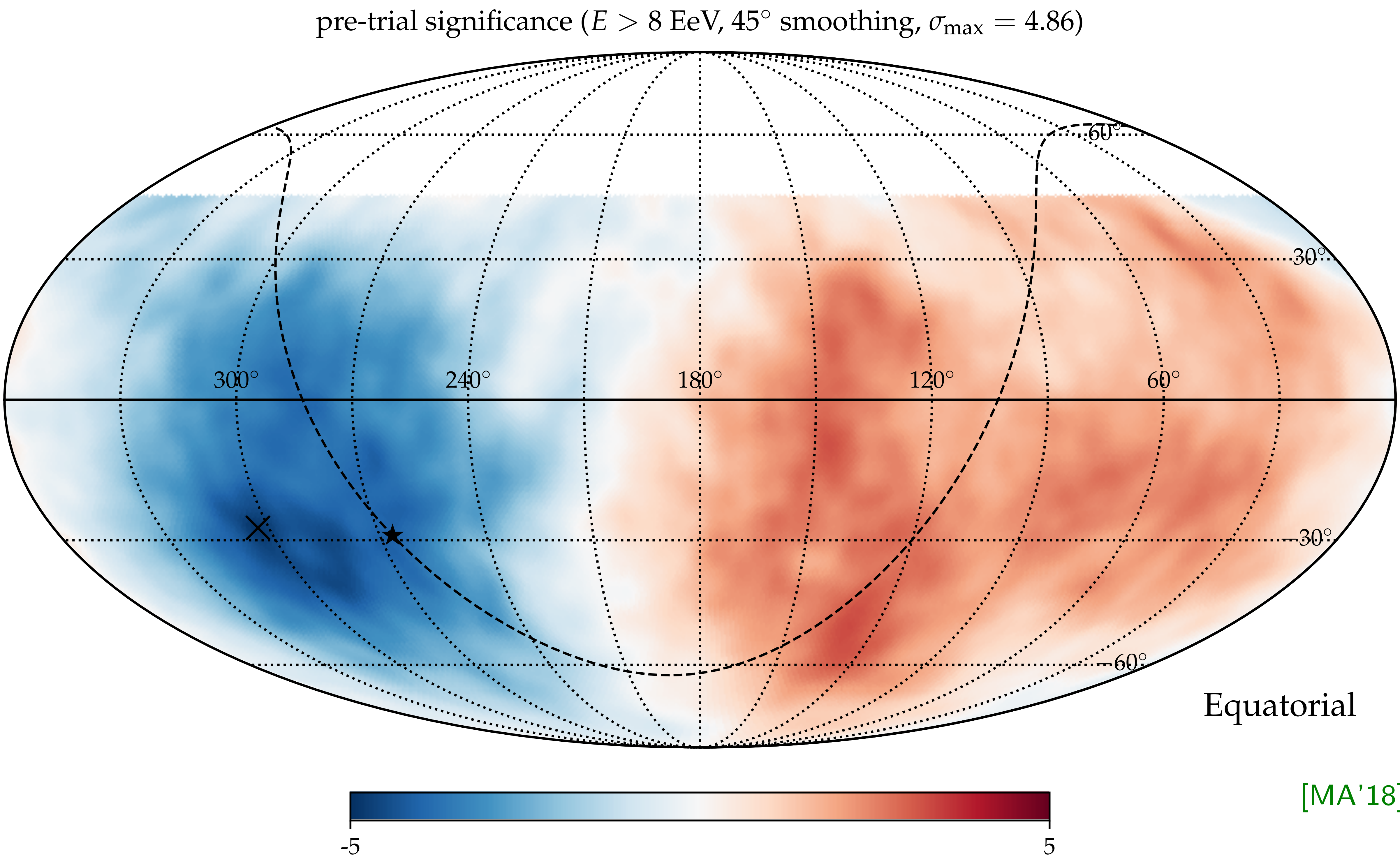

[MA'18]

Method can also be applied to high-energy data beyond the knee, *e.g.* Auger.

Take-Away on Reconstruction

Data-driven methods of anisotropy reconstructions used by ground-based observatories in the TV-PV range are **only sensitive to equatorial dipole** (or, more generally, to all $m \neq 0$ multipole moments).

$$\Delta\delta_\perp \sim \frac{1}{\sqrt{N_{\rm CR}}} \qquad \mathcal{N} \sim \frac{4\pi}{N_{\rm CR}}$$

Monte-Carlo-based methods of anisotropy reconstructions are sensitive to the full dipole, but are severely **limited by systematic uncertainties.**

Particles in Magnetic Fields

- **natural Heaviside-Lorentz units**:

$$\hbar = c = 1 \qquad \mu_0 = \epsilon_0 = 1$$

- For instance, Coulomb force:

$$\mathbf{F} = \frac{q_1 q_2}{4\pi r^2}\mathbf{e_r} = \alpha\frac{Z_1 Z_2}{r^2}\mathbf{e_r}$$

- Lorentz force:

$$\mathbf{F} = q\left(\mathbf{E} + \boldsymbol{\beta}\times\mathbf{B}\right)$$

- EoM in the absence of $\mathbf{E}$:

$$\dot{\mathbf{p}} = \mathbf{p}\times\boldsymbol{\Omega}$$

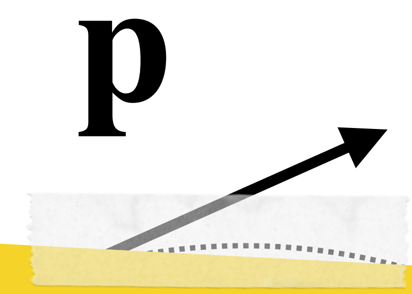

Larmor frequency: $$\boldsymbol{\Omega} \equiv \frac{q}{\gamma m}\mathbf{B}$$

rigidity: $$\mathscr{R} = \frac{|\mathbf{p}|}{q}$$

Larmor radius: $$r_L = \frac{\beta}{|\boldsymbol{\Omega}|} = \frac{\mathscr{R}}{|\mathbf{B}|}$$

$$r_L \simeq 1.1\mathrm{pc}\left(\frac{1\mu\mathrm{G}}{B}\right)\left(\frac{\mathscr{R}}{10^{15}\mathrm{V}}\right)$$

Particle Gyration

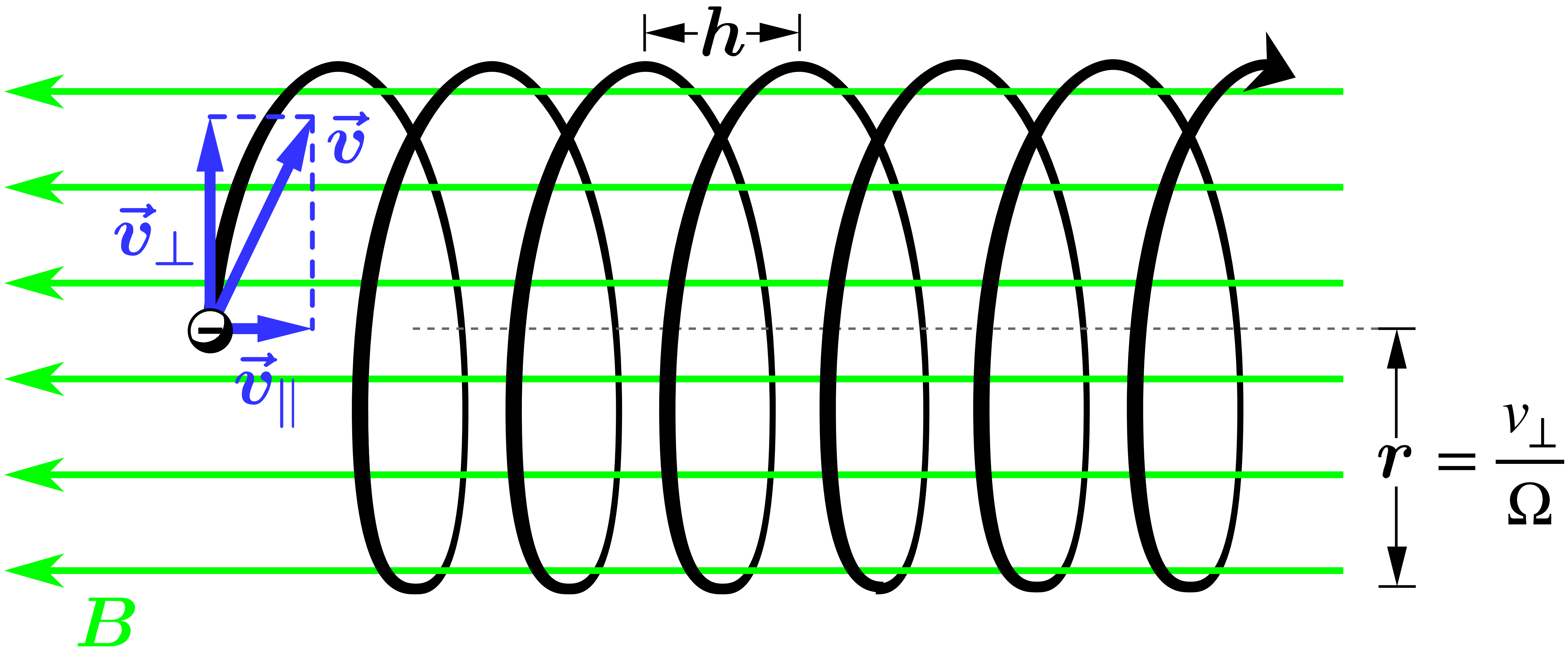

The **pitch angle** θ between $\mathbf{v}(t)$ and $\mathbf{B}_0$ remains constant in time.

The path is a superposition of circular motion in the plane perpendicular to $\mathbf{B}_0$ and linear motion along $\mathbf{B}_0$ with velocity:

$$v_\parallel = \cos\theta v \equiv \mu v.$$

Cosmic Ray Diffusion

- Galactic and extragalactic magnetic fields have a random component (no preferred direction).
- Effectively, after some **characteristic distance** λ, a CR will be scattered into a random direction.
- Cosmic ray propagation follows a random walk.
- After N encounters the CR will have travelled an **average distance**: $$d = \sqrt{N}\lambda$$

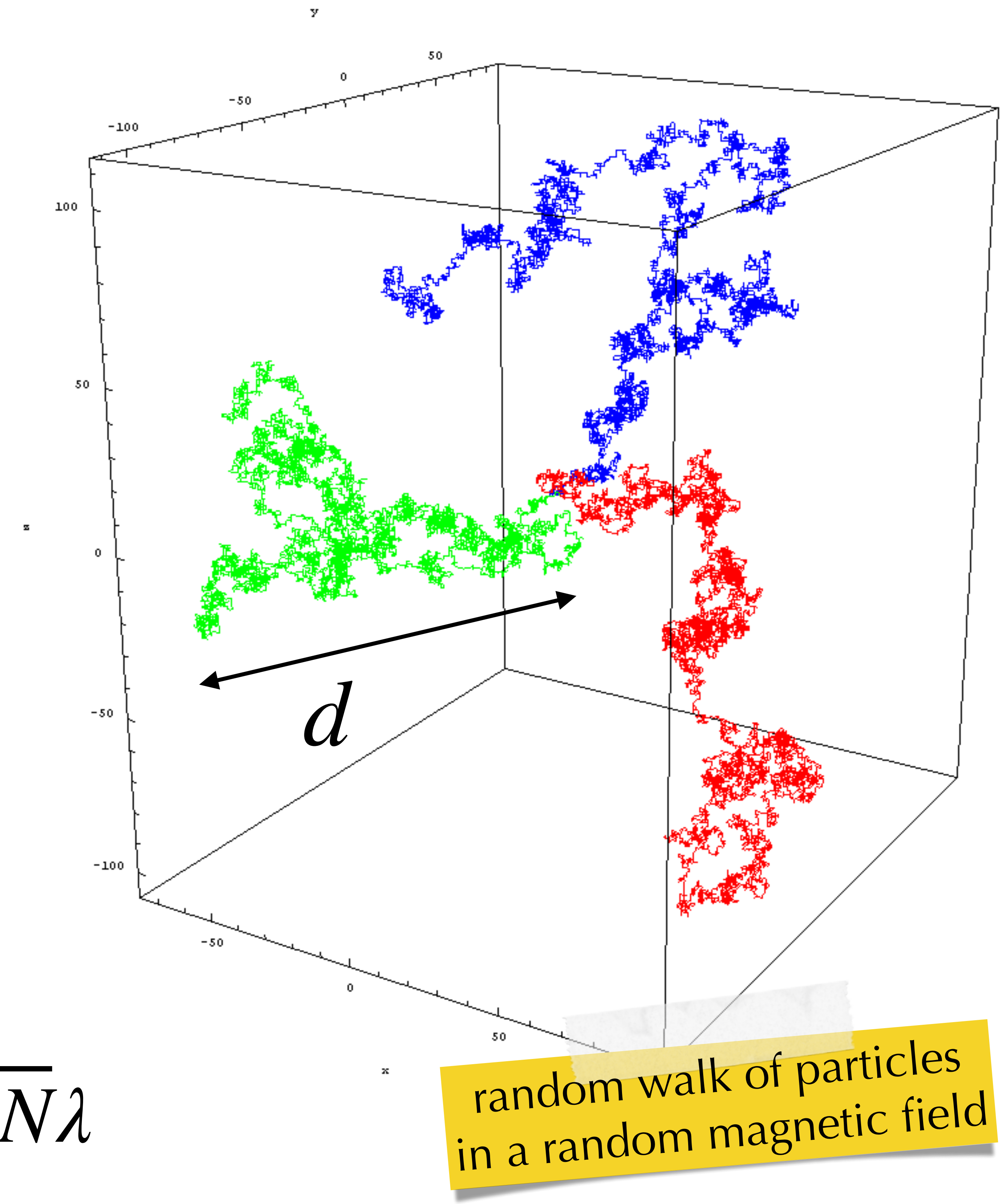

Magnetic Turbulence

- In the following, we consider relativistic particles in magnetic fields with vanishing electric fields ($\mathbf{E} = 0$) due to the high conductivity of astrophysical plasmas:

$$\mathbf{B}(\mathbf{r}) = \underbrace{B_0\mathbf{e}_z}_{\text{ordered}} + \underbrace{\delta\mathbf{B}(\mathbf{r})}_{\text{turbulent}}$$

- We also consider only **homogenous and isotropic turbulence.**

- Turbulence can be characterized by its **two-point correlation function**:

$$\langle \delta B_i(\mathbf{r})\delta B_j(\mathbf{r}')\rangle = C_{ij}(\mathbf{r} - \mathbf{r}')$$

- To characterize the turbulence we look into the Fourier modes:

$$\delta B_i(\mathbf{r}) = \int \mathrm{d}^3k\, \delta\tilde{B}_i(\mathbf{k})e^{i\mathbf{k}\mathbf{r}}$$

Magnetic Turbulence

- Real valued fields obeying $\nabla \delta \mathbf{B} = 0$ require:

$$\delta \tilde{B}_j^*(\mathbf{k}) = \delta \tilde{B}_j(-\mathbf{k}) \qquad \& \qquad \mathbf{k}\delta\tilde{\mathbf{B}}(\mathbf{k}) = 0$$

- The two-point correlation function can be expressed in Fourier space:

$$\langle \delta \tilde{B}_i(\mathbf{k}) \delta \tilde{B}_i^*(\mathbf{k}') \rangle = \delta(\mathbf{k} - \mathbf{k}') \left(\delta_{ij} - \frac{k_i k_j}{k^2} \right) \frac{\mathscr{P}(k)}{4\pi k^2}$$

- The **power spectrum** $\mathscr{P}(k)$ is normalized to the energy density of the turbulence:

$$U_{\delta B} = \frac{1}{2} \langle \delta \mathbf{B}^2 \rangle = \int \mathrm{d}k \mathscr{P}(k)$$

- For instance, in **Kolmogorov turbulence**:

$$\mathscr{P}(k) \propto k^{-5/3} \quad (k_{\min} < k < k_{\max})$$

Phase-Space Density

- We will work in the following with the CR **phase-space density** (PSD):

$$f(t, \mathbf{r}, \mathbf{p}) \equiv \frac{\mathrm{d}N}{\mathrm{d}^3 r\, \mathrm{d}^3 p}$$

- for cosmic rays moving into solid angle Ω with momentum $p = \gamma\beta m$:

$$\mathrm{d}^3 r \times \mathrm{d}^3 p \to \beta\, \mathrm{d}t\, \mathrm{d}A_\perp \times \mathrm{d}\Omega\, p^2 \mathrm{d}p$$

- cosmic ray **intensity** ("spectral flux"):

$$F(t, \mathbf{r}, E, \Omega) \equiv \frac{\mathrm{d}N}{\mathrm{d}t\, \mathrm{d}A_\perp\, \mathrm{d}\Omega\, \mathrm{d}E} = \beta p^2 \frac{\mathrm{d}p}{\mathrm{d}E} f(t, \mathbf{r}, \mathbf{p}) = p^2 f(t, \mathbf{r}, \mathbf{p})$$

- cosmic ray **spectral density**:

$$n(t, \mathbf{r}, E) \equiv \frac{\mathrm{d}N}{\mathrm{d}^3 r\, \mathrm{d}E} = \frac{1}{\beta} \int \mathrm{d}\Omega F(t, \mathbf{r}, E, \Omega) = \frac{4\pi}{\beta} p^2 \langle f(t, \mathbf{r}, \mathbf{p}) \rangle_{4\pi}$$

Liouville's Theorem

- Let's assume that CRs propagate in static magnetic fields without dissipation or sources.

- Number of CRs per PS volume is constant: $\dot{f}(t, \mathbf{r}, \mathbf{p}) = 0$

- Equivalent to **Liouville's equation**: $\partial_t f + \dot{\mathbf{r}}\nabla_{\mathbf{r}} f + \dot{\mathbf{p}}\nabla_{\mathbf{p}} f = 0$

- **Lorentz force** in magnetic field:

$$\dot{\mathbf{p}} = \mathbf{p} \times \left(\boldsymbol{\Omega} + \boldsymbol{\omega}\right) \quad \text{with} \quad \underbrace{\boldsymbol{\Omega} \equiv e\mathbf{B}/p_0}_{\text{background field}} \quad \text{and} \quad \underbrace{\boldsymbol{\omega} \equiv e\delta\mathbf{B}/p_0}_{\text{turbulence}}$$

- **Vlasov equation**: $\partial_t f + \boldsymbol{\beta}\nabla_{\mathbf{r}} f + \left[\mathbf{p} \times (\boldsymbol{\Omega} + \boldsymbol{\omega})\right]\nabla_{\mathbf{p}} f = 0$

Vlasov Equation

- We can express the Vlasov equation in the form ($\mathbf{L} \equiv i\mathbf{p} \times \nabla_{\mathbf{p}}$):

$$\partial_t f + \boldsymbol{\beta} \nabla_{\mathbf{r}} f - i \left[\boldsymbol{\Omega} + \boldsymbol{\omega}\right] \mathbf{L} f = 0 \qquad \text{(A)}$$

- We now look at the **ensemble-average PSD**: $\langle f \rangle$

- Expanding $f = \langle f \rangle + \delta f$ and averaging (A) over magnetic ensemble:

$$\partial_t \langle f \rangle + \boldsymbol{\beta} \nabla_{\mathbf{r}} \langle f \rangle - i\boldsymbol{\Omega}\mathbf{L} \langle f \rangle = \underbrace{i\langle \boldsymbol{\omega}\mathbf{L}\,\delta f \rangle}_{\text{collision term}} \equiv \left(\frac{\partial f}{\partial t}\right)_{\mathrm{c}} \qquad \text{(B)}$$

- The evolution of δf follows from the difference **(A)** - **(B)**:

$$\partial_t \delta f + \boldsymbol{\beta} \nabla_{\mathbf{r}} \delta f - i\boldsymbol{\Omega}\mathbf{L}\,\delta f = i\boldsymbol{\omega}\mathbf{L} \langle f \rangle - \underbrace{\left[i\langle \boldsymbol{\omega}\mathbf{L}\,\delta f \rangle - i\boldsymbol{\omega}\mathbf{L}\,\delta f\right]}_{\simeq 0}$$

Collision Term

- We can solve along **unperturbed particle paths** $\mathscr{P}_0$:

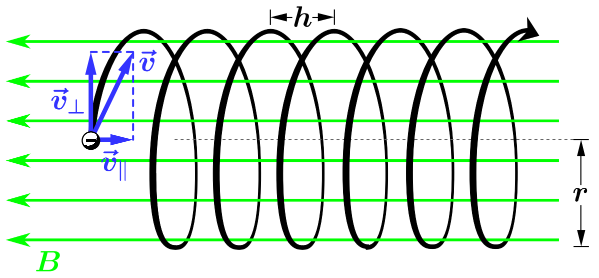

$$\delta f(t, \mathbf{r}_0(t), \mathbf{p}_0'(t)) \simeq -\int_{-\infty}^{t} \mathrm{d}t' \left[i\boldsymbol{\omega}\mathbf{L}\,\langle f \rangle \right]_{\mathscr{P}_0(t')}$$

- This allows to derive a formal solution to the collision term:

$$\left(\frac{\partial f}{\partial t}\right)_{\mathrm{c}} \simeq \left\langle \boldsymbol{\omega}\mathbf{L} \int_{-\infty}^{t} \mathrm{d}t' \left[\boldsymbol{\omega}\mathbf{L}\,\langle f \rangle \right]_{\mathscr{P}(t')} \right\rangle$$

- The collision term on the R.H.S. depends on the form of the magnetic turbulence and can, in general, not be solved analytically.

- In **BGK approximation** we can simplify it as: [Bhatnagar, Gross & Krook'54]

$$\left(\frac{\partial f}{\partial t}\right)_{\mathrm{c}} \to -\nu \left[\langle f \rangle - \frac{1}{4\pi} \int \mathrm{d}\Omega \langle f \rangle \right]$$

Diffusion Approximation

- We will work with the **BGK approximation** in the following.
- Consider the **monopole** and **dipole** contribution of the ensemble averaged PSD:

$$\phi(t,\mathbf{r},p) = \frac{1}{4\pi}\int \mathrm{d}\Omega\langle f(t,\mathbf{r},\mathbf{p}(\Omega))\rangle \quad \& \quad \mathbf{\Phi}(t,\mathbf{r},p) = \frac{1}{4\pi}\int \mathrm{d}\Omega\hat{\mathbf{p}}(\Omega)\langle f(t,\mathbf{r},\mathbf{p}(\Omega))\rangle$$

- Ignoring higher harmonics we can re-write the Vlasov equation as:

$$\partial_t\phi + \beta\nabla\mathbf{\Phi} = 0 \qquad \& \qquad \partial_t\mathbf{\Phi} + \frac{\beta}{3}\nabla\phi + \mathbf{\Omega}\times\mathbf{\Phi} = -\,\nu\,\mathbf{\Phi}$$

- Assuming that $\partial_t|\mathbf{\Phi}| \ll \partial_t\phi$ we arrive at the **diffusion equation**:

$$\partial_t\phi - \partial_i\left(K_{ij}\partial_j\phi\right) = 0 \qquad \mathbf{K} = \frac{\beta^2}{3}\begin{pmatrix} \nu_\perp^{-1} & \nu_A^{-1} & 0 \\ -\nu_A^{-1} & \nu_\perp^{-1} & 0 \\ 0 & 0 & \nu_\parallel^{-1} \end{pmatrix} \qquad \begin{aligned} \nu_\parallel &= \nu \\ \nu_\perp &= \nu + \Omega^2/\nu \\ \nu_A &= \Omega + \nu^2/\Omega \end{aligned}$$

Particle Gyration

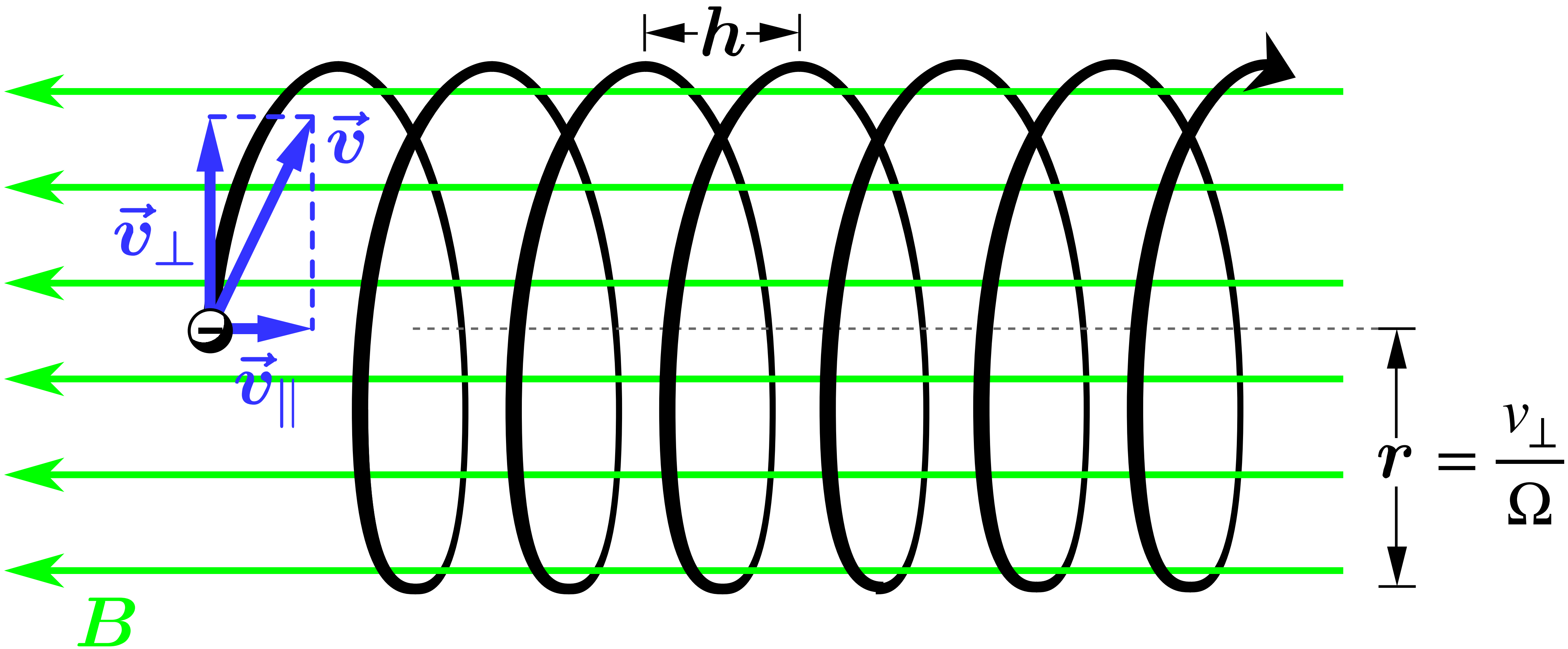

The **pitch angle** θ between $\mathbf{v}(t)$ and $\mathbf{B}_0$ remains constant in time.

The path is a superposition of circular motion in the plane perpendicular to $\mathbf{B}_0$ and linear motion along $\mathbf{B}_0$ with velocity:

$$v_\parallel = \cos\theta v \equiv \mu v.$$

Particle Gyration

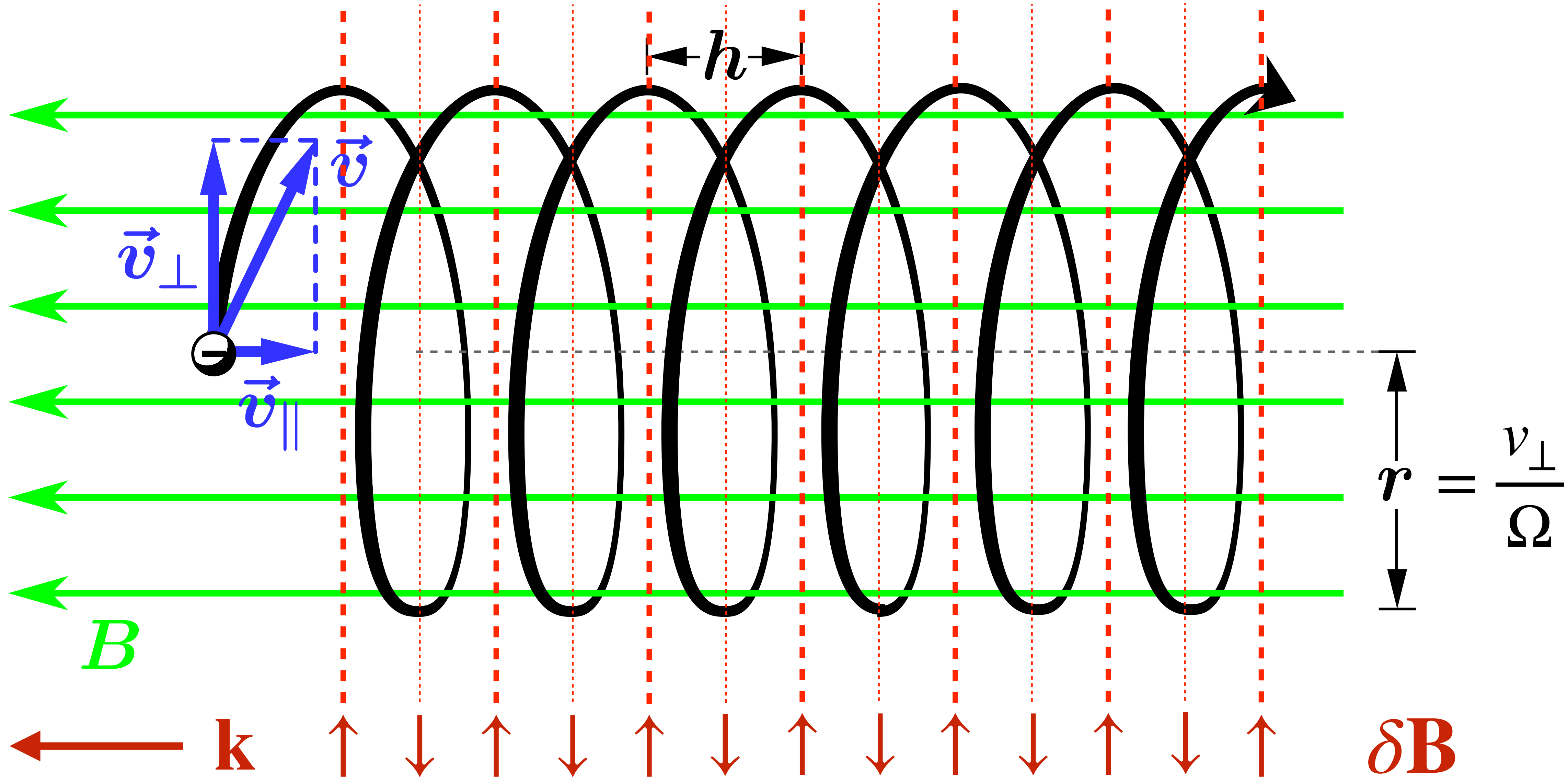

Consider now a **magnetic perturbation** in form of a plane wave:

$$\delta\mathbf{B} = \delta B\mathbf{e}_x \cos(kz + \alpha)$$

Particle Gyration

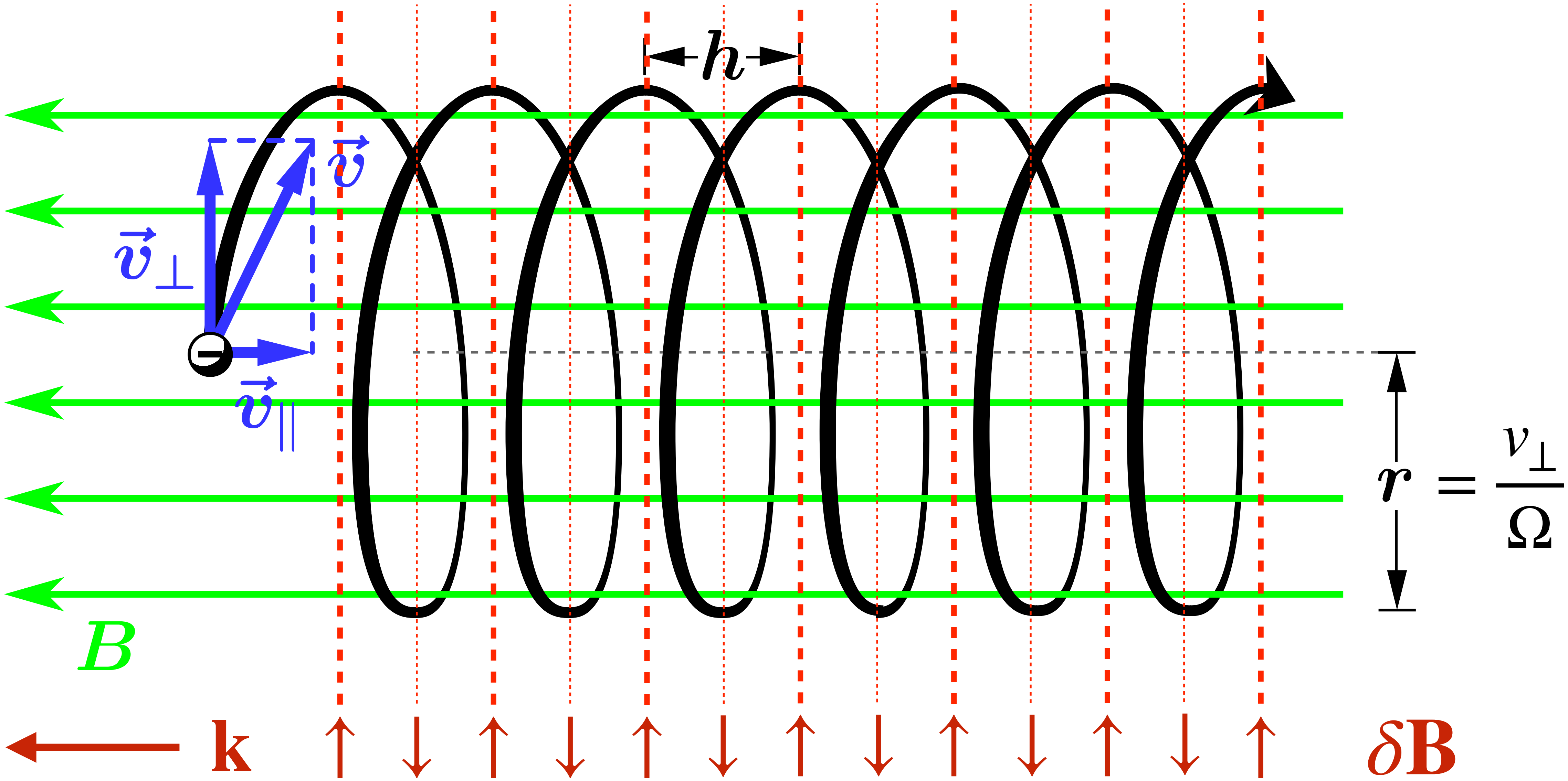

The time-averaged Lorentz force $\delta\mathbf{F}_L = q\boldsymbol{\beta} \times \delta\mathbf{B}$ along the path has the strongest contribution at the **resonance**:

$$kv_\parallel = \pm\,\Omega$$

Resonant Scattering

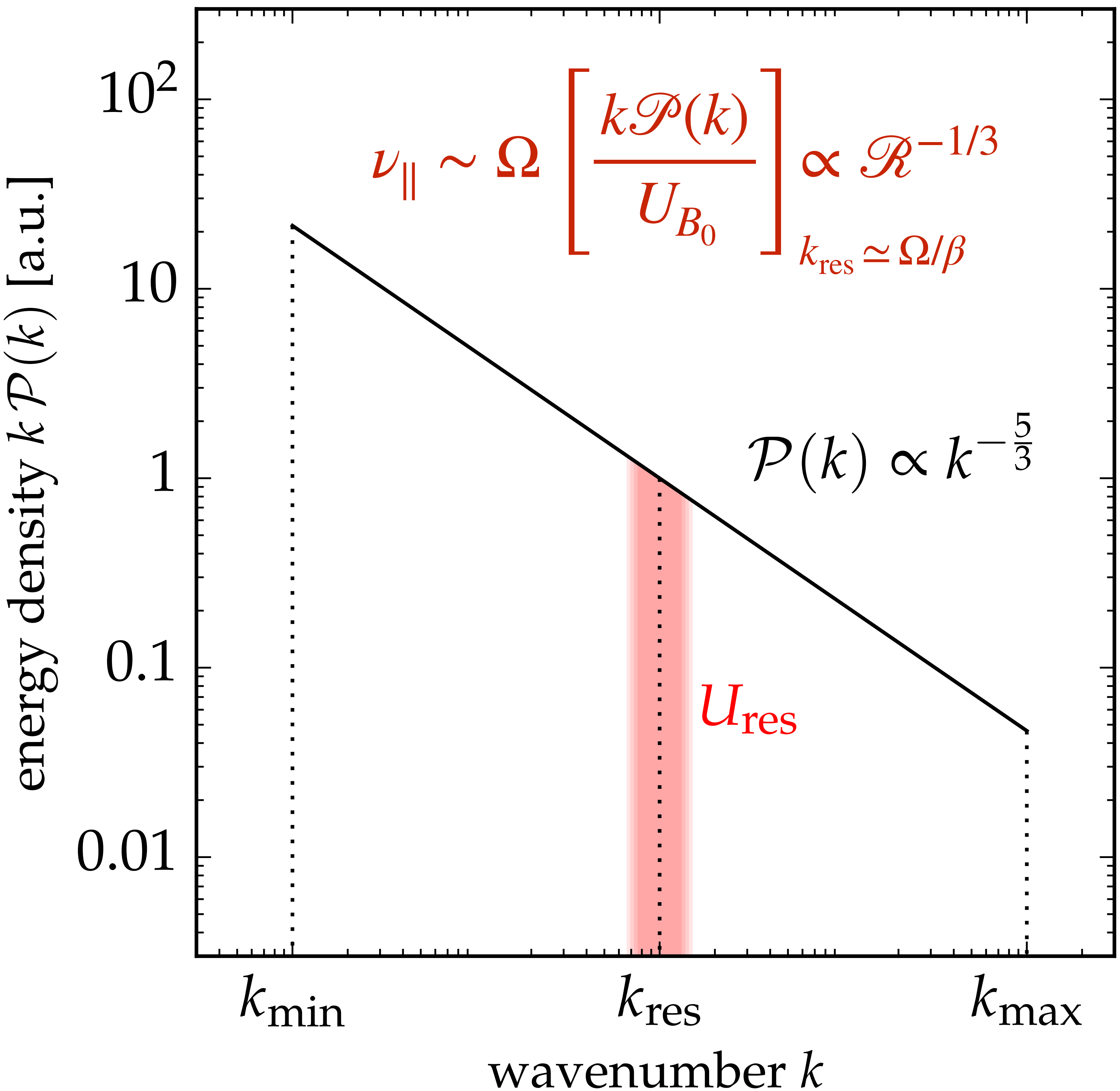

Boron-to-Carbon Ratio

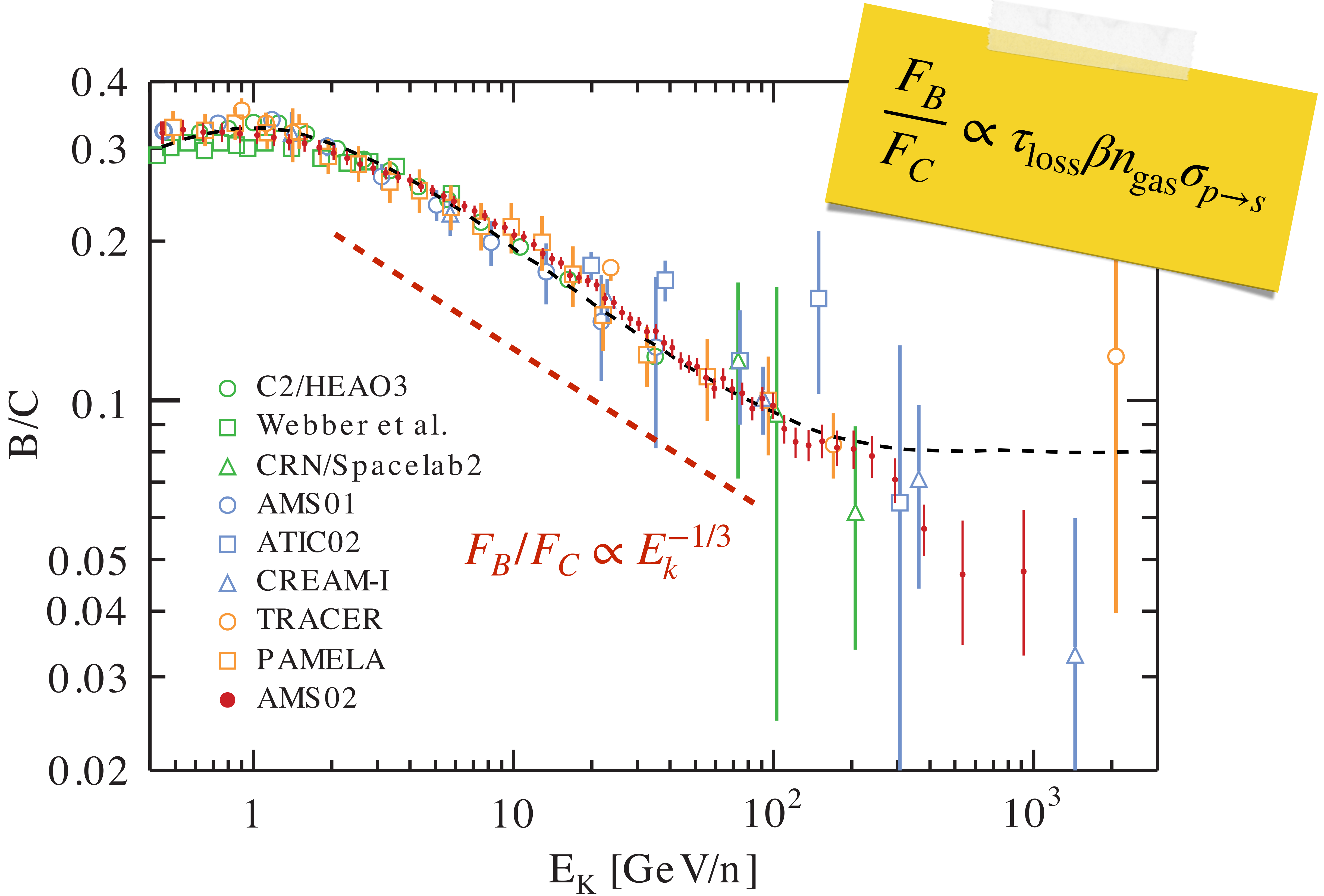

Compton-Getting Effect

- PSD is Lorentz-invariant:

$$f(t, \mathbf{r}, \mathbf{p}) = f^\star(t, \mathbf{r}^\star, \mathbf{p}^\star)$$

- relative motion of observer ($\boldsymbol{\beta} = \mathbf{v}/c$) in plasma rest frame:

$$\mathbf{p}^\star = \mathbf{p} + p\boldsymbol{\beta} + \mathcal{O}(\beta^2)$$

- Taylor expansion:

$$f(\mathbf{p}) \simeq f^\star(\mathbf{p}) + p\boldsymbol{\beta}\nabla_{\mathbf{p}} f^\star(\mathbf{p}) + \mathcal{O}(\beta^2)$$

- dipole term $\boldsymbol{\Phi}$ is not invariant:

$$\phi = \phi^\star \qquad \boldsymbol{\Phi} = \boldsymbol{\Phi}^\star + \frac{1}{3}\boldsymbol{\beta}\frac{\partial \phi^\star}{\partial \ln p} = \boldsymbol{\Phi}^\star + \underbrace{(2+\Gamma)\boldsymbol{\beta}}_{\text{Compton}-\text{Getting effect}}$$

- *What is the plasma rest-frame?* LSR or ISM : $v \simeq 20\,\mathrm{km/s}$

Summary : Dipole Anisotropy

- Spherical harmonics expansion of **relative intensity**:

$$I(\Omega) = 1 + \boldsymbol{\delta}\cdot n(\Omega) + \sum_{\ell\geq 2}\sum_{m=-\ell}^{m} a_{\ell m}Y_{\ell m}(\Omega)$$

- **cosmic ray density** $n_{\rm CR} \propto E^{-\Gamma}$ and **dipole vector** $\boldsymbol{\delta}$ from diffusion theory:

$$\underbrace{\partial_t n_{\rm CR} \simeq \nabla(\mathbf{K}\nabla n_{\rm CR}) + Q_{\rm CR}}_{\text{diffusion equation}} \qquad \underbrace{\boldsymbol{\delta} \simeq 3\mathbf{K}\nabla n_{\rm CR}/n_{\rm CR}}_{\text{Fick's law}}$$

- **diffusion tensor K** in general anisotropic along background field **B**:

$$K_{ij} = \kappa_{\parallel}\hat{B}_i\hat{B}_j + \kappa_{\perp}(\delta_{ij} - \hat{B}_i\hat{B}_j) + \kappa_A\epsilon_{ijk}\hat{B}_k$$

- relative motion of the observer in the plasma rest frame (★):

[Compton & Getting '35]

$$\boldsymbol{\delta} \simeq \boldsymbol{\delta}^\star + (2+\Gamma)\boldsymbol{\beta}$$

TeV-PeV Dipole Anisotropy

- **CG-corrected** dipole:

$$\boldsymbol{\delta}^\star \simeq \boldsymbol{\delta} - (2+\Gamma)\boldsymbol{\beta} = 3\mathbf{K}\nabla n_{\rm CR}/n_{\rm CR}$$

- **projection** onto equatorial plane:

$$\boldsymbol{\delta}^\star \to (\delta^\star_{0h}, \delta^\star_{6h}, 0)$$

- **projection** along strong regular magnetic fields:

[Mertsch & Funk'14; Schwadron *et al.*'14]

$$K_{ij} \simeq \kappa_\parallel \hat{B}_i \hat{B}_j$$

- TeV-PeV dipole data consistent with magnetic field direction inferred from IBEX data.

[McComas *et al.*'09]

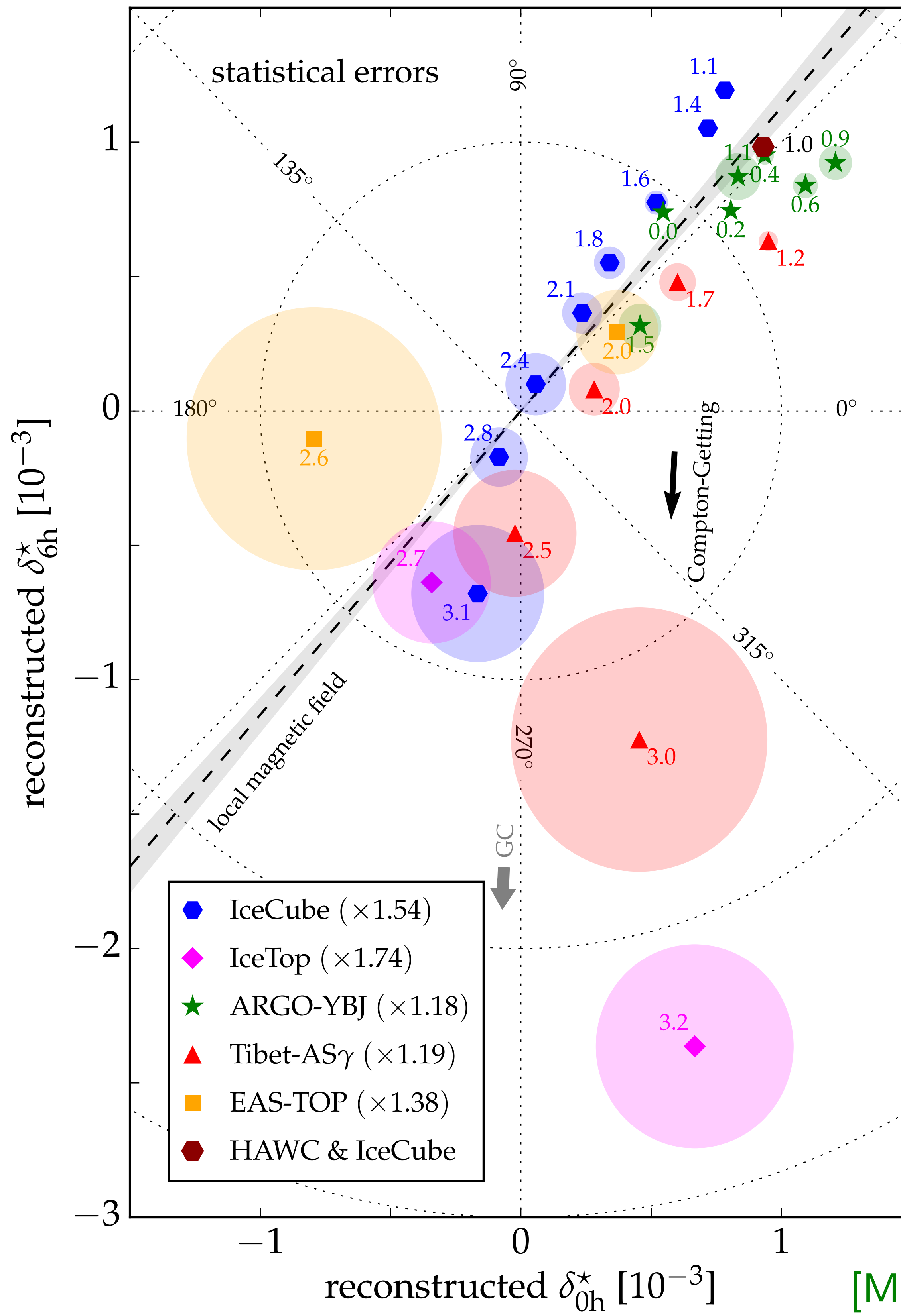

[MA'17]

Local Magnetic Field

- **IBEX ribbon**: enhanced emission of energetic neutral atoms (ENAs) observed with the **I**nterstellar **B**oundary **EX**plorer [McComas *et al.*'09]
- interpreted as local magnetic field ($\lesssim 0.1\,\mathrm{pc}$) draping the heliophere
- ribbon center defines field orientation (Galactic coordinates): [Funsten *et al.*'13]

$$l \simeq 210.5^\circ \quad \& \quad b \simeq -57.1^\circ$$

- consistent with field inferred from polarization of starlight by interstellar dust ($\lesssim 40\,\mathrm{pc}$): [Frisch *et al.*'15]

$$l \simeq 216.2^\circ \quad \& \quad b \simeq -49.0^\circ$$

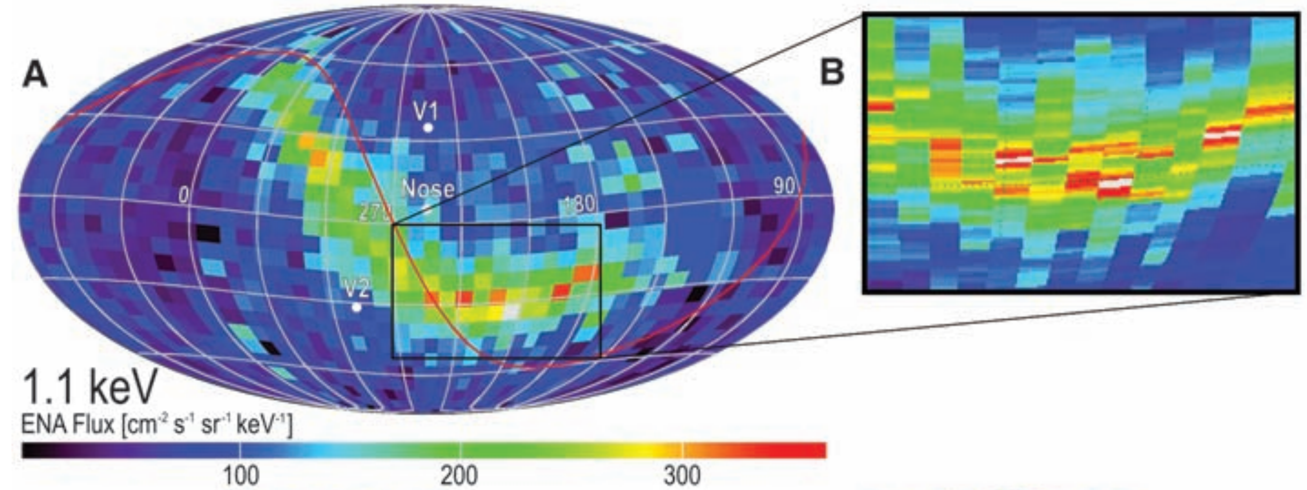

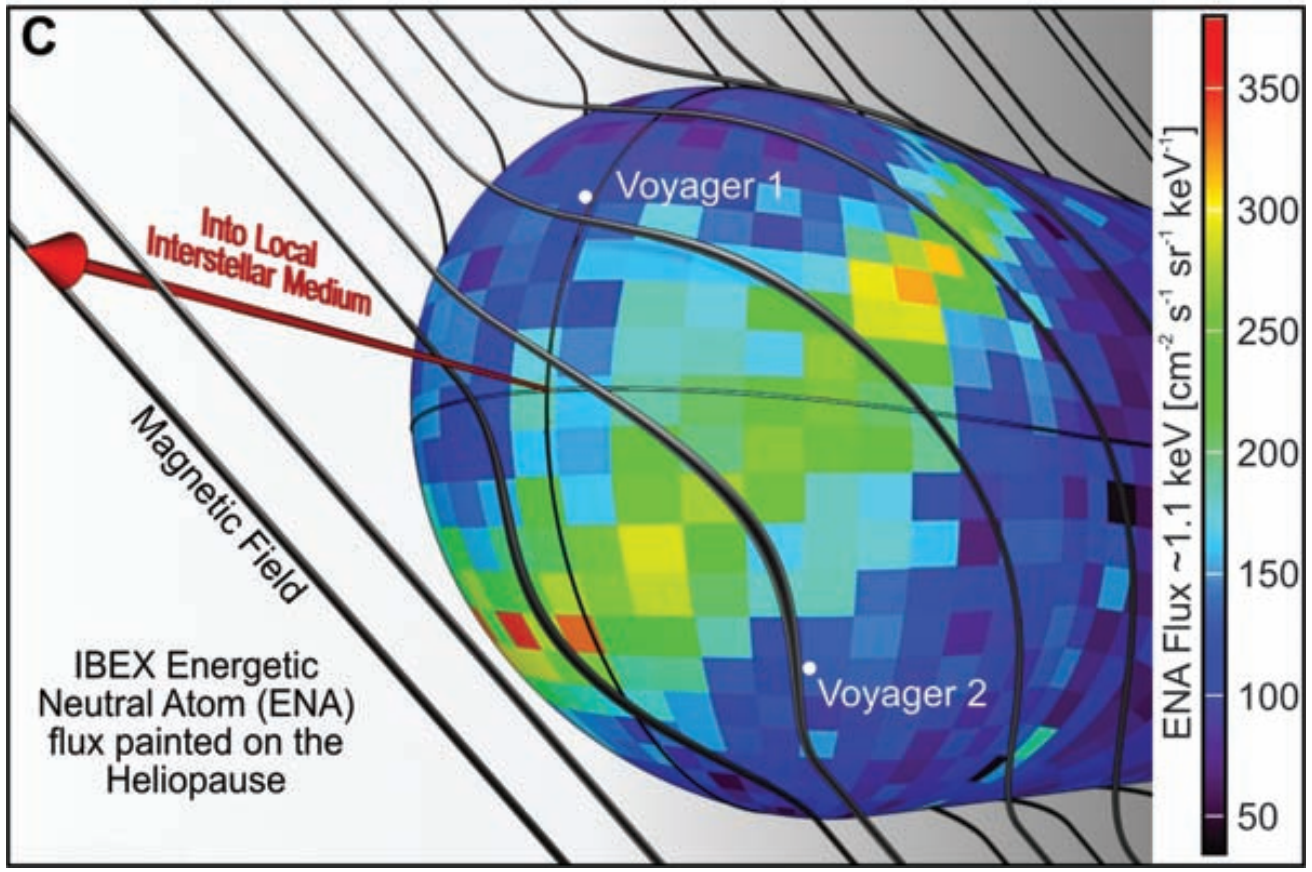

[McComas *et al.*'09]

Known Local SNRs

- projection along magnetic field leaves two possible dipole directions:

$$\boldsymbol{\delta} \propto \pm \hat{\mathbf{B}}_0$$

- **Intersection of magnetic equator with Galactic Plane** defines two regions where CR sources contribute to the dipole with opposite phases:

- $$120^\circ \leq l \leq 300^\circ \rightarrow \alpha_1 \simeq 49^\circ$$

$$-60^\circ \leq l \leq 120^\circ \rightarrow \alpha_1 \simeq 229^\circ$$

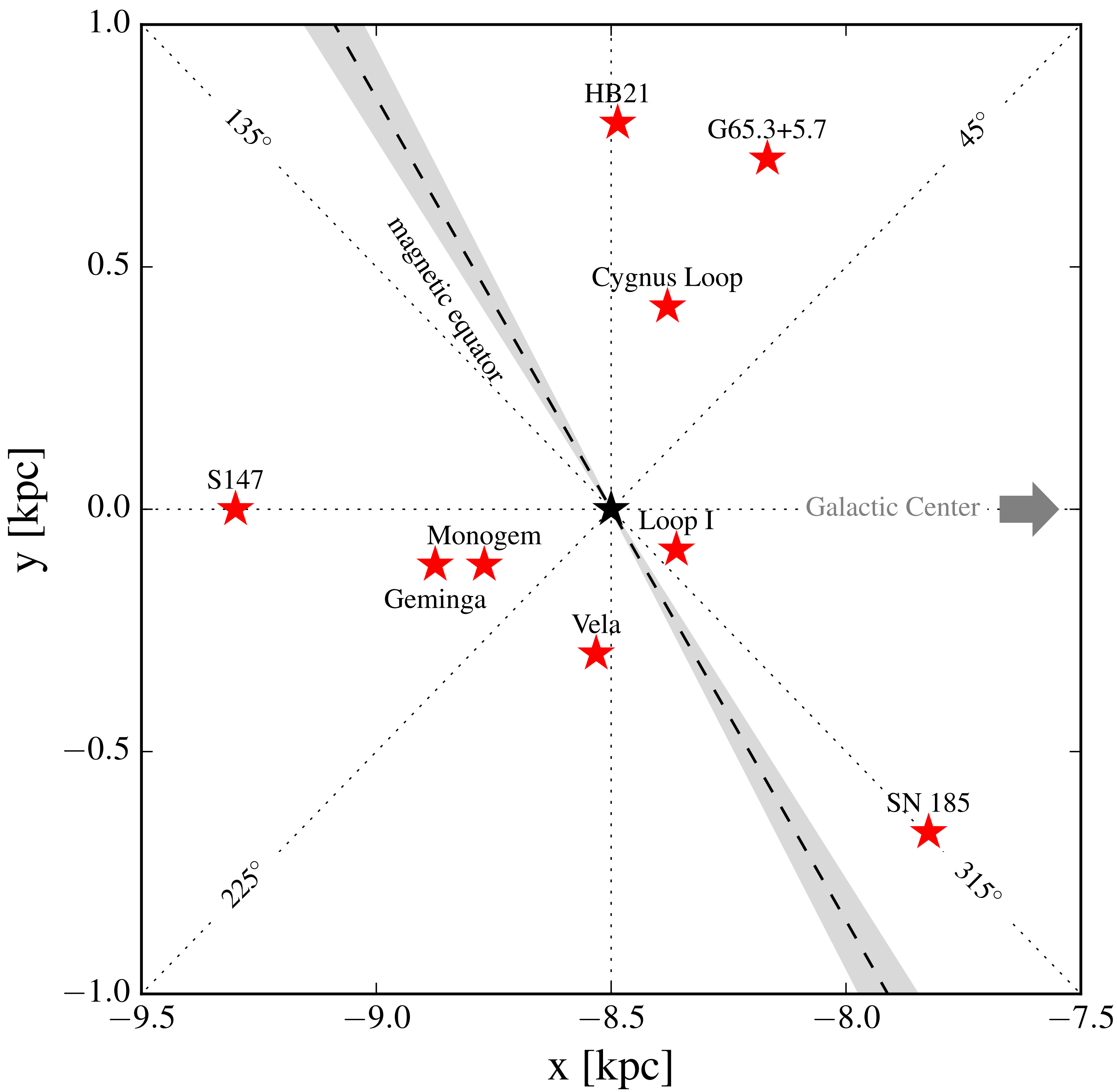

Phase-Flip by Vela SNR?

- Observed 1-100 TeV phase indicates **dominance of a local source** with:

$$120^\circ \leq l \leq 300^\circ$$

- **plausible scenario: Vela SNR**
  - age: $\simeq 11{,}000\,\mathrm{yrs}$
  - distance: $\simeq 1{,}000\,\mathrm{lyrs}$
  - SNR rate: $\simeq 1/30\,\mathrm{yr}^{-1}$
  - (effective) isotropic diffusion:

$$K_{\rm iso} \simeq 3\times 10^{28} E_{\rm GeV}^{1/3}\mathrm{cm}^2/\mathrm{s}$$

  - Galactic halo width: $\simeq 3\,\mathrm{kpc}$
  - instantaneous CR emission $Q_\star$

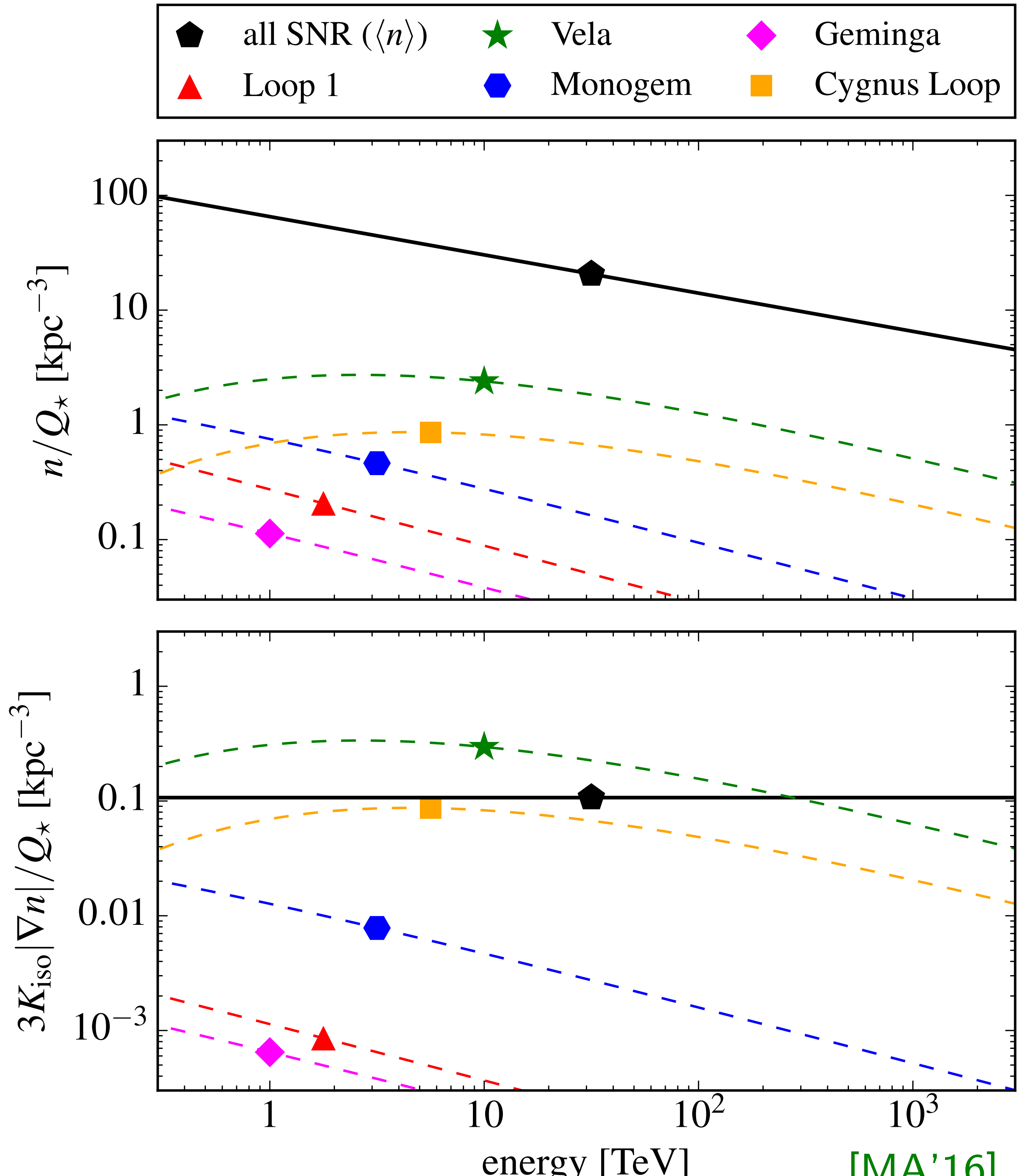

[MA'16]

Position of SNR

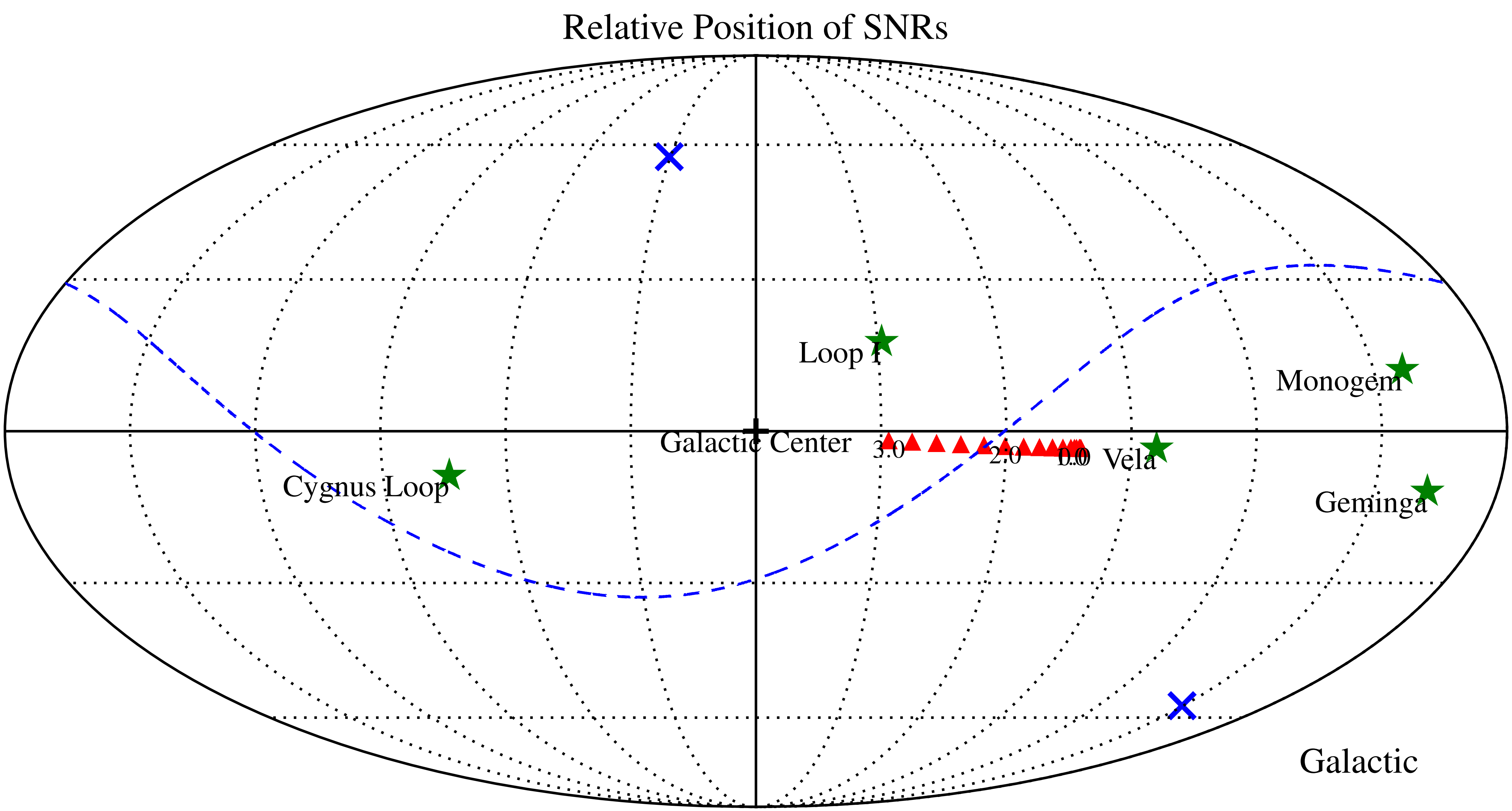

Relative position of the five closest SNRs. The magnetic field direction (IBEX) is indicated by × and the **magnetic equator** by a dashed line.

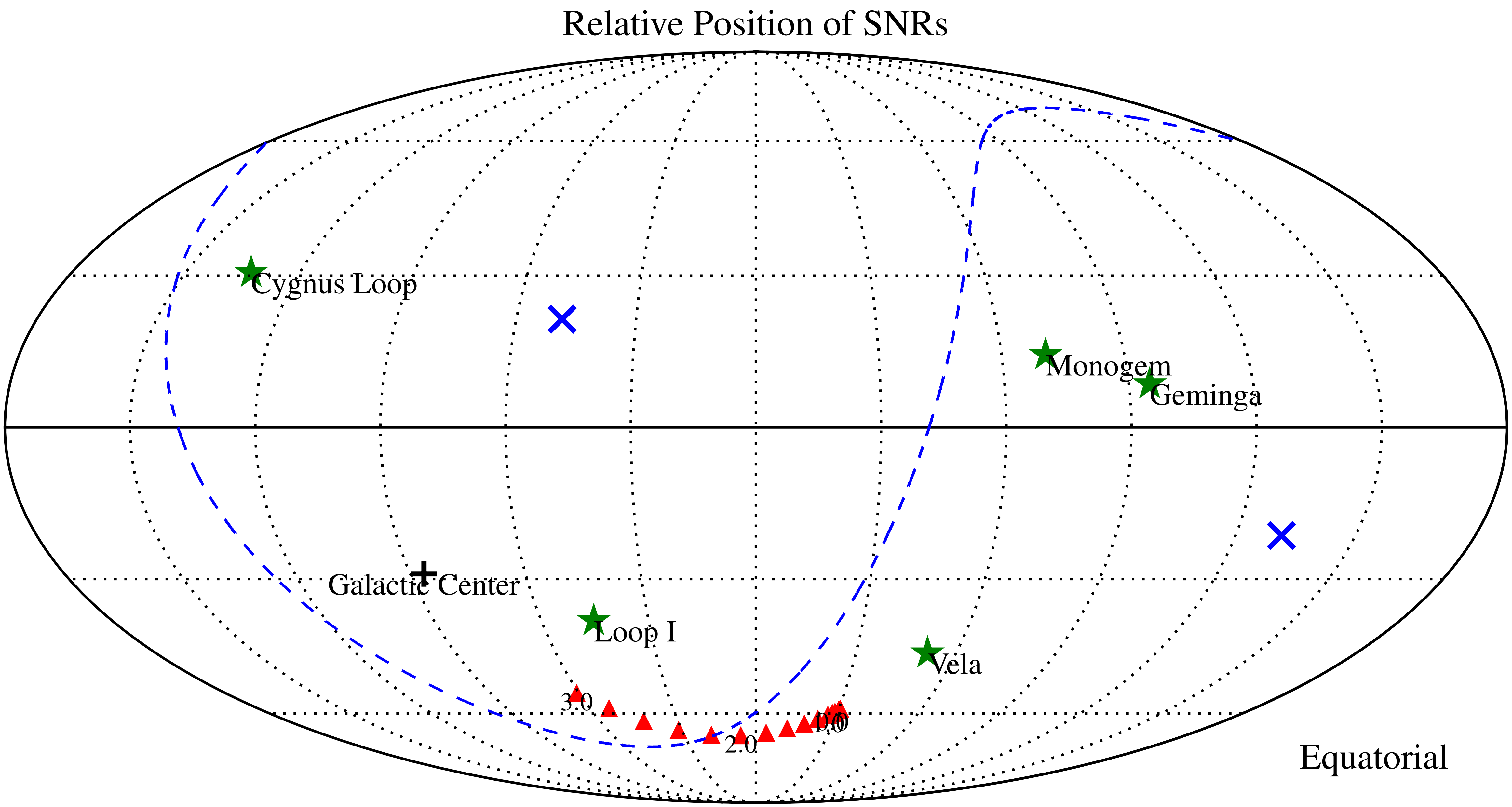

Relative position of the five closest SNRs. The magnetic field direction (IBEX) is indicated by × and the **magnetic equator** by a dashed line.

Phase-Flip by Vela SNR?

- Observed 1-100 TeV phase indicates **dominance of a local source** with:

$$120^\circ \leq l \leq 300^\circ$$

- **plausible scenario: Vela SNR**
  - age: $\simeq 11{,}000\,\mathrm{yrs}$
  - distance: $\simeq 1{,}000\,\mathrm{lyrs}$
  - SNR rate: $\simeq 1/30\,\mathrm{yr}^{-1}$
  - (effective) isotropic diffusion:

$$K_{\rm iso} \simeq 3\times10^{28}E_{\rm GeV}^{1/3}\mathrm{cm}^2/\mathrm{s}$$

  - Galactic halo width: $\simeq 3\,\mathrm{kpc}$
  - instantaneous CR emission $Q_\star$

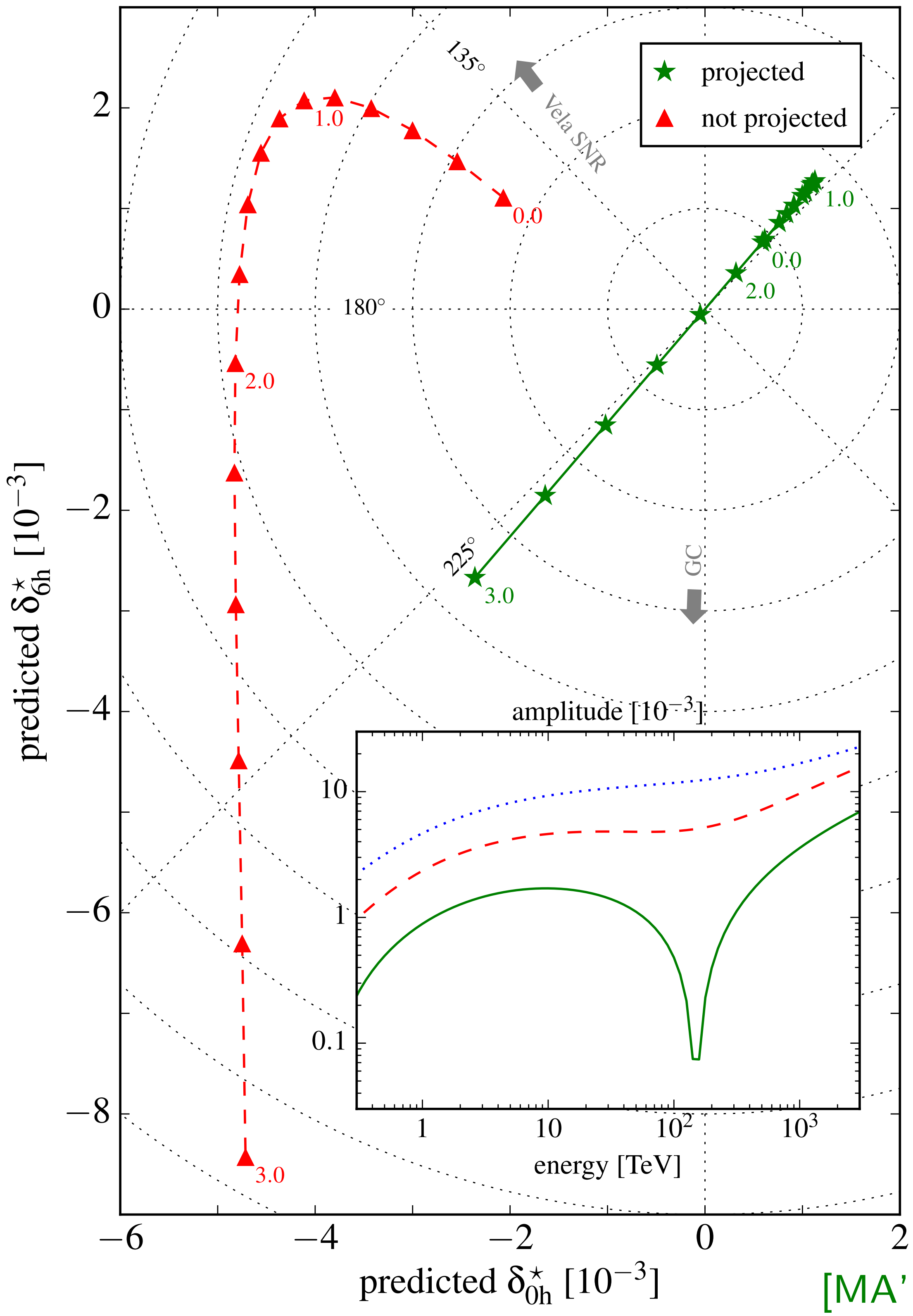

[MA'16]

Small-Scale Anisotropy

- Significant TeV small-scale anisotropies down to angular scales of $\mathcal{O}(10°)$.
- Strong local excess (*region A*) observed by Northern observatories.

  [Tibet-ASγ'06; Milagro'08]
  [ARGO-YBJ'13; HAWC'14]

- Angular power spectra of IceCube and HAWC data show excess compared to isotropic arrival directions. [IC'11; HAWC'14]

$$C_\ell = \frac{1}{2\ell+1}\sum_{m=-\ell}^{\ell}|a_{\ell m}|^2$$

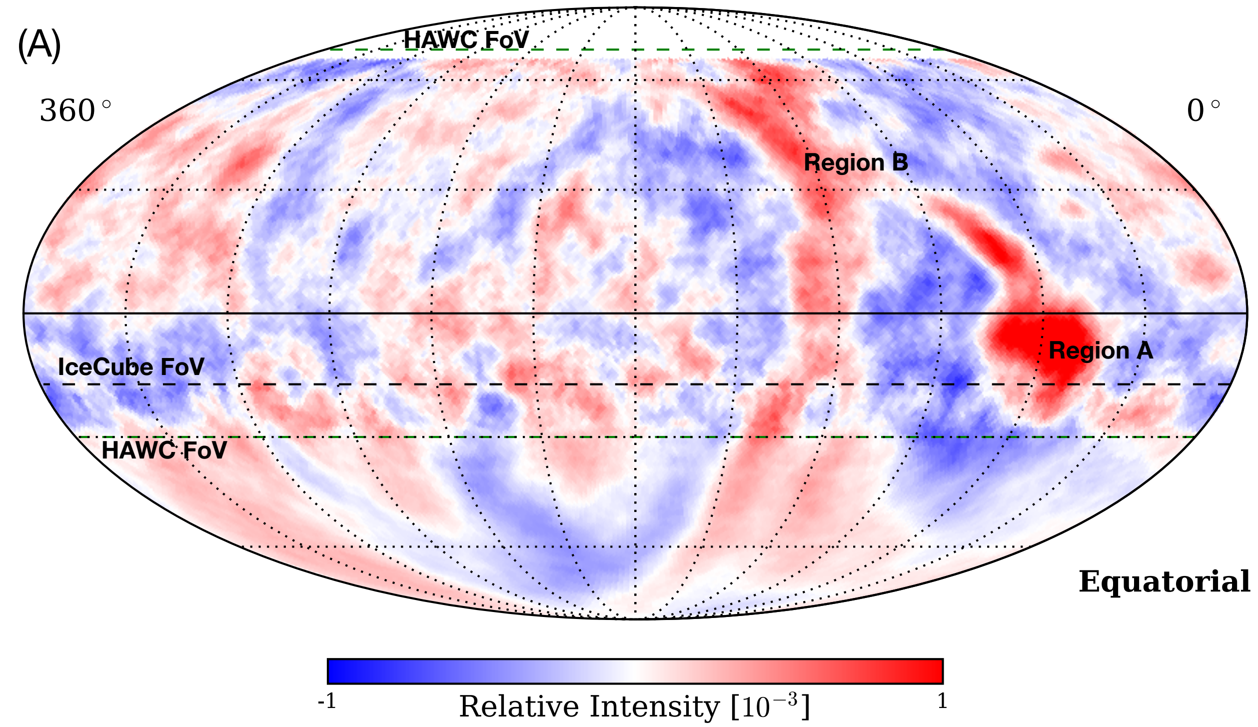

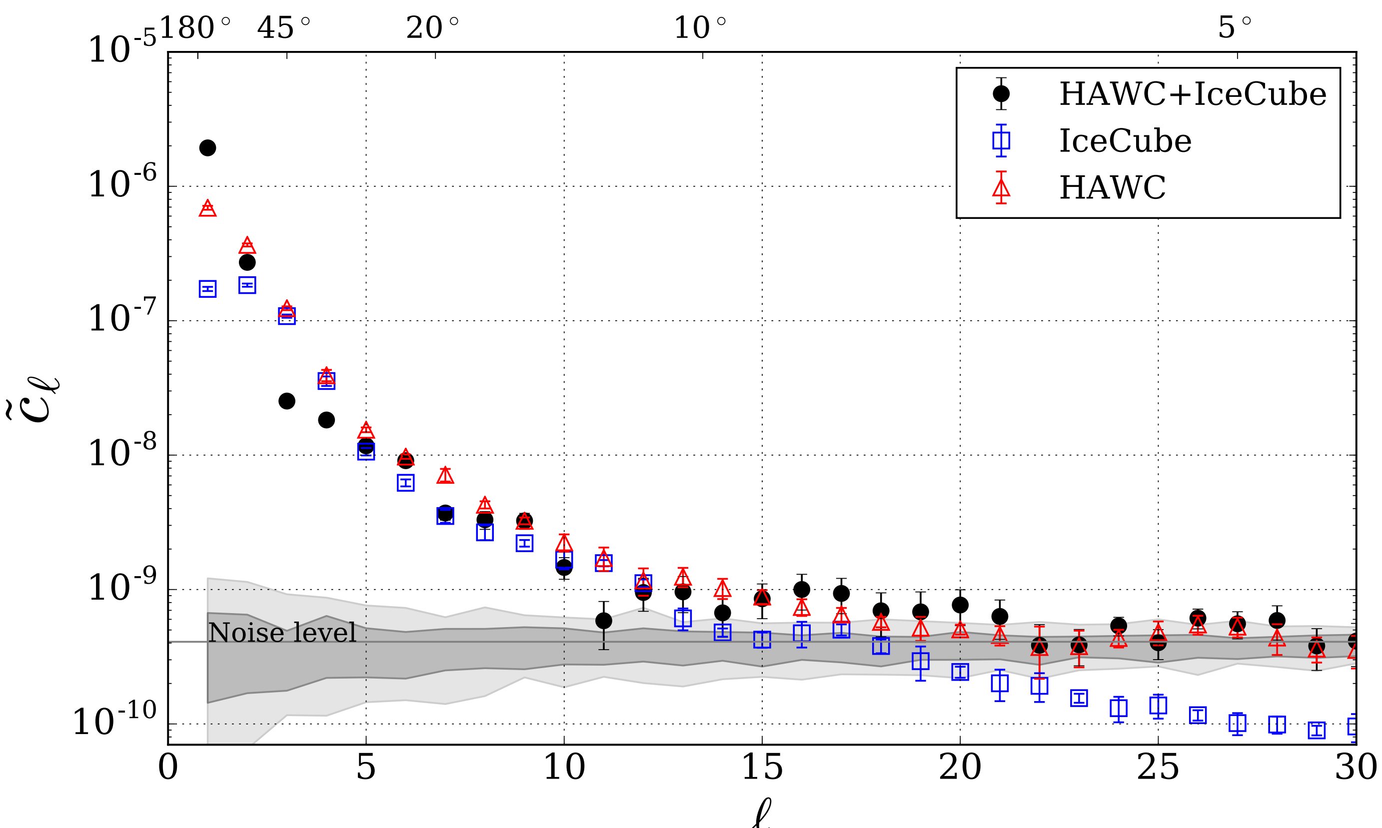

[IceCube & HAWC'18]

Influence of Heliosphere?

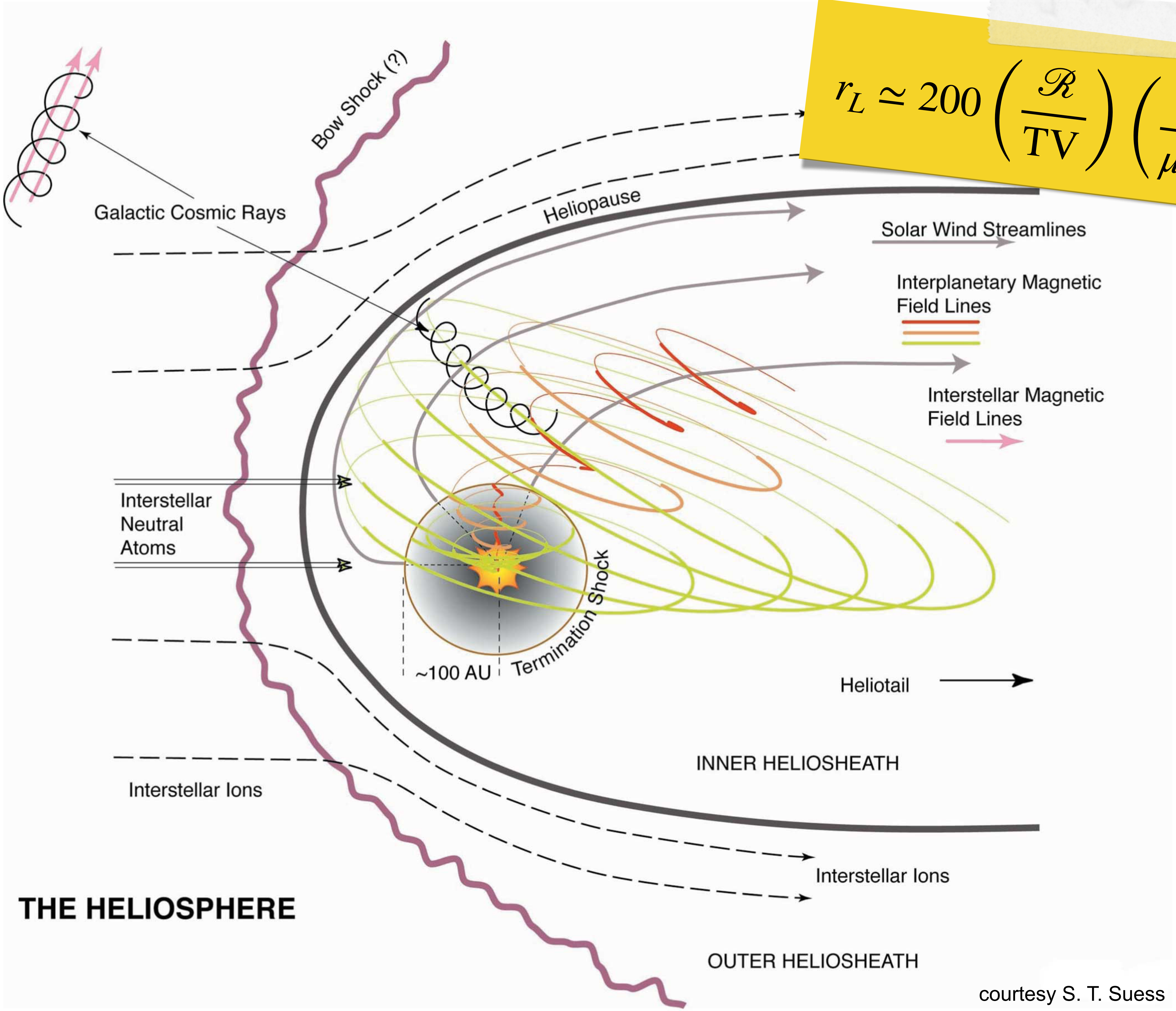

$$r_L \simeq 200 \left(\frac{\mathscr{R}}{\mathrm{TV}}\right)\left(\frac{B}{\mu\mathrm{G}}\right)^{-1} \mathrm{AU}$$

Angular Power Spectrum

- Every smooth function $g(\theta, \varphi)$ on a sphere can be decomposed in terms of spherical harmonics $Y_{\ell m}(\theta, \varphi)$:

$$g(\theta, \varphi) = \sum_{\ell=0}^{\infty} a_{\ell m} Y_{\ell m}(\theta, \varphi) \qquad \leftrightarrow \qquad a_{\ell m} = \int \mathrm{d}\cos\theta \int \mathrm{d}\varphi Y^*_{\ell m}(\theta, \varphi) g(\theta, \varphi)$$

- **angular power spectrum**:

$$C_\ell = \frac{1}{2\ell + 1} \sum_{m=-\ell}^{\ell} |a_{\ell m}|^2$$

- related to the two-point **auto-correlation function**:

$$\xi(\eta) = \frac{1}{8\pi^2} \int \mathrm{d}\Omega_1 \int \mathrm{d}\Omega_2 \delta(\mathbf{n}_1 \cdot \mathbf{n}_2 - \cos\eta) g(\Omega_1) g(\Omega_2) = \frac{1}{4\pi} \sum_{\ell=0}^{\infty} (2\ell + 1) C_\ell P_\ell(\cos\eta)$$

- Note that power C_ℓ is invariant under rotations (assuming 4π coverage).

Non-Uniform Pitch-Angle Diffusion

- stationary pitch-angle diffusion:

$$v\mu\frac{\partial}{\partial z}\langle f\rangle = \frac{\partial}{\partial \mu}\left(D_{\mu\mu}\frac{\partial}{\partial \mu}\langle f\rangle\right)$$

- **non-uniform diffusion**:

$$\frac{D_{\mu\mu}}{1-\mu^2} \neq \text{const}$$

- non-uniform pitch-angle diffusion modifies the large-scale anisotropy aligned with background field
  - **small-scale** excess/deficits for enhanced diffusion towards $\mu = \pm 1$ [Malkov *et al.*'10]
  - **large-scale** features for enhanced diffusion at $\mu = 0$ [Giacinti & Kirk'17]

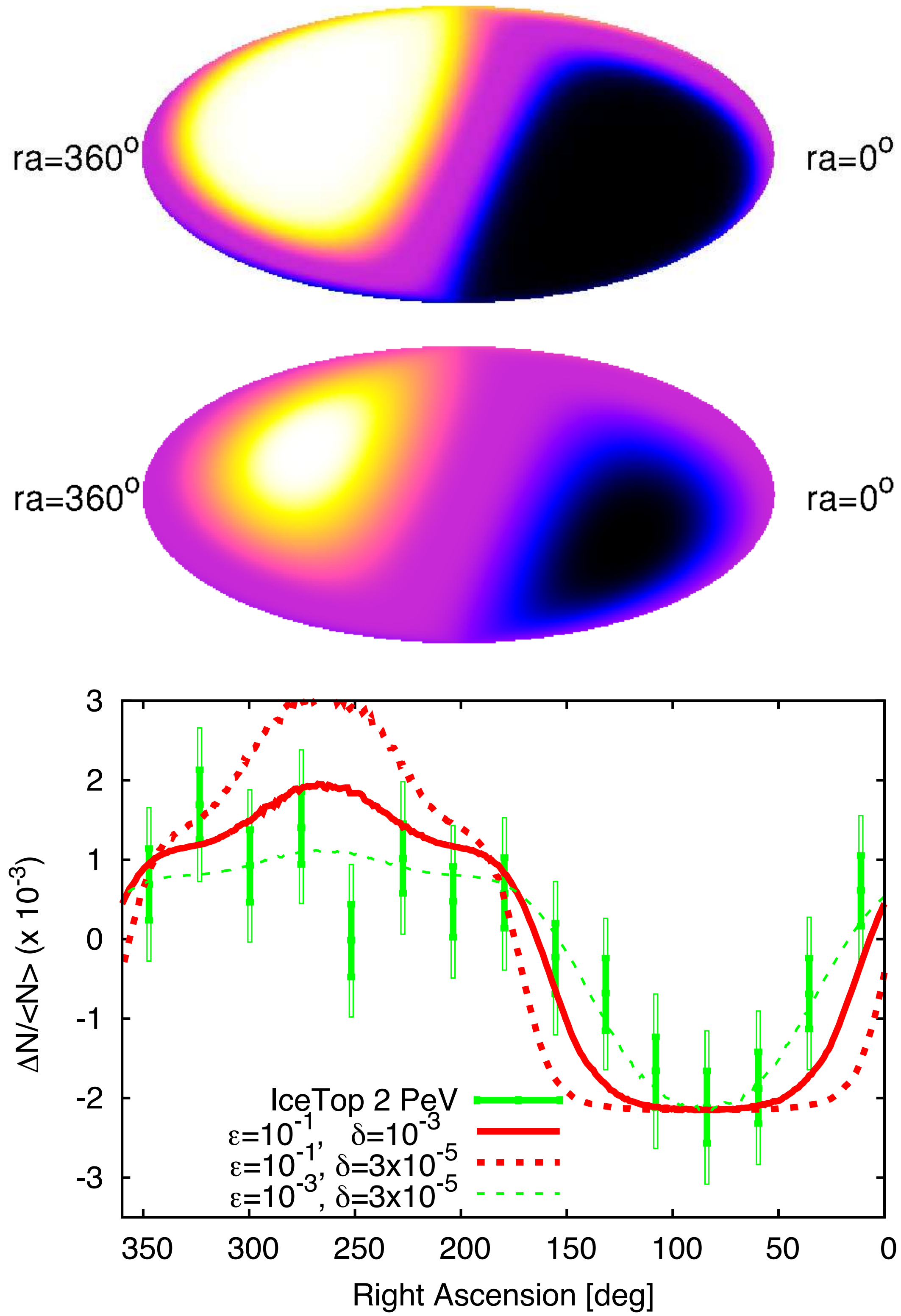

[Giacinti & Kirk'17]

Anisotropy from Local Turbulence

CMB temperature fluctuations

Cosmic Ray Gradient

Large Scale Structure

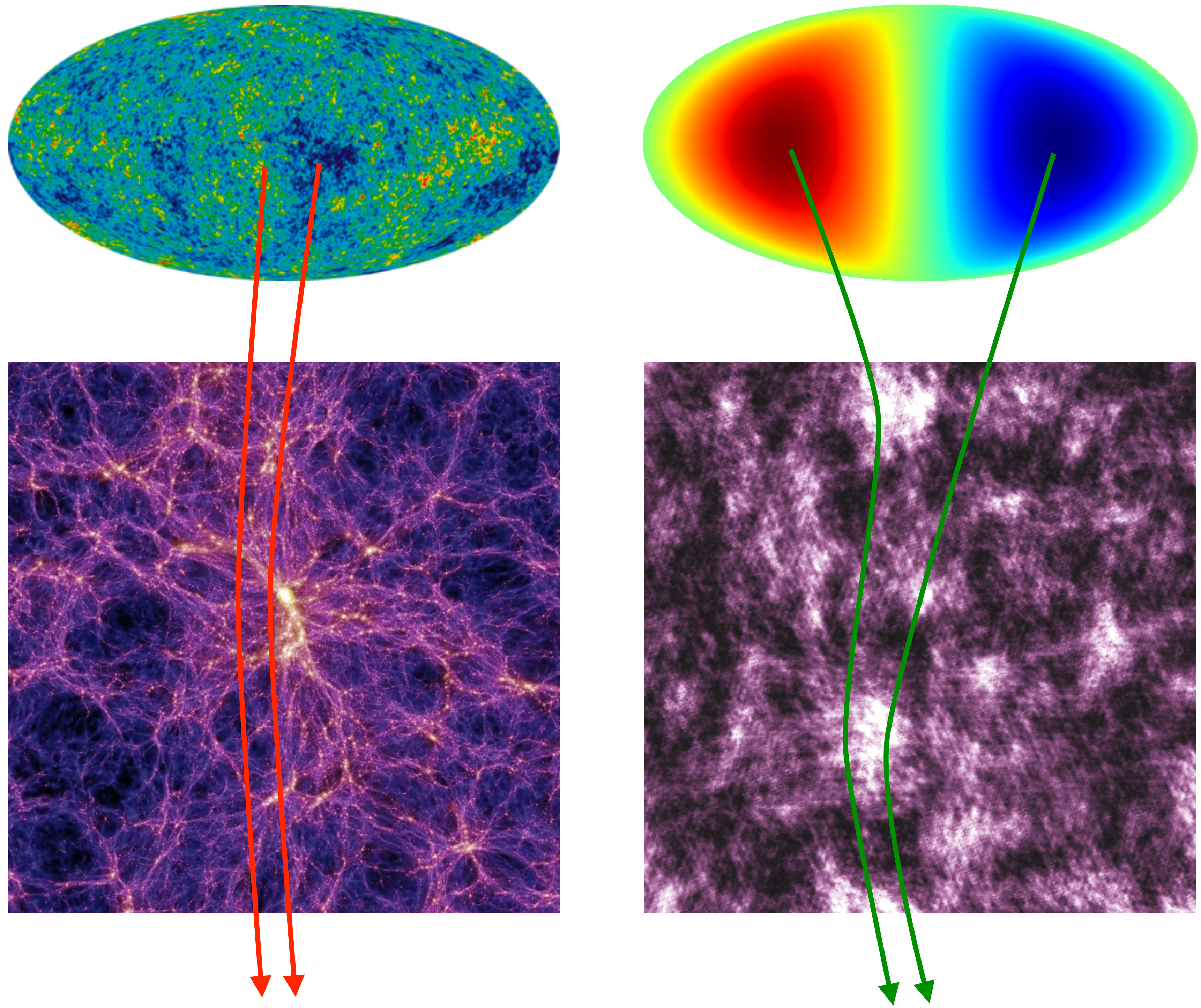

Local Magnetic Turbulence

small scale temperature fluctuations

small scale anisotropies

[Giacinti & Sigl'12]

Small-Scale Theorem

- **Assumptions:**
  - absence of CR sources and sinks
  - isotropic and static magnetic turbulence
  - initially, homogenous phase space distribution
- **Theorem:** *The sum over the ensemble-averaged angular power spectrum is constant*: [MA'14]

$$\sum_{\ell=0}^{\infty}(2\ell+1)\langle C_\ell\rangle \propto \langle\xi(1)\rangle \propto \mathrm{const}$$

- **Proof:** by angular auto-correlation function.
- Wash-out of individual moments by diffusion (rate $\nu_\ell \propto \mathbf{L}^2 \propto \ell(\ell+1)$) has to be compensated by generation of small-scale anisotropy.
- Theorem implies small-scale angular features from large-scale average dipole anisotropy. [Giacinti & Sigl'12; MA'14; MA & Mertsch'15,'20]

Evolution Model

- Diffusion theory motivates that each $\langle C_\ell \rangle$ decays exponentially with an effective relaxation rate:

$$\nu_\ell \simeq \nu \mathbf{L}^2 = \nu \ell(\ell+1)$$

- A linear $\langle C_\ell \rangle$ evolution equation with **partial rates** $\nu_{\ell\to\ell'}$ requires:

$$\partial_t \langle C_\ell \rangle = -\nu_\ell \langle C_\ell \rangle + \sum_{\ell' \geq 0} \nu_{\ell' \to \ell} \frac{2\ell'+1}{2\ell+1} \langle C_{\ell'} \rangle \qquad \text{with} \qquad \nu_\ell \equiv \sum_{\ell' \geq 0} \nu_{\ell \to \ell'}$$

- For $\nu_\ell \simeq \nu_{\ell\to\ell+1}$ and, initially, $C_\ell(t=0) = C_1 \delta_{\ell 1}$ this has an analytic solution:

$$\langle C_\ell \rangle(T) = \frac{3C_1}{2\ell+1} \prod_{m=1}^{\ell-1} \nu_m \sum_n \prod_{p=1(\neq n)}^{\ell} \frac{e^{-T\nu_n}}{\nu_p - \nu_n}$$

- At large times we arrive at the asymptotic ratio:

$$\lim_{T\to\infty} \frac{\langle C_\ell \rangle(T)}{\langle C_1 \rangle(T)} \simeq \frac{18}{(2\ell+1)(\ell+2)(\ell+1)}$$

Comparison with Data

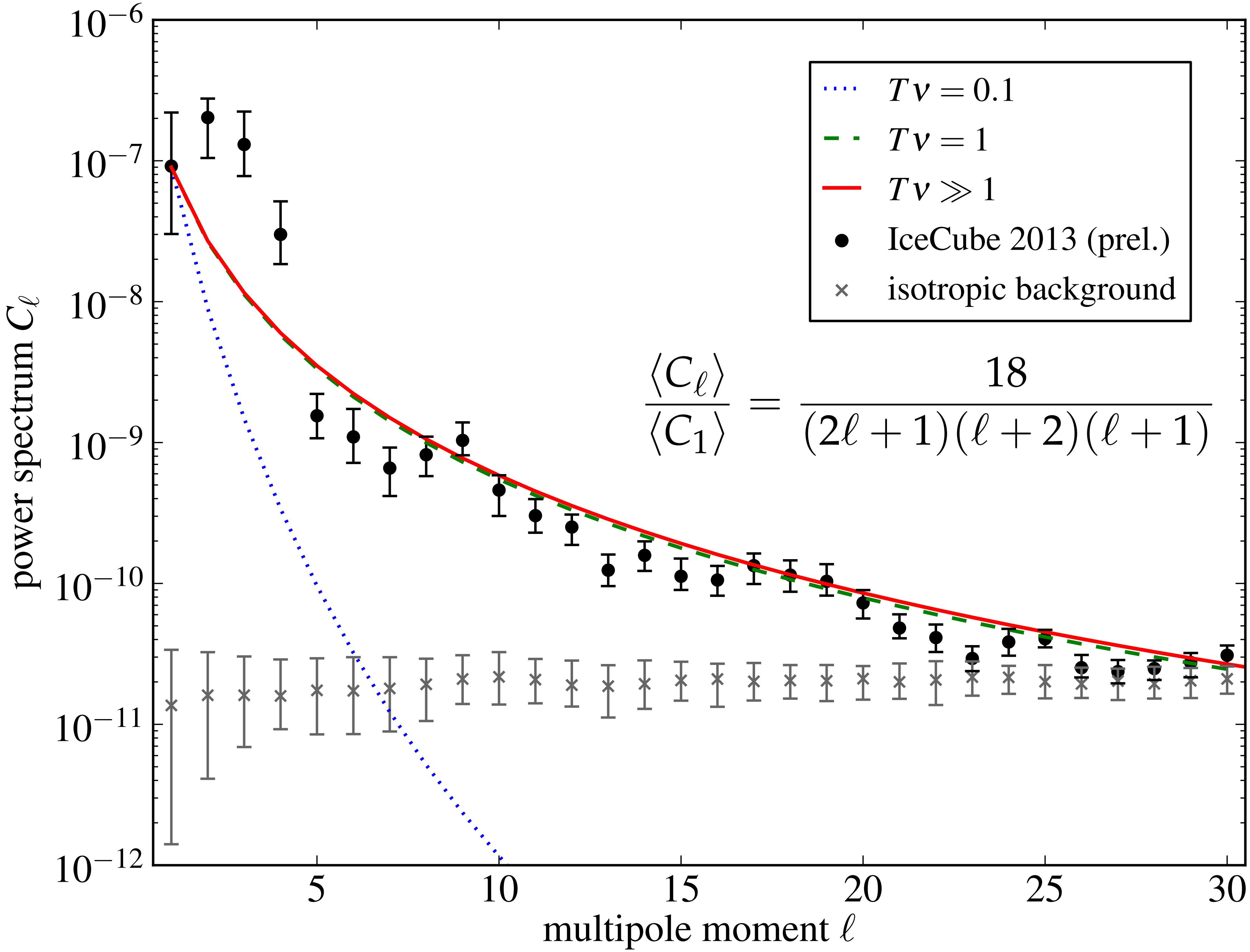

[MA'14]

Cosmic Ray Backtracking

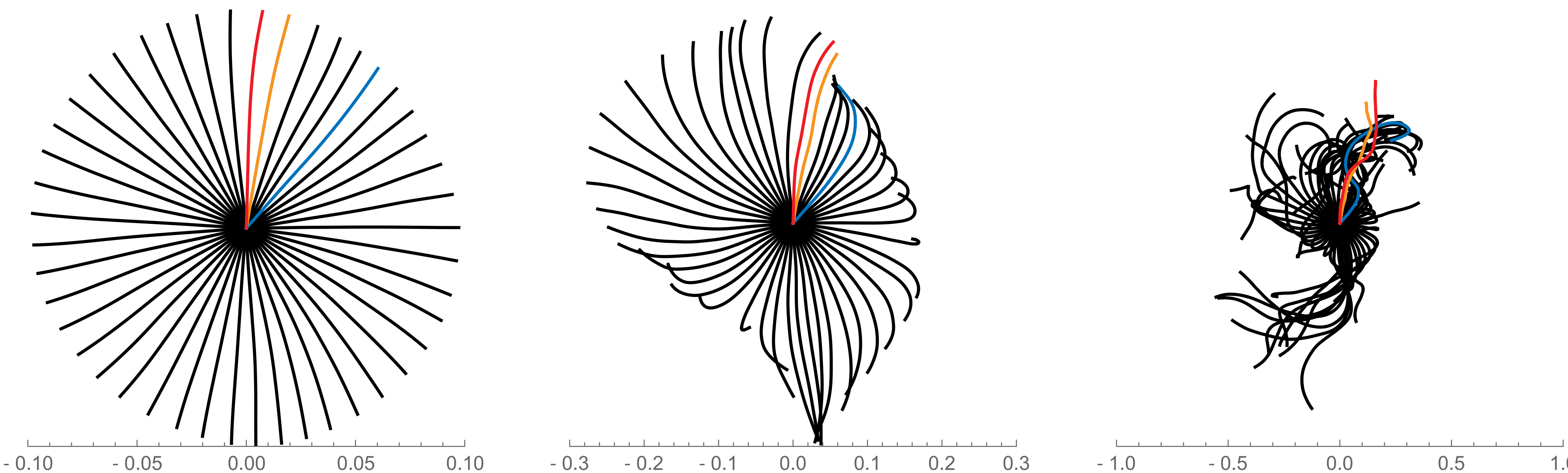

- Consider a local (quasi-)stationary solution of the diffusion approximation:

[MA & Mertsch'15]

$$\langle f \rangle \simeq \phi + (\mathbf{r} - 3\hat{\mathbf{p}}\mathbf{K})\nabla\phi$$

- Ensemble-averaged C_ℓ's ($\ell \leq 1$) from backtacking:

$$\frac{\langle C_\ell \rangle}{4\pi} \simeq \int \frac{\mathrm{d}\hat{\mathbf{p}}_1}{4\pi} \int \frac{\mathrm{d}\hat{\mathbf{p}}_2}{4\pi} P_\ell(\mathbf{p}_1\mathbf{p}_2) \lim_{T\to\infty} \langle \mathbf{r}_{1i}(-T)\mathbf{r}_{2j}(-T)\rangle \frac{\partial_{r_i} n_{\mathrm{CR}} \partial_{r_j} n_{\mathrm{CR}}}{n_{\mathrm{CR}}^2}$$

Cosmic Ray Backtracking

- simulation in isotropic & static magnetic turbulence with:
$$\overline{\delta \mathbf{B}^2} = \mathbf{B}_0^2$$
- relative orientation of CR gradient:
  - *solid lines* : $\mathbf{B}_0 \parallel \nabla n_{\rm CR}$
  - *dotted lines* : $\mathbf{B}_0 \perp \nabla n_{\rm CR}$
- diffusive regime at $T\Omega \gtrsim 100$
- slightly enhanced dipole compared to standard diffusion
- asymptotically limited by simulation noise:
$$\mathcal{N} \simeq \frac{4\pi}{N_{\rm pix}} 2TK_{ij} \frac{\partial_i n_{\rm CR} \partial_j n_{\rm CR}}{n_{\rm CR}^2}$$

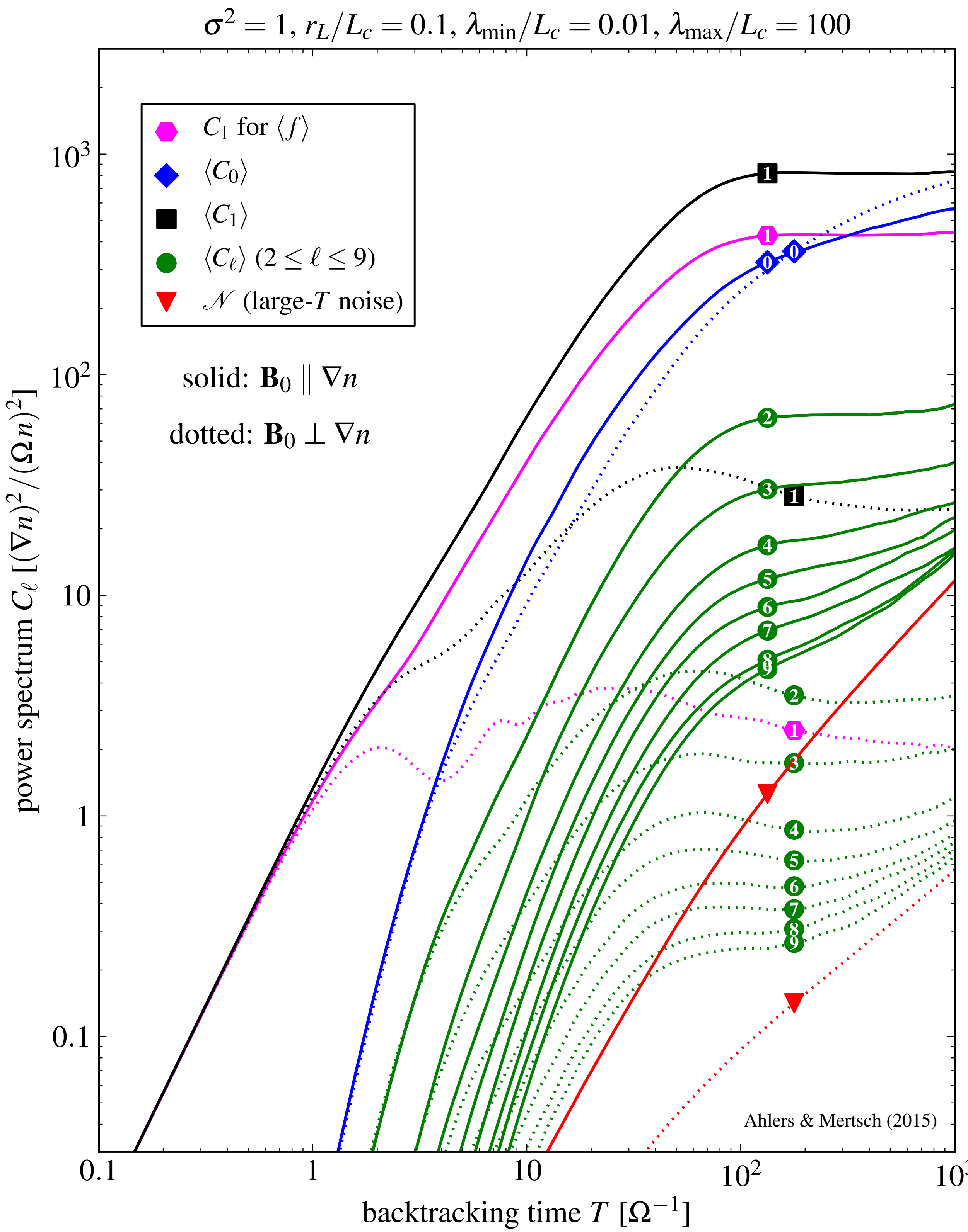

Simulation vs. Data

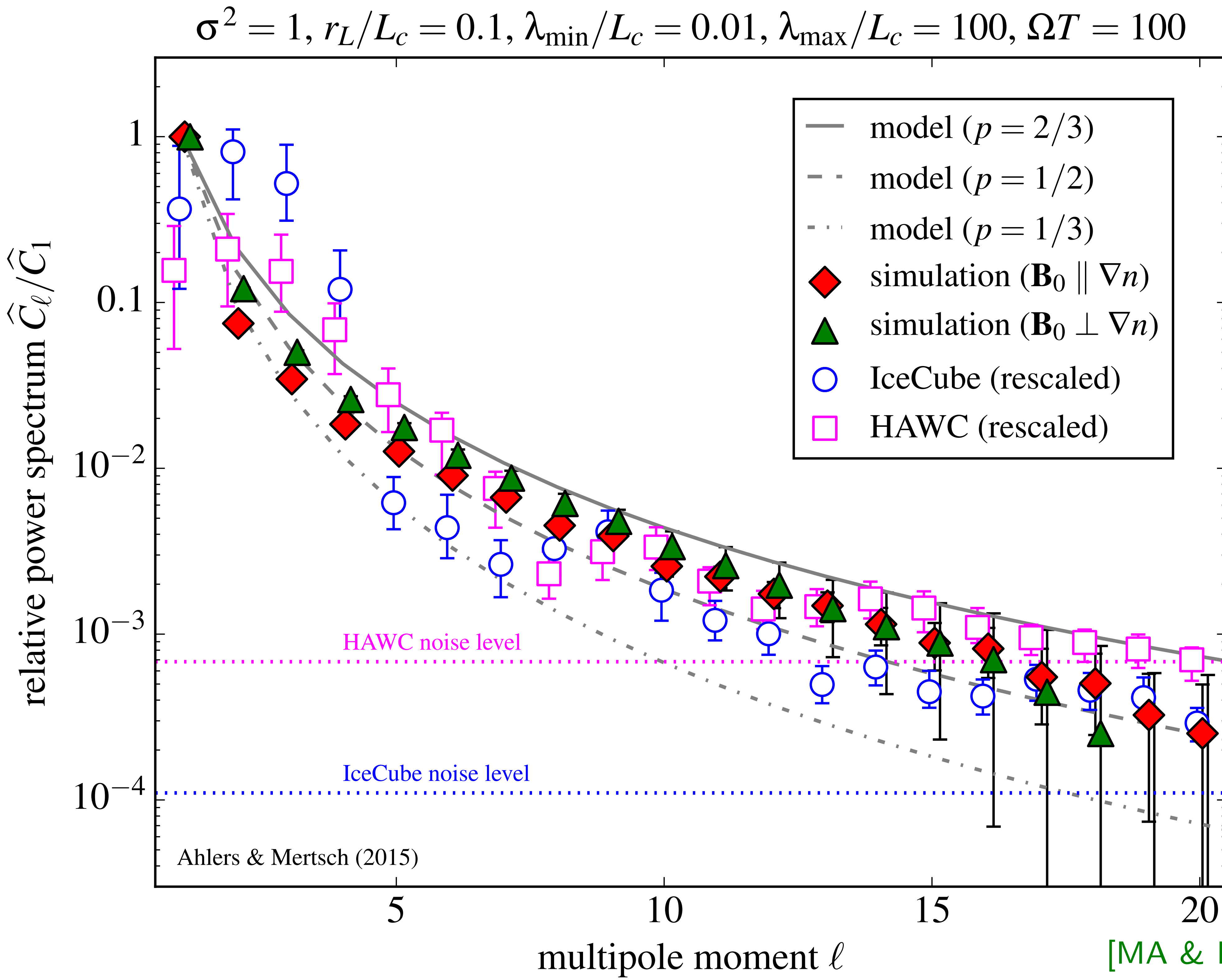

[MA & Mertsch'15]

"Via Lactea Incognita"

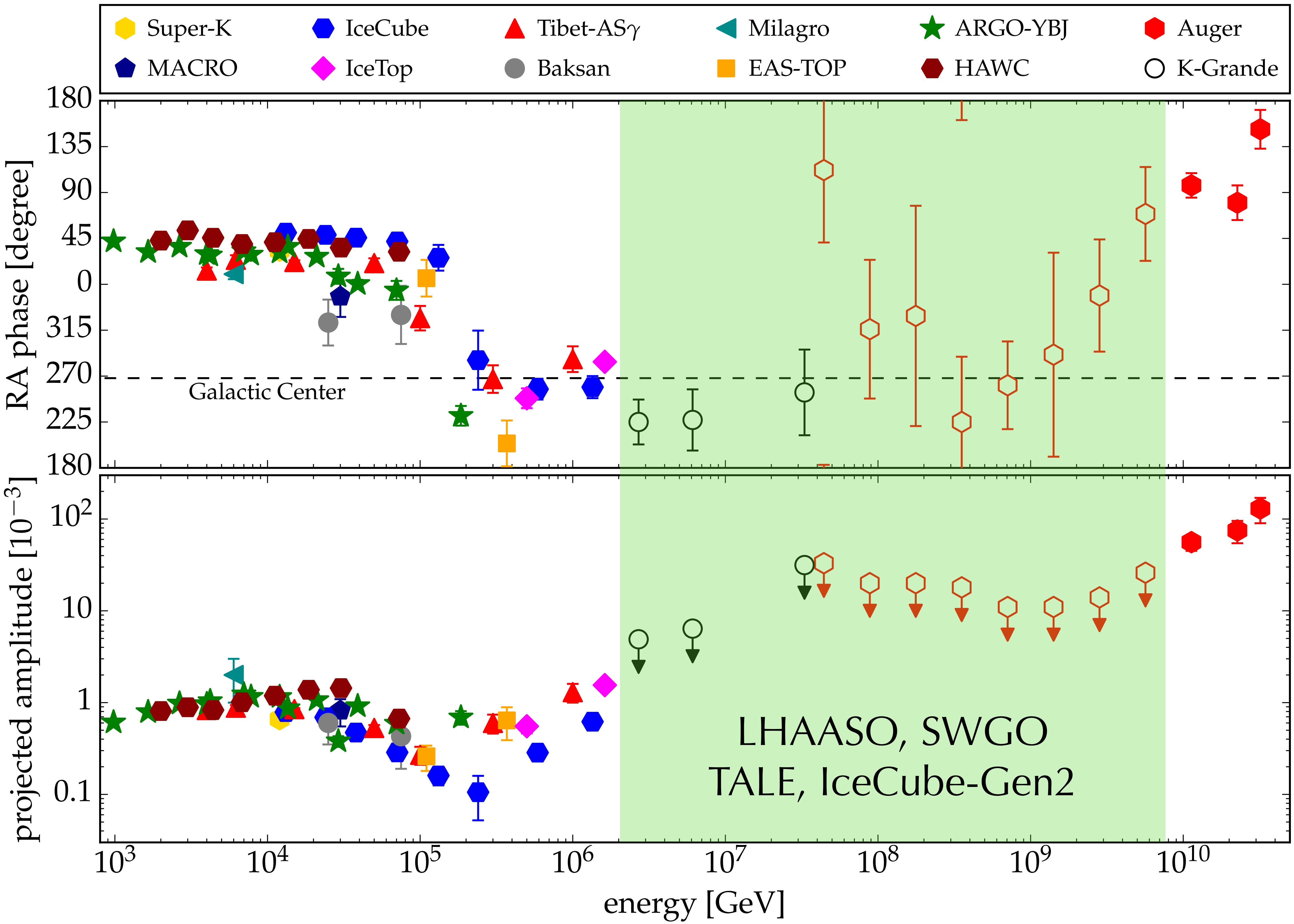

More UHE CR Anisotropies

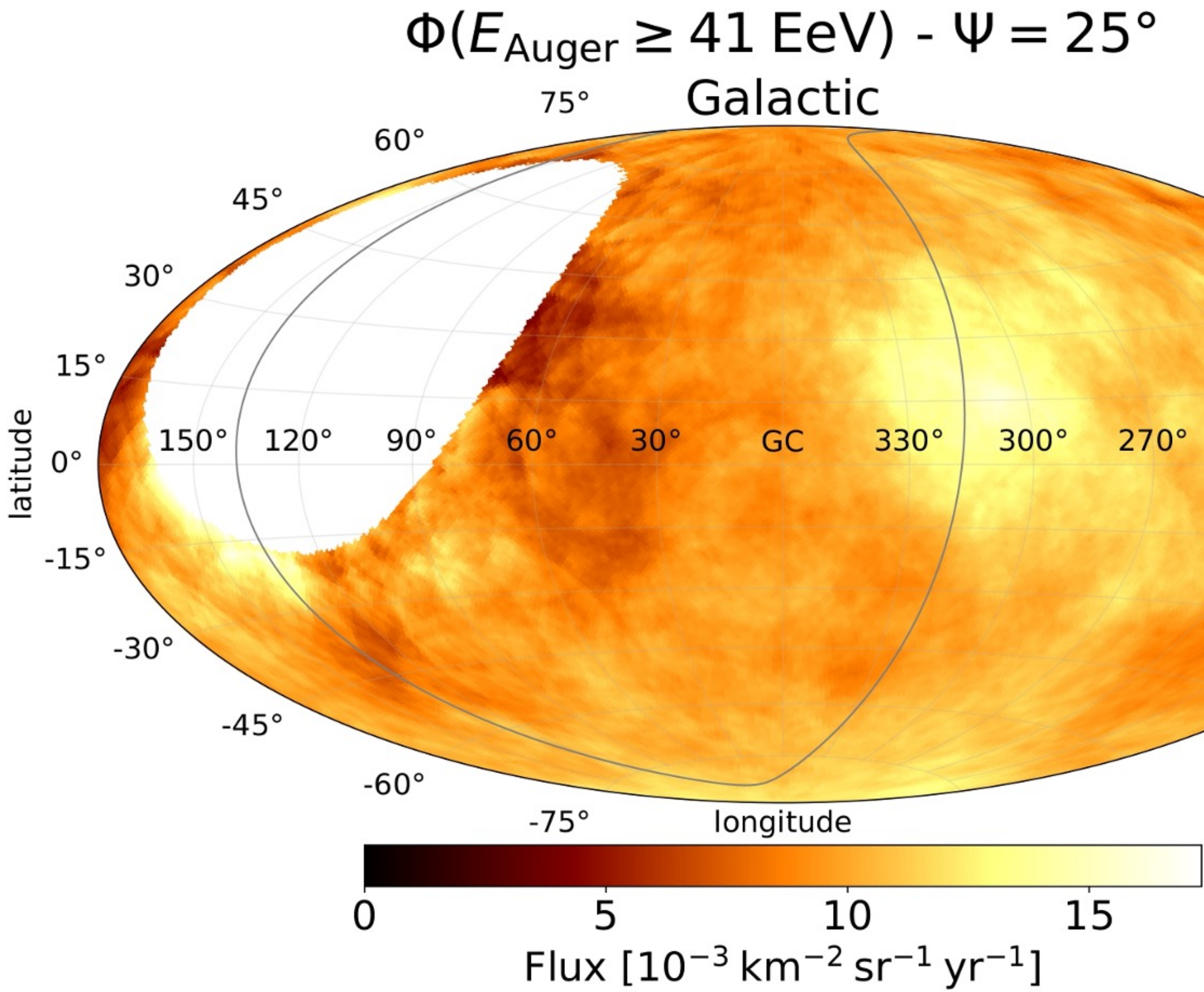

4σ **evidence for small-scale feature**

[Auger, ApJ 935 (2022) 2]

More UHE CR Anisotropies

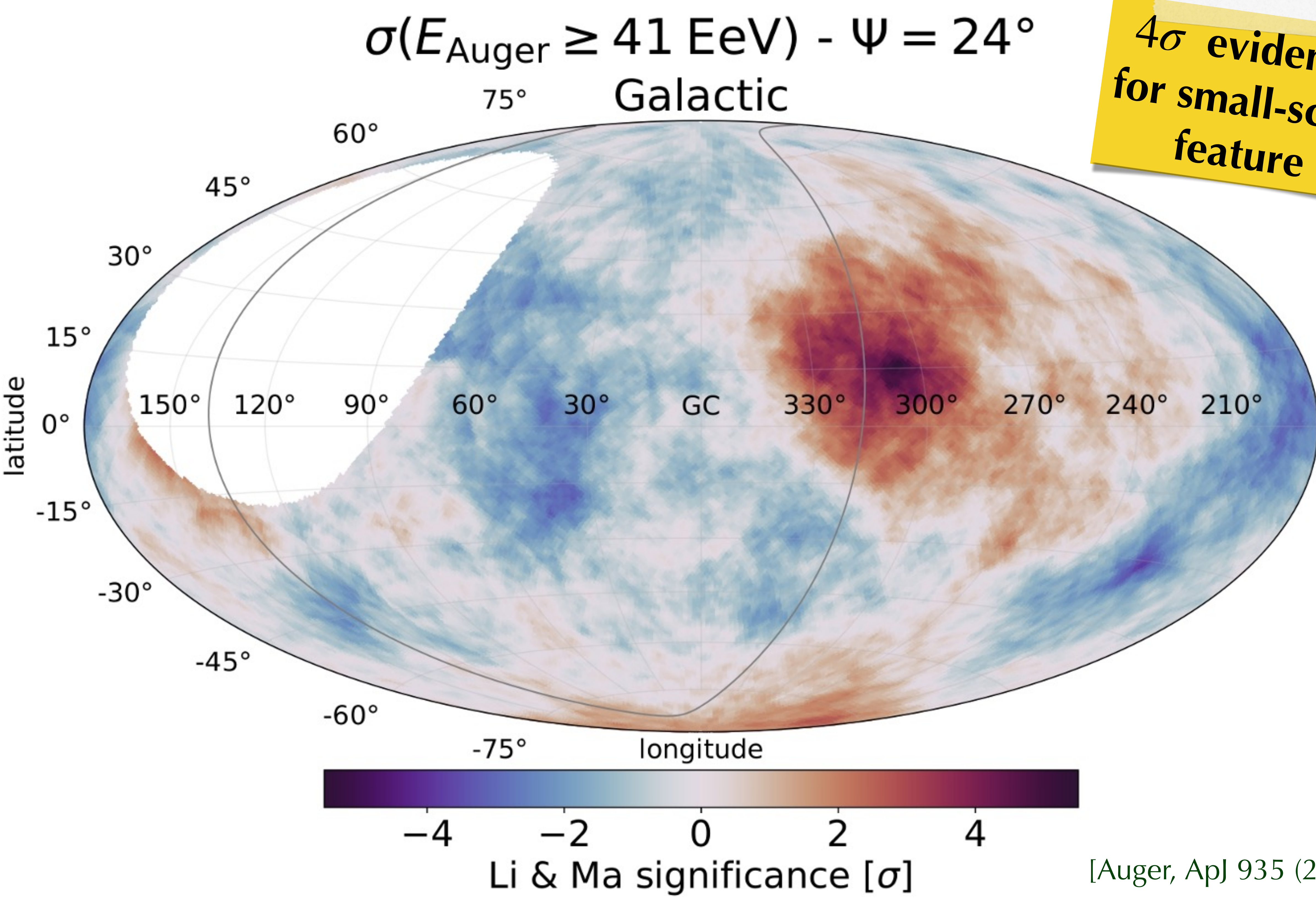

4σ **evidence for small-scale feature**

[Auger, ApJ 935 (2022) 2]

More UHE CR Anisotropies

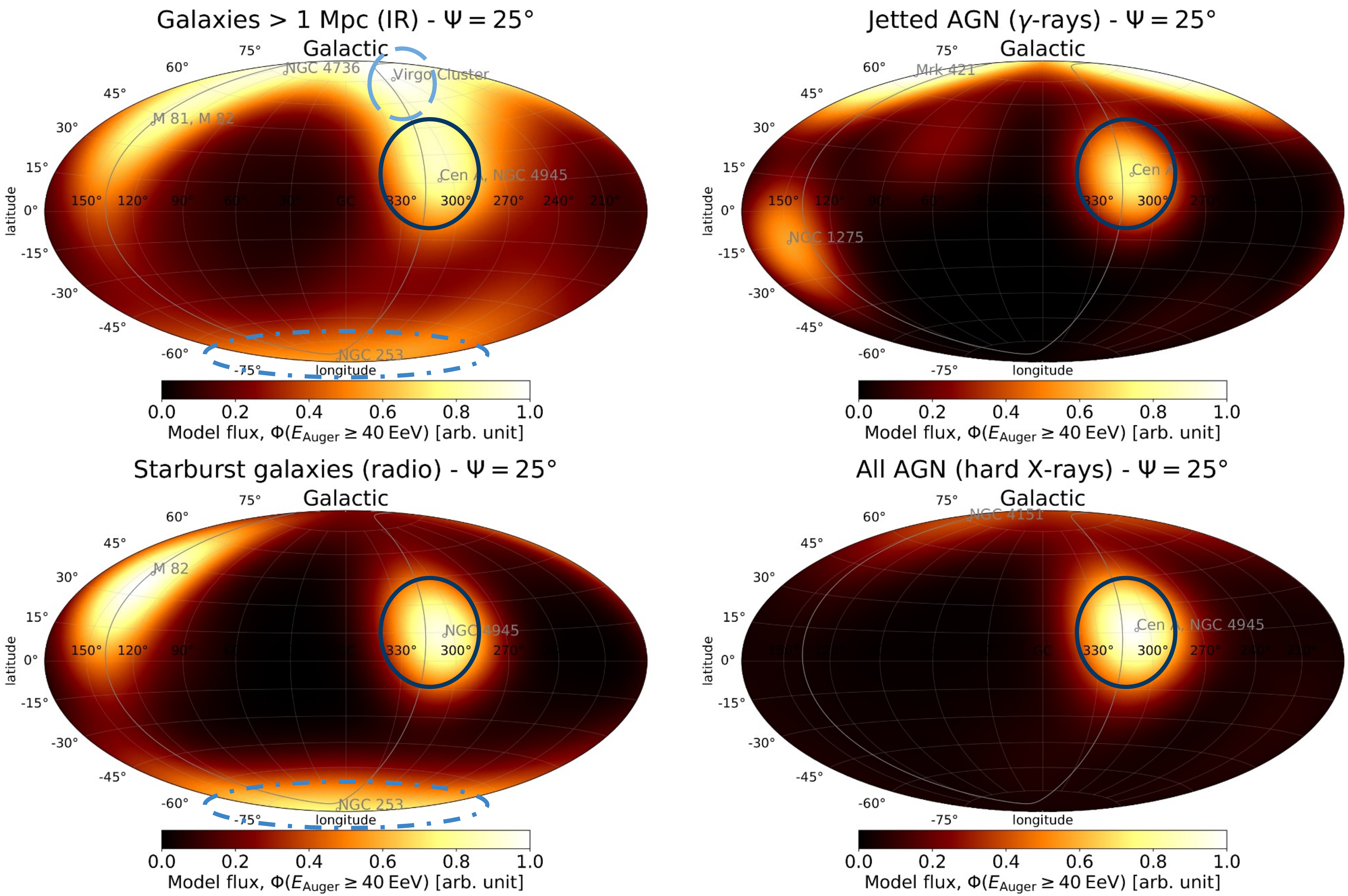

[Auger, ApJ 935 (2022) 2]

Summary

A. Observation of CR anisotropies at the level of one-per-mille is challenging.

- large statistical and systematic uncertainties
- multipole analysis can introduce bias, sometimes not stated or corrected for

B. Dipole anisotropy can be understood in the context of diffusion theory.

- TV-PV dipole phase aligns with the local ordered magnetic field
- amplitude variations as a result of local sources
- plausible candidates are local SNRs, e.g. Vela
- *What is the expected dipole anisotropy in the PV-EV range?*

C. Observed CR data shows also evidence for small-scale anisotropy.

- induces cross-talk with dipole anisotropy in limited field of view
- constitutes a probe of local magnetic turbulence
- *What can we learn about our heliosphere from TV small-scale features?*
- *What is the effect of local (* $\lesssim 10\,\mathrm{pc}$*) magnetic turbulence?*
- *How do we disentangle global CR transport features form local turbulence?*